In presenting the dissertation as a partial fulfillment of the requirements for an advanced degree from the Georgia Institute of Technology, I agree that the Library of the Institute shall make it available for inspection and circulation in accordance with its regulations governing materials of this type. I agree that permission to copy from, or to publish from, this dissertation may be granted by the professor under whose direction it was written, or, in his absence, by the Dean of the Graduate Division when such copying or publication is solely for scholarly purposes and does not involve potential financial gain. It is understood that any copying from, or publication of, this dissertation which involves potential financial gain will not be allowed without written permission.

3/17/65
b

LAMINAR MASS TRANSFER IN THE ENTRANCE REGION OF AN INCLINED TUBE

A THESIS

Presented to

The Faculty of the Graduate Division

by

William Dinsmore Holland

In Partial Fulfillment

of the Requirements for the Degree

Doctor of Philosophy

in the School of Chemical Engineering

Georgia Institute of Technology

May, 1966

LAMINAR MASS TRANSFER IN THE ENTRANCE REGION OF AN INCLINED TUBE

Approved:

[redacted]

[redacted]

Date Approved by Chairman: 5/16/66

ACKNOWLEDGMENTS

The author wishes to express his appreciation to his thesis advisor, Dr. Henderson C. Ward, whose helpful suggestions and encouragement are largely responsible for this work. The advice given by Dr. William M. Newton and Dr. Charles W. Gorton in their reading of this work was most helpful. The interest and cooperation of Dr. Homer V. Grubb, Director of the School of Chemical Engineering, is gratefully acknowledged.

Many graduate and undergraduate students aided in the construction and operation of the experimental equipment. Thanks are due to Mr. A. G. Krigens, Mr. F. M. Gilbert, and Mr. R. A. Hoffman for their assistance in the concentration measurement work, and to Mr. D. M. Turpin, Mr. D. J. DeLong, and Mr. F. N. Tuller, for their aid in obtaining the experimental data. The author is particularly indebted to Dr. William A. Burns, Jr. for his most helpful consultation concerning the computer programming involved in this study and to Mr. J. F. Steadman for his assistance in writing the data reduction program.

The award to the author of the Dow Chemical Company Fellowship for 1961-2 and the Standard Oil Company of California Fellowship for September to December, 1965 greatly assisted in the completion of this work. A Ford Foundation Fellowship and loans provided by the Ford Foundation in 1965 also proved most helpful.

The cooperation of the Lockheed-Georgia Company, and particularly the author's supervisor, Mr. J. F. Cotton, in providing part-time and

summer employment for the author during much of this study is appreciated.

Most of all, the author wishes to thank his wife. Without her encouragement and help, this work could never have been accomplished.

TABLE OF CONTENTS

LIST OF TABLES

LIST OF TABLES (Continued)

LIST OF TABLES (Continued)

LIST OF FIGURES

LIST OF FIGURES (Continued)

LIST OF FIGURES (Continued)

SUMMARY

A study of mass transfer in the entrance region of a 1.60 inch diameter tube was conducted. The inside surface of the tube was coated with a solid material, either naphthalene or para-dichlorobenzene, which sublimed into a laminarly flowing air stream. The system consisting of the air and pipe was maintained at constant temperature during a test run.

Experimental runs were conducted for naphthalene at 30.9°C, 38.2°C, and 50.0°C, and for para-dichlorobenzene at 30.9°C. Reynolds numbers of approximately 500, 1000 , and 1500 were employed for the naphthalene runs, and of approximately 750 and 1500 for para-dichlorobenzene. For each temperature and Reynolds number, runs were conducted for three pipe positions: horizontal, vertical with upflow, and at 45° inclination with upflow.

The test pipe was 81-1/4 inches in length and was made up of short threaded sections of pipe. Thirteen 2-inch long test sections were spaced intermittently between longer sections over the length of the pipe. Mass transfer rates were determined from weight loss measurements on the 2-inch long test sections. From the data collected, local average molar flux at the wall, local Nusselt numbers for mass transfer and logarithmic mean Nusselt numbers for mass transfer were calculated.

Concentration profiles near the exit end of the pipe were measured during several of the naphthalene runs. The profiles were obtained using a method developed during this study which employed a gas chroma-

tograph equipped with an ionization detector system. Gas samples were withdrawn from the test pipe using a heated hypodermic syringe.

A theoretical solution assuming constant physical properties was obtained for the equations describing mass transfer in the laminar entrance region. The solution was obtained by numerically solving the continuity, momentum and diffusion equations using an implicit difference technique that advanced step-wise down the tube. Terms involving radial velocity were included in the equations. The numerical calculations necessary to obtain the solution were made on a Burroughs B-5500 digital computer.

The experimental results for all test runs showed higher mass fluxes and mass transfer Nusselt numbers than predicted by the theoretical solution. In general, the agreement was better near the pipe entrance with deviations increasing further down the pipe. For the naphthalene runs, it was found that agreement with the theoretical solution improved markedly with decreasing temperature. The para-dichlorobenzene runs at 30.9°C showed much larger deviations from the theoretical than the naphthalene runs at the same temperature. Apparently the lack of agreement between the theoretical and the experimental results is caused by free-convection currents initiated by density differences between the fluid near the wall and the fluid near the center of the pipe.

Near the end of the pipe, log mean Nusselt numbers were found to be approximately 60 per cent above the theoretical for naphthalene at 50.0°C, 40 per cent above for naphthalene at 38.2°C, and 20 per cent above for naphthalene at 30.9°C. Para-dichlorobenzene at 30.9°C showed deviations of about 60 per cent. Over the range tested, pipe inclination

was found to have little effect on the overall mass transfer rates. A tendency for the runs made at higher Reynolds numbers to give higher transfer rates was noted for all inclinations and temperatures; however, the effect was usually small.

The effect of pipe inclination was more readily seen by considering local results. Local Nusselt numbers for vertical and 45° angle runs showed generally better agreement with theory than those for the horizontal case; however, the horizontal runs showed better agreement close to the pipe entrance. Except at axial locations close to the entrance, deviations of over 100 per cent were quite common for the local Nusselt numbers obtained during high Grashof number runs. These runs were naphthalene at $50.0^{\circ}C$ and para-dichlorobenzene at $30.9^{\circ}C$. Best agreement in local values occurred for naphthalene at $30.9^{\circ}C$, but even for this case local results were frequently over 30 per cent above the theoretical results.

Local mass fluxes measured for the horizontal runs with naphthalene at $50.0^{\circ}C$ were compared to similar results obtained by Bosworth (6). Fluxes near the pipe entrance were found to be considerably lower than those determined by him. Further down the pipe, the results of this study were higher than those measured by Bosworth at corresponding positions. The negative mass fluxes reported by him at certain axial locations were not found to occur in any of the test runs conducted during this study.

An attempt was made to correlate the experimentally determined log mean Nusselt numbers for mass transfer using available heat transfer expressions which consider free-convection. An equation presented by

Jackson, Spurlock and Purdy (16) which is based on heat transfer data obtained in the laminar entrance region of a horizontal pipe was found to give good agreement for the higher Grashof number horizontal mass transfer runs. For the lower Grashof number runs, the equation predicted results which were too high. No success was had in correlating the results for the vertical runs. For these runs, free-convection and forced-convection were acting in opposite directions. All available heat transfer correlations predict the effect of opposed free- and forced-convection to be a reduction in Nusselt number from the theoretical value. The experimental mass transfer runs for the vertical case resulted in higher than theoretical Nusselt numbers.

The experimental concentration profiles showed generally higher concentrations than predicted by the theoretical solution. Agreement was fair near the wall, but the center of the pipe was found to have considerably higher concentrations than theoretically predicted. Experimental profiles for the horizontal runs exhibited skewness, sometimes above and sometimes below the centerline. The one profile obtained for a vertical run was found to be quite symmetrical. These results seem to verify the finding from the weight loss measurements that free convection is significant over the range of variables studied.

NOMENCLATURE

In this tabulation, dimensions are given in terms of mass (M), length (L), time (t), and temperature (T). Equations referred to are defining equations in the body of the text.

Symbol	Definition
c_p	heat capacity at constant pressure per unit mass, L^2/t^2T
C	total molar concentration, moles/L^3
C_A	molar concentration of species A, moles/L^3
C_B	molar concentration of species B, moles/L^3
C^*	dimensionless concentration of species A, equation (2-12)
C_b^*	dimensionless bulk concentration of species A, equation (2-20)
$\mathscr{D}_{AB}$	binary diffusivity of system A-B, L^2/t
D	pipe diameter, L
D_m	experimentally determined average pipe diameter, L

Symbol	Definition
g	gravitational acceleration, L/t^2
h	heat transfer coefficient, M/t^3T
k	thermal conductivity, ML/t^3T
k_x	mass transfer coefficient, moles/tL^2
$k_{x,loc}$	local mass transfer coefficient, moles/tL^2, equation (2-16)
L	length of pipe, L
M_A	molecular weight of species A, M/mole
M_B	molecular weight of species B, M/mole
N_{Aw}	molar flux of species A at pipe wall, moles/L^2t
N_{Bw}	molar flux of species B at pipe wall, moles/L^2t
p	pressure, M/Lt^2
P	dimensionless pressure, equation (2-11)
r	radial distance, L
R	dimensionless radial distance, equation (2-9)
t	time, t

Symbol	Definition
T	absolute temperature, T
u	axial velocity, L/t
$\bar{u}$	average axial velocity, L/t
U	dimensionless axial velocity, equation (2-7)
v	radial velocity, L/t
V	dimensionless radial velocity, equation (2-8)
VP	vapor pressure, M/Lt^2
X	mole fraction, dimensionless
X_A	mole fraction of species A, dimensionless
z	axial distance, L
Z	dimensionless axial distance, equation (2-10)

Greek Symbols

β	coefficient of thermal expansion, 1/T
ζ	concentration coefficient of volumetric expansion, dimensionless
μ	viscosity, M/Lt

Symbol	Definition
υ	kinematic viscosity, (μ/ρ), L^2/t
ρ	fluid density, M/L^3
ω_A	molar mass transfer rate of species A, moles/t

Dimensionless Groups

Gr	Grashof number for heat transfer, $\rho^2\beta g D^3(\Delta T)/\mu^2$
Gr_{AB}	Grashof number for mass transfer, $\rho^2\zeta g D^3(\Delta X_A)/\mu^2$
Nu	Nusselt number for heat transfer, hD/k
Nu_{AB}	Nusselt number for mass transfer, $\frac{k_x D}{C\mathscr{D}_{AB}}$
Pr	Prandtl number, $c_p\mu/k$
Re	Reynolds number, $\bar{u}D/\upsilon$
Sc	Schmidt number, $\upsilon/\mathscr{D}_{AB}$

Subscripts

am	arithmetic mean value
A	component A
b	bulk condition

Symbol	Definition
B	component B
j	axial location of mesh point
k	radial location of mesh point
lm	logarithmic mean value
m	mean or average value
o	quantity evaluated at pipe inlet
w	quantity evaluated at the pipe wall

CHAPTER I

INTRODUCTION

In the design of experimental models to obtain mass transfer data, the use of a solid material which sublimes into an air stream has often been found convenient. The mass transfer rate in such a system is easily determined either by direct weight loss measurements or by determining thickness changes in the material, called "profilometric techniques." Of the subliming materials available for use in such models, naphthalene is by far the most often used (1,2,3,4,5). One of the major reasons for its widespread use is its rate of sublimation near room temperature, which is high enough to allow accurate determination of mass transfer rates but low enough that dimensions of the test piece are not significantly changed over normal testing periods. The rate of sublimation is also an important consideration in the design of mass transfer models to represent analogous heat transfer situations. The relatively low rate of sublimation of naphthalene allows its use in such cases without the analogy to heat transfer being lost. Other factors, such as cost, ease of machining and casting, and fairly well determined physical properties, also make it attractive for use in experimental studies.

The present study stems from mass transfer experiments involving naphthalene which were performed by Bosworth (6) in 1962. Bosworth measured mass transfer rates to laminarly flowing air in the entrance region of a 2 inch diameter, constant temperature, horizontal pipe.

The interior surface of the pipe was coated with naphthalene. The experiments covered the range 50° C to 60° C with Reynolds numbers between 500 and 2000. Using a profilometric technique based on the output of a strain gage attached to a tracer arm, the mass transfer rate was determined as a function of axial and angular position.

The results were compared to a theoretical solution obtained numerically in a manner similar to that presented by Kays (7) for laminar heat transfer in the entrance length of a tube with constant wall temperature. The velocity profiles of Langhaar (8) were used in an explicit difference scheme which advanced stepwise down the pipe. In the solution of the diffusion equation, the effect of the radial velocity term was neglected.

Near the entrance, Bosworth's experimental results were generally higher than the predicted values with deviations of up to 60 per cent. A sharp drop off in mass flux was also detected at certain axial locations and, once this occurred, subsequent fluxes were much less than theoretical and in some cases became negative. Local fluxes were also found to be strongly dependent on angular position with the bottom of the pipe showing higher fluxes.

The purpose of this study was to re-examine the system studied by Bosworth using a different measuring technique. Since free convection was considered to be a likely cause of the difference between theoretical and experimental results, it was decided to extend the experiments over a wider temperature range, and, in addition, study the effect of pipe inclination on the results. It was also deemed desirable to develop a concentration measuring technique to determine

concentration profiles in the air stream. It was felt that a knowledge of the profiles might aid in explaining some of the results obtained from the measured mass fluxes. To determine if the discrepancy between the theoretical and experimental results found by Bosworth (6) was caused by some characteristic peculiar to naphthalene, some experiments using another subliming solid, para-dichlorobenzene, were conducted.

Because considerably more computer capability had become available since the time of Bosworth's theoretical solution, it was decided to obtain a new theoretical solution which included the radial velocity terms. Before the new solution was obtained, two theoretical studies (9, 10) were completed which show that radial velocity terms do have a significant effect on entrance length heat transfer calculations.

It was hoped that through this study additional knowledge would be obtained which would allow more confident use of experimental mass transfer results obtained from subliming solid materials. It is necessary to develop this confidence by studying systems which are amenable to theoretical analysis before moving on to the more difficult (though industrially more important) problems for which theoretical solutions are not available.

CHAPTER II

MATHEMATICAL MODEL

The system under consideration consists of the interior of a cylindrical pipe of diameter D and length L. The interior surface of the pipe is made of a subliming solid material, A. A fluid, B, enters the pipe at z = 0 with uniform axial velocity $\bar{u}$ and zero radial velocity. As the fluid flows down the pipe, its velocity changes toward a more developed profile while simultaneously A diffuses into B.

The following assumptions concerning the above system are made:

(1) The flow is laminar and steady.

(2) The system consisting of the fluid and the solid surface is isothermal.

(3) The conditions are such that the ideal gas law applies.

(4) The concentration of A at the interior surface, C_{Aw}, is constant and equal to the concentration corresponding to saturation at the temperature of the system.

(5) The concentration of A in the fluid at z = 0, C_{Ao}, is uniform.

(6) The axial velocity, u, is zero at the solid surface.

(7) The fluid is Newtonian and of constant viscosity.

(8) The density, total molar concentration, and binary diffusivity of the system are constant.

(9) There are no body forces on the fluid and angular symmetry

is attained.

(10) Pressure is a function of axial position only.

(11) Momentum and mass transfer by diffusion in the z-direction are negligible.

(12) There is no significant change in the diameter of the pipe due to loss of material at the surface.

Under the above assumptions, the equation of motion in the z-direction is:

$$u \frac{\partial u}{\partial z} + v \frac{\partial u}{\partial r} = \frac{-1}{\rho} \frac{\partial p}{\partial z} + \upsilon \left[\frac{\partial^2 u}{\partial r^2} + \frac{1}{r} \frac{\partial u}{\partial r} \right] \qquad (2\text{-}1)$$

The equation of continuity is:

$$\frac{r \partial u}{\partial z} + \frac{\partial (vr)}{\partial r} = 0 \qquad (2\text{-}2)$$

The equation of continuity of material A is:

$$u \frac{\partial C_A}{\partial z} + v \frac{\partial C_A}{\partial r} = \mathcal{D}_{AB} \left[\frac{\partial^2 C_A}{\partial r^2} + \frac{1}{r} \frac{\partial C_A}{\partial r} \right] \qquad (2\text{-}3)$$

The following boundary conditions are applicable to equations (2-1), (2-2), and (2-3):

$$(1)\ u(r,0) = \bar{u} \qquad 0 \leqslant r < r_w$$

$$(2)\ v(r,0) = 0 \qquad 0 \leqslant r < r_w$$

$$(3)\ u(r_w,z) = 0 \qquad z > 0$$

$$(4)\ \frac{\partial u}{\partial r}(0,z) = 0 \qquad z > 0$$

$$(5)\ C_A(r,0) = C_{Ao} \qquad 0 \le r < r_w$$

$$(6)\ C_A(r_w,z) = C_{Aw} \qquad z > 0$$

$$(7)\ \frac{\partial C_A}{\partial r}(0,z) = 0 \qquad z > 0$$

Equations (2-1), (2-2), and (2-3) and their boundary conditions may be put in dimensionless form

$$U\frac{\partial U}{\partial Z} + V\frac{\partial U}{\partial R} = -\frac{\partial P}{\partial Z} + \left[\frac{\partial^2 U}{\partial R^2} + \frac{1}{R}\frac{\partial U}{\partial R}\right] \tag{2-4}$$

$$R\frac{\partial U}{\partial Z} + \frac{\partial (VR)}{\partial R} = 0 \tag{2-5}$$

$$V\frac{\partial C^*}{\partial R} + U\frac{\partial C^*}{\partial Z} = \frac{1}{Sc}\left[\frac{\partial^2 C^*}{\partial R^2} + \frac{1}{R}\frac{\partial C^*}{\partial R}\right] \tag{2-6}$$

(BC 1) $U(R,0) = 1 \qquad 0 \le R < 1$

(BC 2) $V(R,0) = 0 \qquad 0 \le R < 1$

(BC 3) $U(1,Z) = 0 \qquad Z > 0$

(BC 4) $\frac{\partial U}{\partial R}(0,Z) = 0 \qquad Z > 0$

(BC 5) $C^*(R,0) = 0 \qquad 0 \le R < 1$

$$(BC\ 6)\quad C^{*}(1,Z) = 1 \qquad Z > 0$$

$$(BC\ 7)\quad \frac{\partial C^{*}}{\partial R}(0,Z) = 0 \qquad Z > 0$$

Definitions of variables used in converting equations (2-1), (2-2), and (2-3) to (2-4), (2-5), and (2-6), respectively, are:

$$U = \frac{u}{\bar{u}} \tag{2-7}$$

$$V = \frac{r_w v}{\nu} \tag{2-8}$$

$$R = \frac{r}{r_w} \tag{2-9}$$

$$Z = \frac{\nu z}{r_w^2 \bar{u}} \tag{2-10}$$

$$P = \frac{p}{\rho \bar{u}^2} \tag{2-11}$$

$$C^{*} = \frac{C_A - C_{Ao}}{C_{Aw} - C_{Ao}} \tag{2-12}$$

$$Sc = \frac{\nu}{\mathcal{D}_{AB}} \tag{2-13}$$

Due to the assumptions concerning constant physical properties, equations (2-4), and (2-5) are almost independent of equation (2-6). However, a connection between the equations exists because the dimensionless radial velocity at the wall $V_w(Z)$ is related to the molar

wall flux N_{Aw} by

$$V_w(Z) = \frac{M_A r_w N_{Aw}}{\rho \nu} \tag{2-14}$$

and N_{Aw} is dependent upon the concentration gradient at the wall, which is determined by equation (2-6).

Assuming the solubility of B in solid A is negligible, $X_A \ll 1$, and constant molar density, Fick's first law of diffusion can be used to obtain an expression for the molar flux of A at the wall

$$N_{Aw} = \frac{-\mathcal{D}_{AB}(C_{Aw} - C_{Ao})}{r_w} \left.\frac{\partial C^*}{\partial R}\right|_{R = 1,Z} \tag{2-15}$$

A numerical solution to equations (2-4), (2-5), and (2-6) using the appropriate boundary conditions and equations (2-14) and (2-15) was obtained using finite difference techniques. A detailed discussion of the methods used in obtaining the solution is presented in Appendix A. In general, the method consisted of a marching procedure in which the solution was advanced stepwise down the pipe. At each new step, an initial value for $V_w(Z)$ was assumed and difference representations of equations (2-4) and (2-5) were solved for U and V as functions of radial position. These values were then used in a difference representation of equation (2-6) to solve for C^* at each radial position. From the known values of C^*, the concentration gradient at the pipe wall was evaluated and equation (2-15) was solved for N_{Aw}. This was then used in equation (2-14) to calculate a new value for $V_w(Z)$. The procedure was repeated until successive values of $V_w(Z)$ varied by less than 2 per cent.

The local mass transfer coefficient, $k_{x,loc}$ is defined by

$$k_{x,loc} = \frac{N_{Aw} - X_{Aw}(N_{Aw} + N_{Bw})}{X_{Aw} - X_{Ab}} \tag{2-16}$$

Assuming $X_{Aw} \ll 1$ and N_{Bw} is zero (B not soluble in A), equations (2-16) and (2-15) may be combined to give

$$k_{x,loc} = \frac{-\mathcal{D}_{AB}(C_{Aw} - C_{Ao})}{r_w (X_{Aw} - X_{Ab})} \frac{\partial C^*}{\partial R} \Bigg|_{R = 1,Z} \tag{2-17}$$

X_{Ab} is the bulk or cup-mixing mole fraction of A in the mixture of A and B. Since $C_A = C\, X_A$, equation (2-17) can be written

$$k_{x,loc} = \frac{-\mathcal{D}_{AB} C(C_{Aw} - C_{Ao})}{R_w (C_{Aw} - C_{Ab})} \frac{\partial C^*}{\partial R} \Bigg|_{R = 1,Z} \tag{2-18}$$

or

$$k_{x,loc} = \frac{-\mathcal{D}_{AB} C}{r_w (1 - C_b^*)} \frac{\partial C^*}{\partial R} \Bigg|_{R = 1,Z} \tag{2-19}$$

In equation (2-19), C_b^* is the dimensionless bulk concentration defined as

$$C_b^* = \frac{C_{Ab} - C_{Ao}}{C_{Aw} - C_{Ao}} = \frac{\int_0^{2\pi} \int_0^1 U(R,Z) C^*(R,Z) R\, dR\, d\theta}{\int_0^{2\pi} \int_0^1 U(R,Z) R\, dR\, d\theta} \tag{2-20}$$

The local Nusselt number for mass transfer $(Nu_{AB})_{loc}$ is defined as

$$(Nu_{AB})_{loc} = \frac{k_{x,loc} D}{C \mathcal{D}_{AB}} \tag{2-21}$$

Substituting equation (2-19) into (2-21), and noting that D = $2r_w$, the local Nusselt number can be expressed in terms of dimensionless quantities as

$$(Nu_{AB})_{loc} = \frac{-2 \left(\frac{\partial C^*}{\partial R}\right)\Big|_{R = 1,Z}}{1 - C_b^*} \tag{2-22}$$

The logarithmic mean Nusselt number for mass transfer for a tube of length L is

$$(Nu_{AB})_{lm} = \frac{1}{L} \int_o^L (Nu_{AB})_{loc} \, dz \tag{2-23}$$

The average mass transfer coefficient $k_{x,m}$ obtained from

$$k_{x,m} = \frac{(Nu_{AB})_{lm} C \mathcal{D}_{AB}}{D} \tag{2-24}$$

can be used to evaluate the total molar mass transfer rate from a cylindrical tube of length L by the equation

$$\omega_A = k_{x,m} (\pi DL)(\Delta X_A)_{lm} \tag{2-25}$$

where $(\Delta X_A)_{lm}$ is the logarithmic mean driving force for diffusion, defined by

$$(\Delta X_A)_{lm} = \frac{(X_{Aw} - X_{Ao})\Big|_{z=0} - (X_{Aw} - X_{Ab})\Big|_{z=L}}{\ln \dfrac{(X_{Aw} - X_{Ao})\Big|_{z=0}}{(X_{Aw} - X_{Ab})\Big|_{z=L}}} \quad (2\text{-}26)$$

For use in the correlation of the experimental results, a theoretical Grashof number for mass transfer was calculated. The Grashof number for mass transfer, based on tube diameter, is defined (11) as

$$Gr_{AB} = \rho^2 \zeta g D^3 (\Delta X_A) / \mu^2 \quad (2\text{-}27)$$

where the concentration coefficient of volumetric expansion ζ is

$$\zeta = -\frac{1}{\rho}\left(\frac{\partial \rho}{\partial X_A}\right)_T \quad (2\text{-}28)$$

Assuming constant total molar concentration, the Grashof number based on the logarithmic mean concentration difference may be represented by

$$Gr_{AB} = \rho g D^3 (M_A - M_B) (\Delta C_A)_{lm} / \mu^2 \quad (2\text{-}29)$$

where $(\Delta C_A)_{lm}$ is defined analogously to $(\Delta X_A)_{lm}$ in equation (2-26).

CHAPTER III

EXPERIMENTAL EQUIPMENT AND INSTRUMENTATION

The experimental equipment used in conducting the mass transfer runs is first described. During several of the mass transfer runs, concentration profiles within the pipe were also determined. The equipment used to measure concentrations is discussed in the second section of this chapter.

Mass Transfer System

General

The mass transfer system consisted of a test pipe coated on the inside with a subliming material, an air supply system which delivered a measured quantity of dry air at a constant rate, an inlet plenum chamber to give the desired velocity profile at the pipe inlet, and a heating system to maintain the air and test pipe at a constant temperature. The subliming material used was either naphthalene or p-dichlorobenzene. A schematic diagram of the mass transfer system is shown in Figure 1.

Test Pipe

The test pipe was an assembly of small sections made from standard 2 inch brass pipe. The test sections were threaded on each end and assembled as shown in Figure 2. When assembled, the test pipe was 81-1/4 inches in length and consisted of fourteen 2-inch long sections, six 9-1/8 inch long sections and one 6-1/2 inch long section. The order of

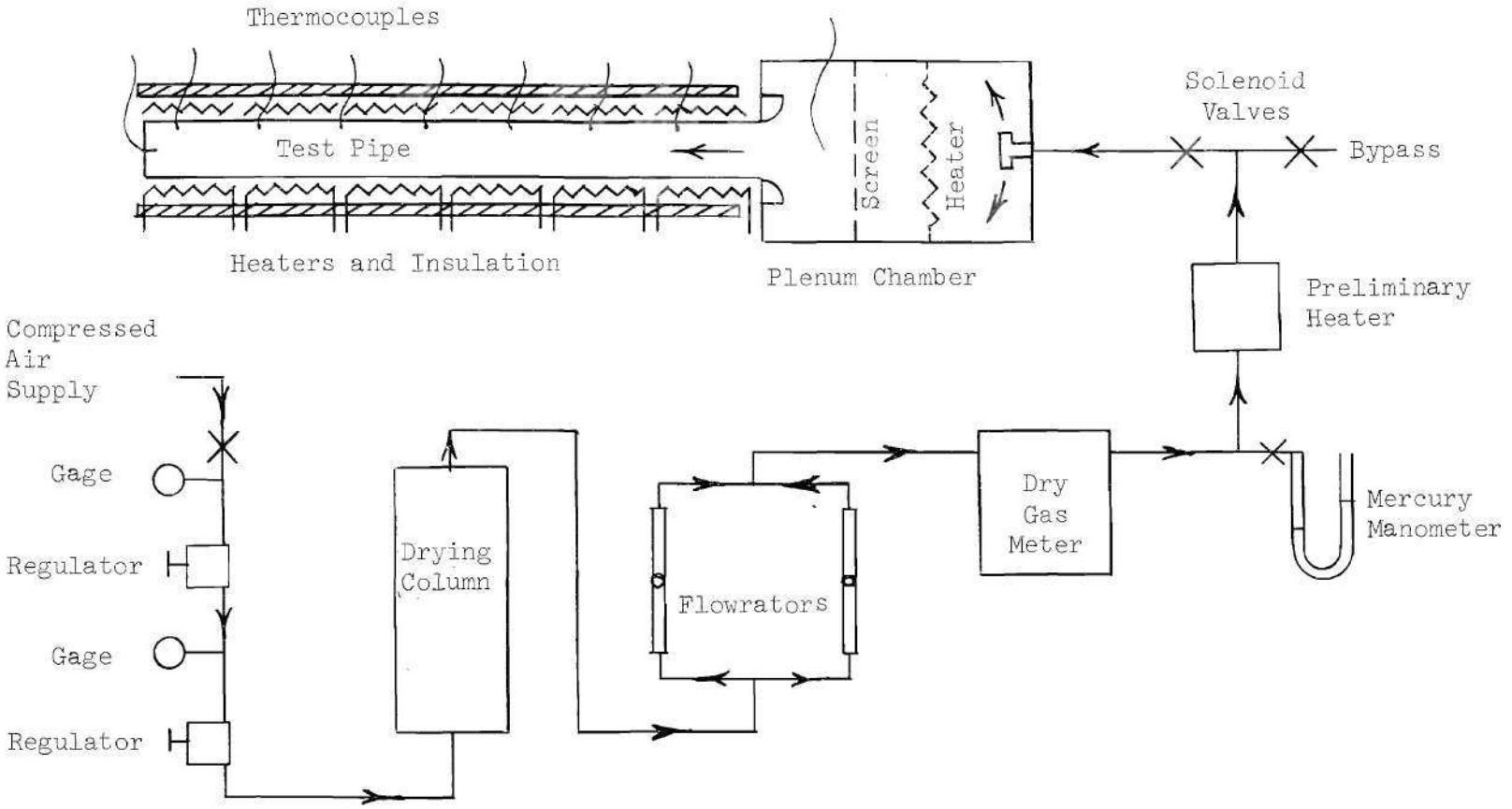

Figure 1. Schematic Diagram of the Mass Transfer System

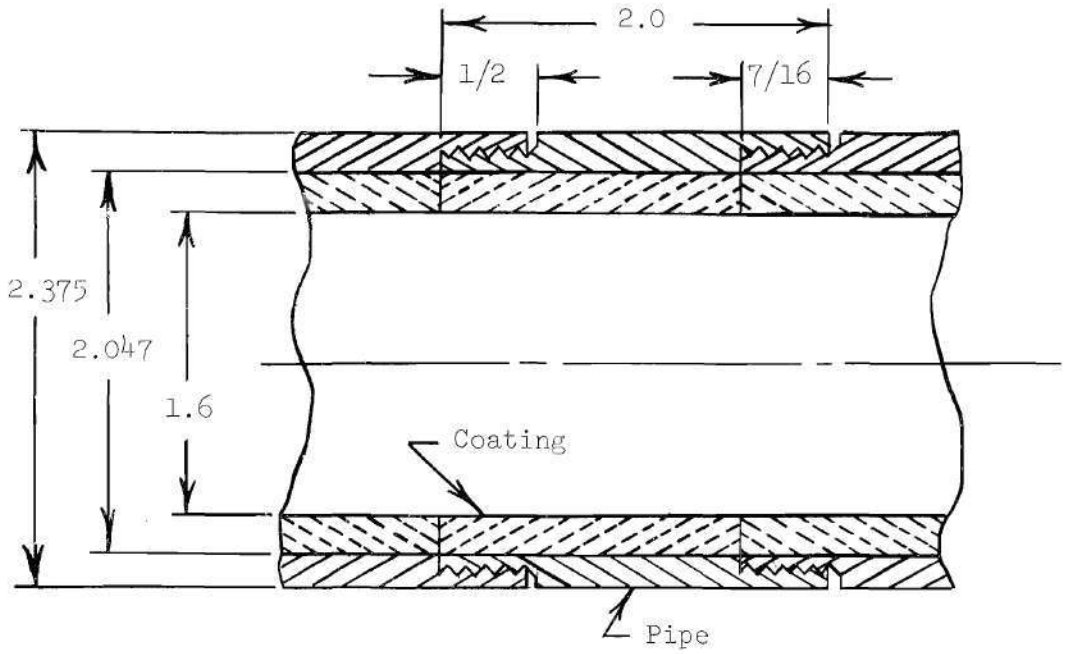

Figure 2. Typical Test Section Assembly

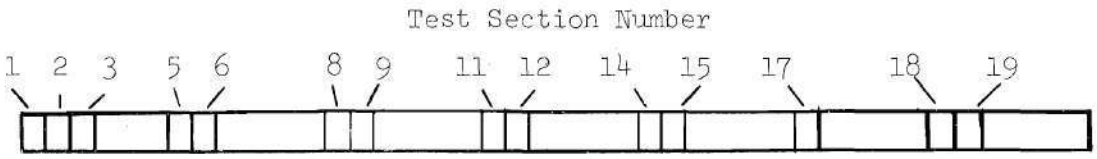

Figure 3. Arrangement of Test Sections

arrangement of these sections in the test pipe is shown in Figure 3.

The first section in the pipe was machined to an inside diameter of 2.063 inches for a depth of 0.375 inches to allow for a slip fit over the exit section of the plenum chamber. A 0.063 inch diameter hole was drilled through the wall near the center of each of the larger sections to allow for insertion of thermocouples or of a gas sampling probe. A coating of naphthalene or p-dichlorobenzene was applied to the interior of each section by a casting procedure. The inside diameter of the cast coating was initially 1.59 inches. When assembled, the pipe presented a smooth coating of solid material over its entire interior surface.

A supporting frame was constructed of 1-1/2 x 1-1/2 in. slotted angle iron to accommodate the test pipe and the inlet plenum chamber. The frame was designed such that the axis of the test pipe could be maintained horizontal, vertical or 45° from the horizontal. For the 45° position, a second supporting structure made from 2 x 4 inch lumber was also used.

Figures 4, 5, and 6 show the test pipe and its supporting structure in the three positions mentioned above.

Air Supply System

Air used in all tests was obtained from a compressed air source located in the Chemical Engineering Building. The air was first passed through two Model 17, Rockwell Manufacturing Company pressure regulators connected in series. The regulators were manually adjusted to give the desired flow rate. The air then passed through a packed column 4-1/2 inches in diameter and 16 inches deep containing 1/8 inch pellets of

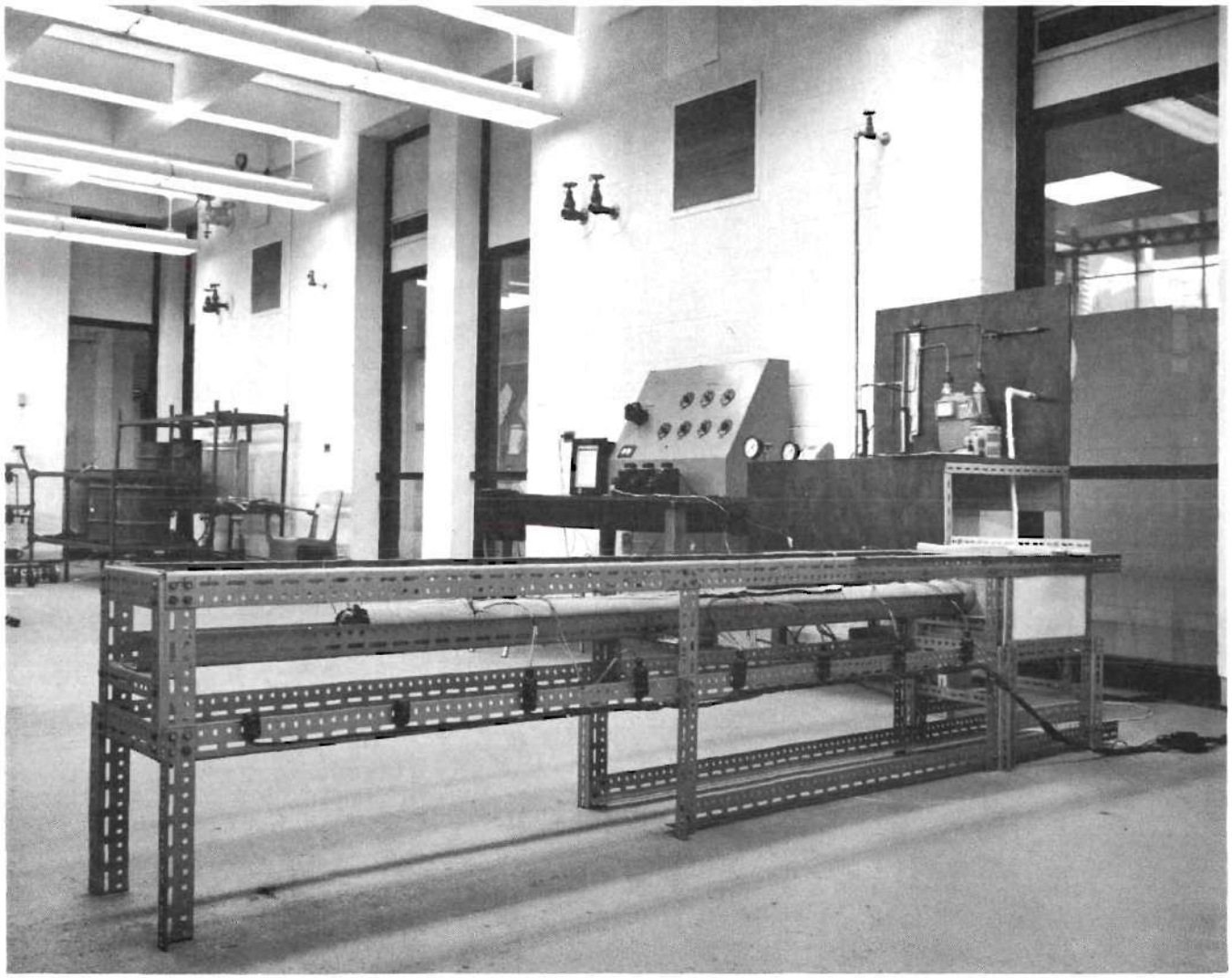

Figure 4. Test Pipe in Horizontal Position.

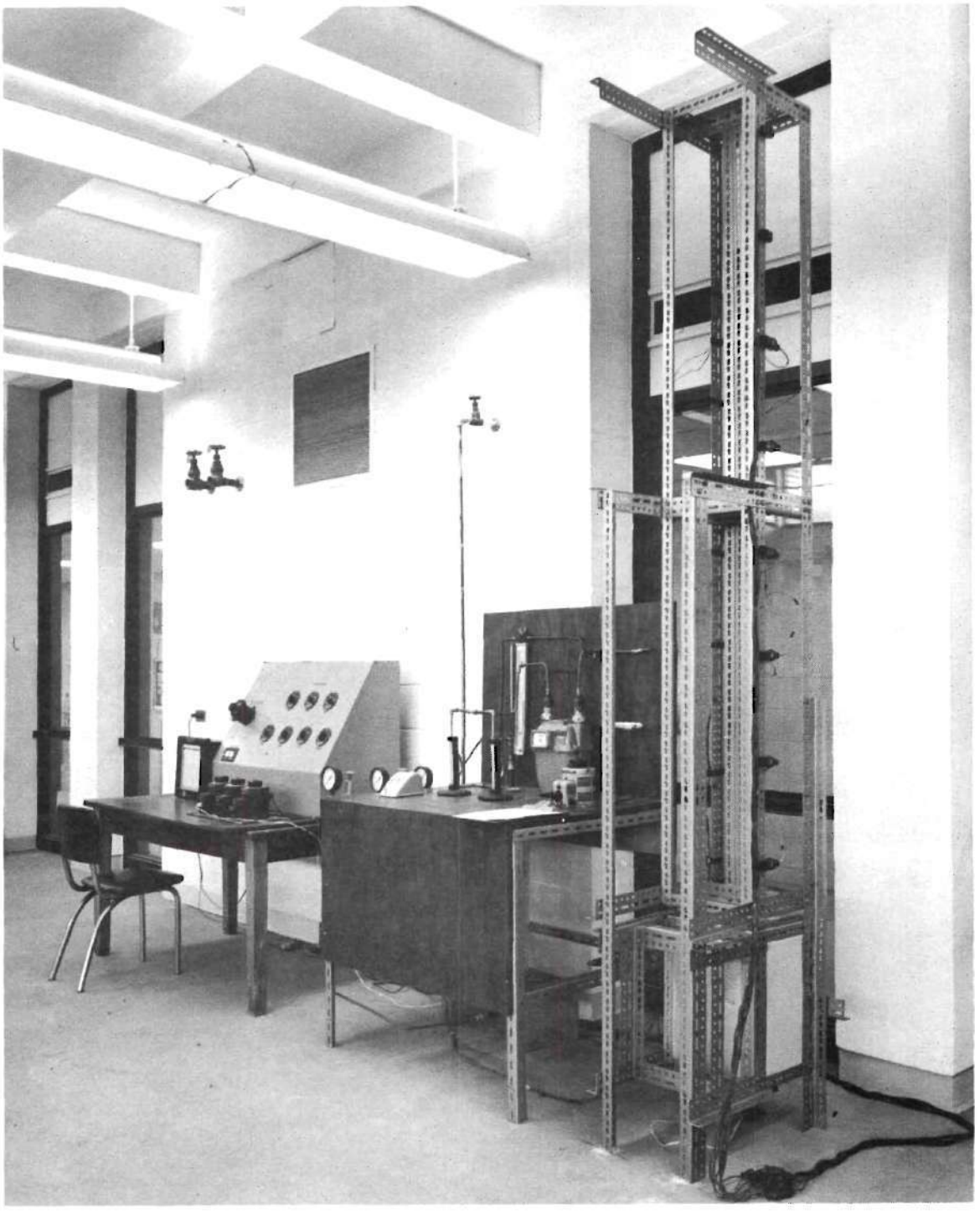

Figure 5. Test Pipe in Vertical Position.

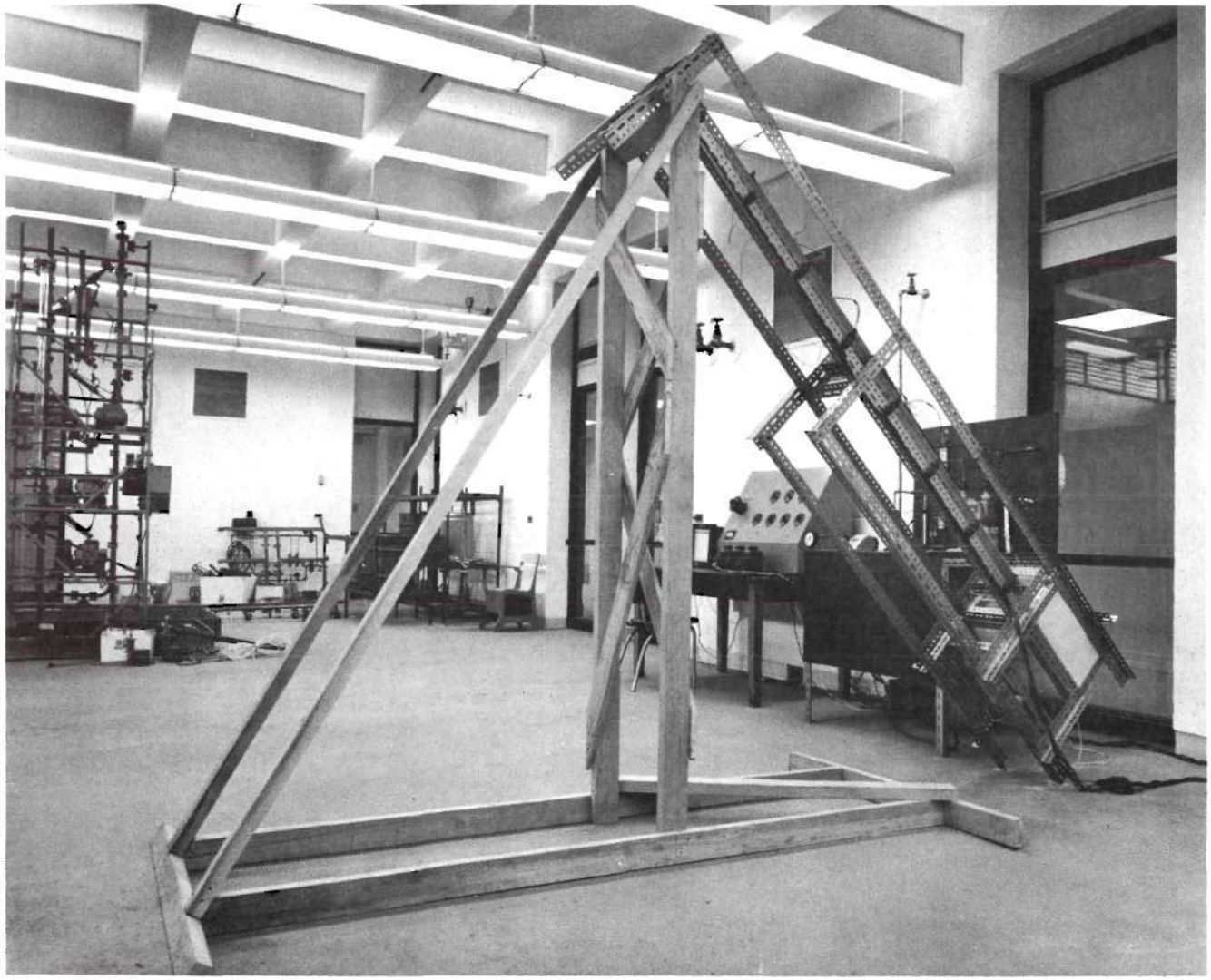

Figure 6. Test Pipe at 45° Inclination.

Linde Type 5A Molecular Sieve material. The packed column served to dry the air and also remove any entrapped oil.

The air next passed through two Fisher and Porter flowrators connected in parallel. Each flowrator had a capacity of 1.3 SCFM at 1 atmosphere and 70° F. The flowrators were used primarily as an aid in adjusting the air flow rate.

The air flow was measured by means of a Rockwell Model S dry gas meter having a capacity of 150 cubic feet per hour. Pressure of the air passing through the meter was measured with a mercury filled U-tube manometer. From the dry gas meter, the air passed into a preliminary heater.

The preliminary heater consisted of a coil of approximately 20 feet of 3/8 inch O.D. copper tubing wrapped with a layer of electrical heating tape and two layers of asbestos tape insulation. A 115 volt variable transformer was used to supply power to the preliminary heater.

The air then passed through one of two ASCO Model 82653R solenoid valves. The valves were arranged so that one acted as a by-pass and directed the air out of the test system while the other allowed the air to pass into the inlet plenum chamber. The solenoid valves were connected to a power source through separate switches so that each could be operated independently.

The air supply system downstream of the pressure regulators was made using 3/8 inch O.D. copper tubing with flared or compression type brass fittings. The system was tested for leaks by applying a soap solution around each joint.

Inlet Plenum Chamber

The inlet plenum chamber consisted of an airtight insulated box, 10 x 10 x 16 in., made from 1/8 inch aluminum plate. At one end of the chamber, incoming air passed through a 3/8 inch O.D. brass fitting and was deflected 90° by use of a tee. As the air flowed through the chamber, it was caused to pass in series through a layer of electrical heating tape and a section of 16 mesh aluminum wire screen. These were supported by a metal frame across the entire cross-section of the chamber. The tape was connected to a variable transformer and was used as a final air heater. The purpose of the screen was to insure mixing of the heated air and provide more constant velocity across the chamber.

The outlet section of the chamber was provided with a bell-shaped opening having a throat of 1.875 in. diameter with the flared section having a one inch radius of curvature. This was similar in design to the opening used by Bosworth (6) and its purpose was to give as flat a velocity profile as possible at the pipe entrance.

A copper-constantan thermocouple was suspended in the center of the chamber approximately two inches away from the bell-shaped opening. It was used to determine the temperature of the inlet air to the pipe.

All joints in the chamber, and the holes through the chamber walls which were necessary for electrical connections, were sealed with epoxy cement. The top of the chamber was removable and was held in place by a flanged connection using a one inch wide rubber gasket. The chamber was insulated on all sides using one inch thick polyurethane foam insulation attached to the outside.

The outlet side of the plenum chamber was made to slip inside the first section of the test pipe to a depth of three-eighths of an inch.

During preliminary tests, no leakage could be found at this joint. Since the inside diameters of the throat of the bell-shaped opening and the coated test pipe were not equal, several brass inserts were made which could be slipped into the throat and thus give a smaller diameter. These inserts had inside diameters of 1.60, 1.65, 1.70, and 1.75 inches, respectively, and, during testing, the one which more closely matched the inside diameter of the first section of the test pipe was used.

Heating System

The test pipe was maintained at the desired operating temperature by the use of six heaters made from one inch wide electrical heating tape. Each heater was approximately 13 inches long and 9 inches wide and encased in a bag made of heavy cotton duck which provided electrical insulation between the pipe and the heater.

The voltage to each heater could be controlled independently by the use of six small variacs connected to a larger variac as a common source. The larger variac was used to reduce the line voltage to about 40 volts. Since the voltage requirement for each heater was about 15 volts, the smaller variacs could be operated near the midpoint of the full range and finer voltage adjustments were possible.

During operation, each heater was wrapped completely around the pipe and the pipe was covered over its entire length. The heaters were held in place against the pipe by wrapping over them a piece of one inch thick fiberglass insulation. The insulation was encased in four fabric bags having one inch wide Velcro seams sewed to the edges running lengthwise. The use of this type insulation enabled the test

pipe to be mounted in place or disconnected quickly and easily and also provided convenient passage for thermocouples through the insulation.

Temperature Measurements

In addition to the thermocouple located in the plenum chamber, seven thermocouples were inserted through the pipe wall approximately equidistant down the length of the pipe and one was inserted approximately four inches from the exit of the test pipe. All thermocouples used were 24 gage copper-constantan wrapped in thermoplastic insulation.

The thermocouples spaced along the length of the test pipe were inserted through 1/16 inch holes drilled through the large test sections. They were placed as closely as possible to the solid-air interface by sighting down the test pipe.

A sealing arrangement was made to prevent air leakage through the thermocouple ports and yet provide for convenient assembly and disassembly. This arrangement consisted of passing each thermocouple through a 3/16 inch diameter by 1/8 inch disc of rubber septum material and then inserting the disc in a 3/16 inch diameter hole drilled out through most of the pipe wall above the thermocouple port.

The exit thermocouple was used to measure the exit air temperature and was placed near the axis of the pipe. All thermocouples were referenced to an ice-water bath and were connected by means of an 11 channel thermocouple switch to a 0 to 5 millivolt Leeds and Northrup Speedomax H recorder. Using this arrangement, thermocouple readings could be taken very quickly and it was possible to see at a glance if any of the thermocouples deviated from the desired temperature reading.

Figure 7 shows the test pipe mounted in the frame with the

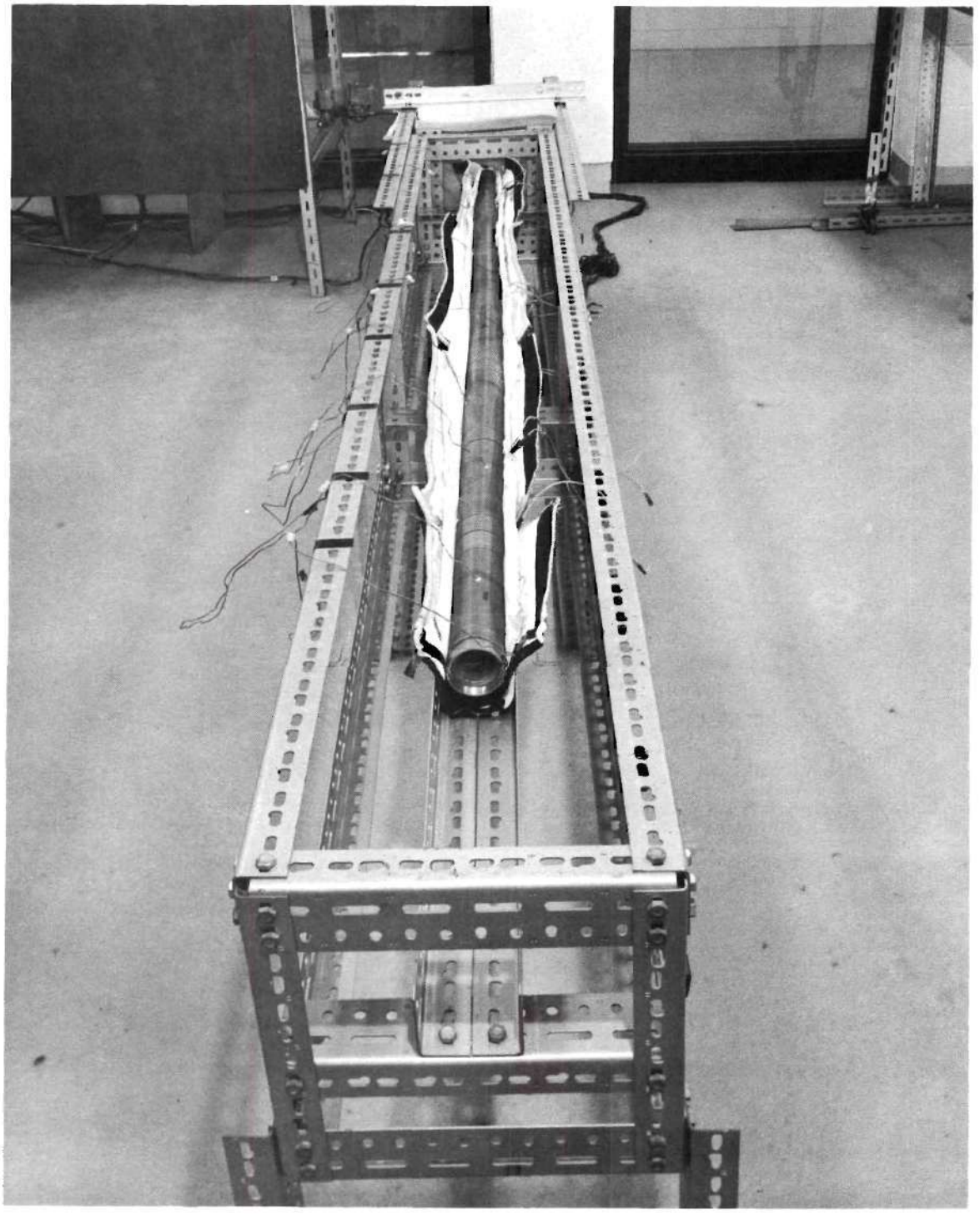

Figure 7. Test Pipe and Thermocouples with Insulation Open.

thermocouples in place and the insulation open.

Concentration Measuring System

General

The concentration measuring system was used to determine concentration profiles within the test pipe. A sampling system consisting of a heated hypodermic syringe and spacers was used to withdraw gas samples at known locations in the pipe. A detection system employing a gas chromatograph and associated equipment was used to analyze the samples.

Sampling System

Gas samples were taken in a 1 cc glass syringe equipped with a 2 inch long, 25 gauge stainless steel needle. Since preliminary investigations indicated that reproducible results could not be obtained unless the syringe was heated above about 175° C, a heating unit for the syringe was constructed. This unit consisted of a 4-1/4 inch section of 1/2 inch brass pipe wrapped with electrical heating tape and asbestos insulation. A variable transformer was used to supply electrical power to the heater. The pipe was large enough to allow the syringe and an iron-constantan thermocouple, used to measure temperature, to be inserted into it.

Gas samples were obtained by inserting the needle through rubber septums fitted in holes drilled in the test pipe. Spacers placed between the pipe wall and the top shoulder of the needle were used to control the depth of insertion. The spacers were 1/2 inch diameter stainless steel discs with 1/16 inch diameter holes drilled through the centers. They were machined to thicknesses of 0.063, 0.125, 0.250, 0.500 and 1.000 inches. Other thicknesses were obtained by stacking two or

more of the spacers. The needle was inserted through the 1/16 inch diameter holes in the spacers and then into the rubber septum.

It was found that a 0.750 inch spacer located the end of the sampling needle exactly on the pipe centerline. Thus, by knowing the amount of spacer used to obtain a particular sample, the location of the tip of the needle from the pipe centerline could be easily calculated.

Detection System

The gas samples were analyzed for naphthalene content using a Perkin-Elmer Model 810 gas chromatograph. This unit is equipped with dual columns and a flame ionization detector system. A Sargent Model SR recorder with a 0 to 1 millivolt range was used to record the output signal from the chromatograph. High purity hydrogen and air were used to maintain the flame in the detector system. Nitrogen was used as the carrier gas.

Preliminary tests on naphthalene-air mixtures using packed columns coated with SE-30 silicone gum rubber and with carbowax showed an excessive amount of "tailing" of the naphthalene peak. This made determination of the area under the peak, which is proportional to the amount of naphthalene injected, quite difficult. Also, determining the amount of sample injected using the heated syringe presented problems. For these reasons, the use of columns containing a stationary liquid phase was abandoned and columns packed with fine glass beads were installed. These columns were 3 foot long sections of 1/8 inch diameter copper tubing. Calibration tests showed that this arrangement gave peaks whose height was proportional to naphthalene concentration

over the range of interest. The height of these peaks was also insensitive, over a wide range, to the amount of gas injected.

The columns were operated at 200° C with the injector at about 300° C. The flow rates used were approximately those recommended by the manufacturer. These were set using pressure regulators attached to the gas cylinders. As the flow rates probably varied from day to day, a new calibration was made for each run.

CHAPTER IV

EXPERIMENTAL PROCEDURE

In this chapter the experimental procedures used in conducting the mass transfer runs are presented. During several of these runs, concentration profiles within the pipe were measured. The procedures used in obtaining the concentration profiles are also discussed.

Mass Transfer Procedures

General

The experimental procedures used were essentially the same for all pipe inclinations. The procedure for a typical run consisted of the following steps:

(1) Casting a coating of the solid subliming material inside each section of the test pipe.

(2) Determining the physical dimensions of the system necessary for reduction of the test data.

(3) Initial weighing of the smaller test sections.

(4) Conducting a warm-up period to bring the system to operating temperature.

(5) Conducting the test run by passing air at a known flow rate through the test pipe for a measured period of time while maintaining all temperatures at a constant predetermined value.

(6) Reweighing the smaller test sections at the end of the run.

(7) Determining a correction term to be applied to account for

mass transfer losses not associated with the actual runs.

(8) Reduction of the test data.

While not every step above was taken for every run, this was the general procedure followed. A detailed description of each step is given in the following sections.

Casting Method

All test sections were initially washed with soap and water, rinsed with methyl-ethyl ketone and dried. A mold, shown in Figures 8 and 9, consisting of a base and a constant diameter center piece was manufactured from brass rod stock. The test section to be coated was screwed onto the base of the mold and the center piece was inserted through the test section and also screwed into the base. The material to be cast was melted and poured into the annular space formed between the center piece and the walls of the test section.

Best results were obtained if the molten material was heated to just under its boiling point. Due to shrinkage on solidification, several pourings were necessary to fill the annular space and build up a layer of solid material slightly above the top edge of the test section. After disassembly of the mold, all excess solid material was trimmed away and the top edge of the solid was cut down even with the top edge of the test section. Two different center pieces, both of 1.590 inch diameter, were used. One was longer than the other and was used to cast the long test sections.

It was found that a small amount of mold release agent on the center piece prevented chipping or scratching of the solid surface on disassembly. A light coating of Dow Corning High Vacuum Grease was

Figure 8. Disassembled Mold and Test Section.

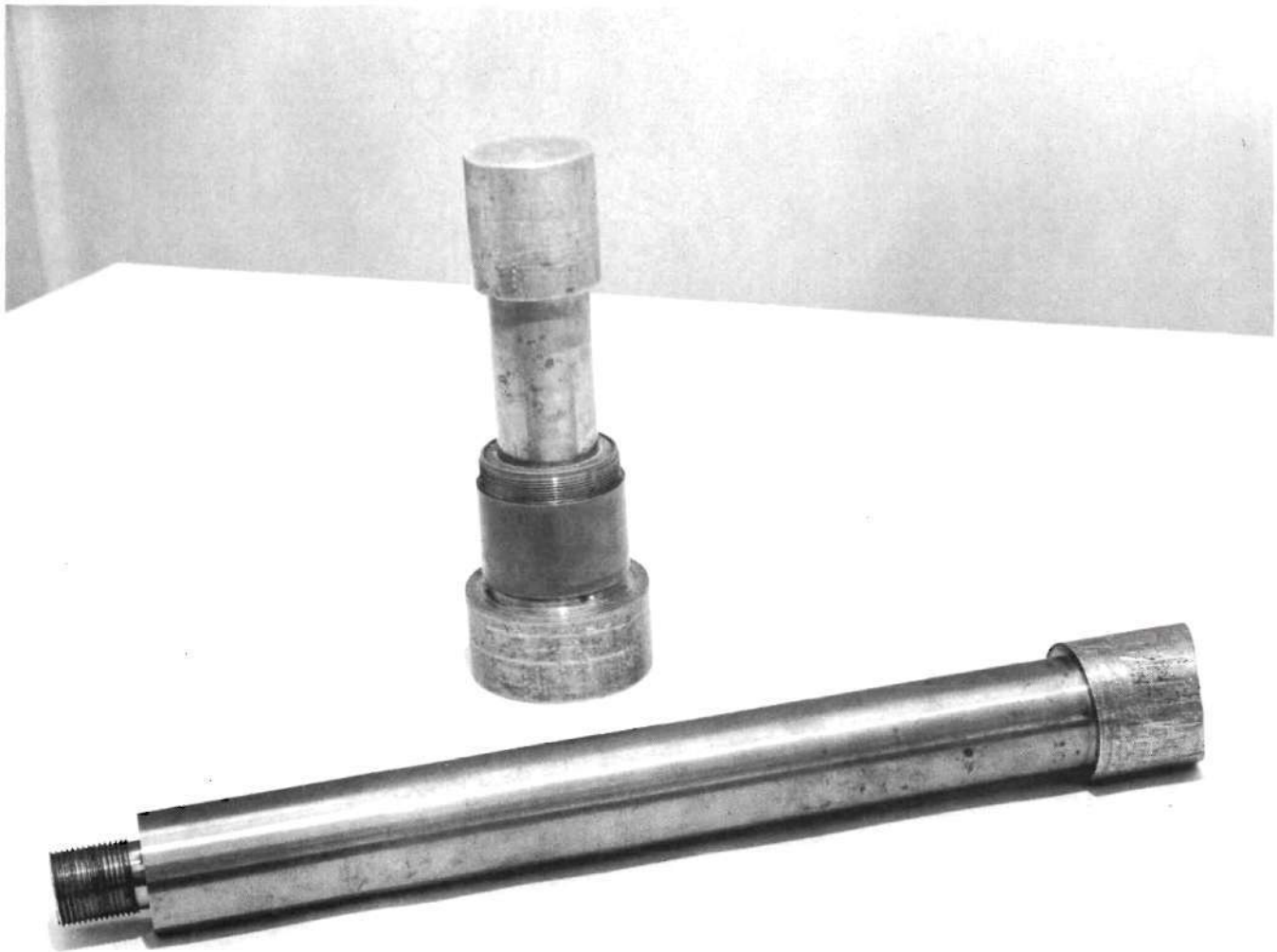

Figure 9. Assembled Mold with Long Center Piece in Foreground.

applied to the center piece of the mold and then the surface was wiped repeatedly with clean paper towels until all visible traces disappeared. Christian and Kezios (12) used this procedure to cast naphthalene test pieces in a mass transfer study and found no measurable effect of the release agent on the sublimation rate in either free or forced convection.

After all test sections were cast and their exterior surfaces cleaned of any excess solid material, they were assembled to form the test pipe. During storage, the ends of the test pipe were wrapped with aluminum foil to prevent evaporation losses.

Casting of new test sections was not done for every run but only when the inside diameters of the entrance and exit sections became significantly different or when it was desired to change to a new test material.

Dimensions of the System

The following dimensions of the system were determined:

(1) The length of the coated interior surface of each small test section.

(2) The distance from the beginning of the coating to the midpoint of the coated surface for each small test section when the test pipe was assembled.

(3) The inside diameters of test section number 3, located near the entrance of the test pipe, and test section number 19, located near the exit.

The measurements described in (1) and (2) above were made at the beginning of the test series. Since the pipe was always assembled in

the same order, these values were assumed to be constant throughout the test series. Results of these measurements are presented in Table 1. Measurements described in (3) above were made at the beginning and end of each test run.

Table 1. Dimensions of Test Sections

Test Section Number	Length of Test Section, centimeters	Distance from Beginning of Coating to Midpoint of Test Section, inches
2	4.0	1.97
3	4.1	3.59
5	3.7	11.31
6	4.3	12.88
8	3.9	23.34
9	4.0	24.91
11	4.0	35.35
12	4.0	36.88
14	4.1	47.28
15	4.0	48.94
17	4.1	59.28
18	4.3	69.72
19	4.1	71.41

Weighing of the Test Sections

All small test sections with the exception of the first section of the test pipe were weighed prior to conducting a test run. The first section was not weighed because it was found that during a run some of the solid coating was transferred from this section to the edge of the connecting piece on the inlet plenum chamber. Weighings were made on an analytical balance to the nearest one thousandth of a gram. The approximate weight of a test section was 275 grams.

A weighing routine was developed in which each test section was

disassembled from the pipe, weighed, and reassembled before another section was disassembled. This routine was designed to minimize exposure of the sections to the ambient air.

A similar weighing procedure was used at the end of each test run. After each weighing a sheet of aluminum foil was wrapped around each end of the test pipe.

Warm-up Procedure

After weighing, the test pipe was placed in the mounting frame, the thermocouples were inserted and the pipe was wrapped with the heaters and then the fiberglass insulation. The ends of the test pipe remained covered with aluminum foil. Electric power to the heaters was turned on and adjustments were made to the individual heater power supplies to eliminate any temperature gradients along the length of the pipe as the temperature was increased.

While the pipe was heating up, the air supply was turned on and the air flow rate was adjusted using the pressure regulators to give the desired reading on the flowrators. The air flow was directed through the inlet plenum chamber by the solenoid valves and the preliminary and final air heaters were turned on and adjusted to bring the air to the desired operating temperature. During this period the air flowed through the plenum chamber and out into the room since the chamber was not connected to the test pipe.

The warm-up period lasted approximately one hour. During this time, thermocouple readings and heater adjustments were made every five to ten minutes. For all test runs, the warm-up period was conducted with test pipe in the horizontal position.

Test Run Procedure

When the desired test temperature was attained, the following procedure was employed to begin a test run:

(1) The air flow was diverted through the by-pass solenoid valve.

(2) The aluminum foil was removed from the ends of the test pipe and the pipe was connected to the inlet plenum chamber. The exit thermocouple was then inserted into position on the pipe axis, about four inches inside the last section.

(3) The test pipe was placed in the desired position.

(4) The air flow was directed through the inlet plenum chamber and down the pipe using the solenoid valves. Simultaneously, an electric timer used to time the run was started. The initial reading of the dry gas meter was recorded.

The above steps took from three to four minutes to accomplish. During the first hour of a run, thermocouple readings were taken every three to five minutes and the power to the heaters was adjusted to balance all temperatures. After about thirty minutes, a steady state was attained and only minor adjustments to the power to the heaters was required.

In addition to the thermocouple readings, the following data were recorded every 1000 seconds (16.67 minutes) during a test run:

(1) The dry gas meter reading.

(2) The flowrator readings.

(3) The pressure difference between the outlet of the dry gas meter and the atmosphere.

(4) The room temperature of the laboratory.

The difference between dry gas meter readings was calculated for the 1,000 second intervals, and when necessary, adjustments were made in the air flow rate to keep this value constant. A barometer reading was taken at the end of the test period. The test period lasted approximately two hours for the para-dichlorobenzene runs and three to five hours for the naphthalene runs.

At the end of the test period, the air was diverted through the by-pass valve, power to the heaters was shut off and the test assembly was disassembled as quickly as possible. Aluminum foil covers were placed over the ends of the test pipe. The shut-down procedure took about three minutes to accomplish.

The test pipe was then allowed to cool approximately thirty minutes to room temperature and the small test sections were reweighed. After reweighing, the inside diameters of sections number 3 and number 19 were remeasured.

Weight Loss Correction Term

A correction term was applied to the weight loss measurements made on each test section. The correction term was found to be dependent on the test material and on the temperature of the run. Weight loss correction terms were measured for naphthalene for the three test temperatures used and for para-dichlorobenzene for the one test temperature used.

The method used to evaluate the correction term consisted of the following steps:

(1) Weighing the small test specimens using the normal weighing routine.

(2) Heating the test pipe to the desired temperature exactly as described in the warm-up procedure above.

(3) Connecting the pipe to the air supply system but not turning on the air supply.

(4) Disconnecting the pipe and reweighing the small sections after a cool down period exactly as described in the preceding section.

The weight loss obtained is the proper correction term to be subtracted from the total weight loss for runs of the corresponding material and temperature. In most cases, it was found that the weight loss correction varied only slightly from one test section to another for the same test. Consequently, an average correction term was determined by averaging the individual terms for each test section obtained for one particular set of conditions. This average correction term was then applied to every section for each test run at the specified conditions.

The average correction terms determined by the above described procedure are presented in Table 2.

Table 2. Average Weight Loss Correction Terms

Material	Temperature	Correction Term
Naphthalene	30.9°C	0.006 gms.
Naphthalene	38.2°C	0.007 gms.
Naphthalene	50.0°C	0.008 gms.
Para-dichlorobenzene	30.9°C	0.022 gms.

The individual values for the correction terms are given in Table 19, Appendix C.

Concentration Measuring Procedures

Concentration measurements were taken on six of the naphthalene runs. All concentration profiles were measured at an axial position 64.32 inches from the pipe entrance. For the horizontal and 45° angle pipe positions, the profiles were measured along a line running from the top to the bottom of the pipe and perpendicular to the direction of flow.

During a warm-up period before sampling, the chromatograph was turned on and brought up to operating temperature and the sampling syringe was placed in the heater and heated to $180^{\circ}C$. To obtain a sample, the syringe was removed from the heater and the desired spacers were placed on the needle. The insulation was then peeled back around the sampling port and the needle inserted as shown in Figure 10. A gas sample of approximately 1 cc was slowly withdrawn. The insulation was replaced and the sample injected into the chromatograph. A peak was produced on the recorder approximately 5 seconds after the injection. The syringe was then replaced in the heater and 4 to 5 minutes were allowed for reheating before another sample was taken. The time required to take a sample was approximately one minute.

The centerline concentration was measured first and then concentrations were measured at specified intervals, alternately on each side of the centerline, toward the wall. Usually two samples were taken from each location; however, if agreement between these samples was con-

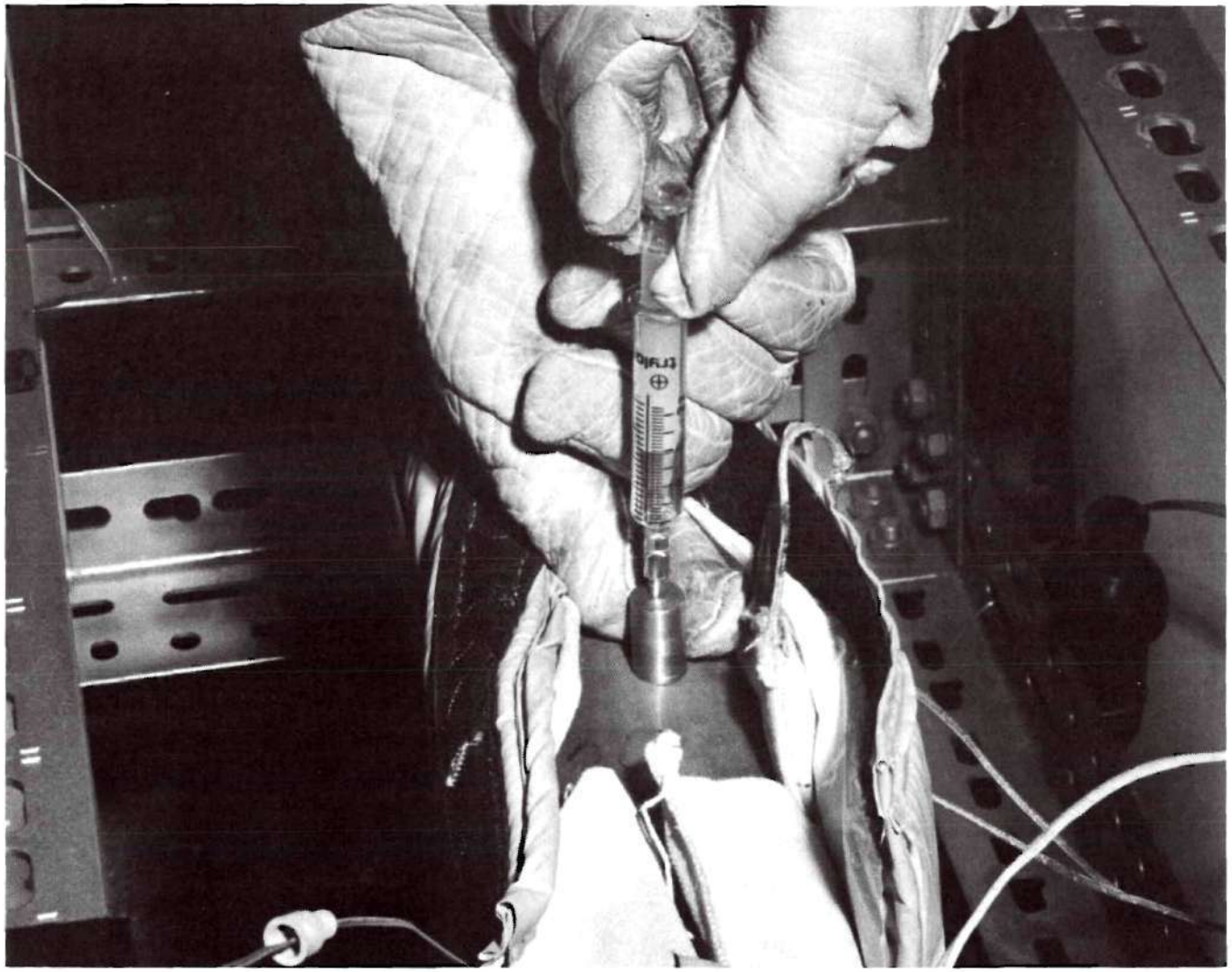

Figure 10. Withdrawal of Gas Sample.

sidered poor, additional samplings were made. In general, the agreement between successive samples from the same location were within about 5 per cent of the full scale reading. However, for some locations agreement was found to be poor even after five or six samplings.

It was found convenient to check the stability of the chromatograph by injecting samples of natural gas-air mixtures. These mixtures were made by injecting 2 or 3 cubic centimeters of natural gas into stoppered 1 liter flasks. It was found that these mixtures gave easily reproducible peaks even with the syringe at room temperature. These samples were injected from time to time during a test run to insure that the chromatograph output was not drifting.

Tests were made to determine if the rate of sample withdrawal could cause the scatter in readings found at some locations. Samples taken at somewhat faster and slower rates than those normally used showed no apparent effect on results, even at locations close to the pipe wall.

CHAPTER V

DATA REDUCTION METHOD

The experimental data obtained from the mass transfer runs were reduced using procedures given below. In essence, these procedures convert the measured weight losses for the test sections to mass fluxes and Nusselt numbers for mass transfer. For those runs in which concentration measurements were also made, the method used to convert the output signal of the chromatograph to concentration is presented.

Reduction of Mass Transfer Data

A computer program utilizing a Burroughs 220 digital computer was written to speed up the data reduction technique. A summary of the calculations made using this program is presented below. For the actual calculations, appropriate conversion factors were included to insure dimensional consistency. The method of data reduction for a typical mass transfer run consisted of the following steps:

(1) The physical properties μ, ρ, $\mathcal{D}_{AB}$ and Sc were obtained by the methods described in Appendix B. Values of ρ and $\mathcal{D}_{AB}$ were corrected to the measured atmospheric pressure.

(2) The initial and final diameters of test sections no. 3 and no. 19 were numerically averaged to obtain an average diameter D_m.

(3) The average velocity of the air $\bar{u}$ was calculated by correcting the total volume of air passed through the dry gas meter

to the temperature and pressure of the system and dividing this value by the average cross-sectional area of the pipe $\pi D_m^2/4$, and the total time of the run.

(4) The Reynolds number, based on the pipe diameter, was calculated from

$$Re = D_m \bar{u} \rho / \mu \tag{5-1}$$

(5) Assuming the ideal gas law, the molar concentration of the test material at the wall, C_{Aw}, was calculated from

$$C_{Aw} = (VP)/RT \tag{5-2}$$

where VP = vapor pressure at T obtained from equation (B-1) or (B-2), Appendix B

T = system temperature, ^{o}K

R = gas constant

(6) For each of the small test sections, an average molar wall flux, N_{Aw}, was calculated from

$$N_{Aw} = \frac{(\Delta \text{ wt. - corr.})}{(M_A)(\pi D_m \; l)t} \tag{5-3}$$

where Δ wt. = weight loss of test section

corr. = weight loss correction term

l = length of test section

t = time of test run

(7) The dimensionless length parameter ReScD/z was calculated from

$$ReScD/z = (Re)(Sc)D_m/z \tag{5-4}$$

where z is the distance from the entrance to the midpoint of the coating as given in Table 1.

(8) The expression $\int_o^z N_{Aw}dz$ was evaluated for the z values corresponding to each test section. Near the pipe entrance, where the value of N_{Aw} is strongly dependent on z, a relation of the form

$$N_{Aw} = A_o(ReScD/z)^{B_o} \tag{5-5}$$

A_o and B_o = constants

was assumed. This assumption was based on the relationship between N_{Aw} and z shown by both the theoretical and experimental results. The constants A_o and B_o were evaluated from the measured N_{Aw} and z values for the first two test sections. If N_{Aw1} and z_1 represent the measured flux and distance, respectively, for the first test section, equation (5-5) may be integrated to give

$$\int_o^{z_1} N_{Aw}dz = N_{Aw1}z_1/(1-B_o) \tag{5-6}$$

Further integration was performed numerically using the trapezoidal rule over each incremental Δz value between the test sections.

(9) The bulk concentration at each test section was determined from

$$C_b = \frac{4 \int_o^z N_{Aw} dz}{D_m \bar{u}} \tag{5-7}$$

The logarithmic mean average concentration difference applicable to the particular test section was determined from

$$(\Delta C)_{lm} = \frac{C_b}{\ln \frac{C_{Aw}}{C_{Aw} - C_b}} \tag{5-8}$$

since $C_{Ao} = 0$ for all test runs. The dimensionless bulk concentration, C_b^*, was evaluated at each test section from

$$C_b^* = \frac{C_b}{C_{Aw}} \tag{5-9}$$

(10) The logarithmic mean Nusselt number at each test section was calculated from

$$(Nu_{AB})_{lm} = \frac{D_m \int_o^z N_{Aw} dz}{z \mathcal{D}_{AB} (\Delta C)_{lm}} \tag{5-10}$$

and the local Nusselt number for each test section was calculated from

$$Nu_{loc} = \frac{2 \left. \frac{\partial C^*}{\partial R} \right|_{R = 1,Z}}{1 - C_b^*} \tag{5-11}$$

where

$$\left.\frac{\partial C^*}{\partial R}\right|_{R = 1,Z} = \frac{N_{Aw} D_m}{2 \mathcal{D}_{AB} C_{Aw}} \qquad (5\text{-}12)$$

Reduction of Concentration Data

The peak heights obtained from the chromatographic analysis were converted to concentrations by use of a calibration factor. This factor was obtained from the peak height produced by an air-naphthalene mixture of known concentration. The known sample was obtained from a saturated mixture of naphthalene in air at room temperature. The concentration of this mixture was calculated from a knowledge of the vapor pressure of naphthalene at the system temperature. A new calibration factor was determined for each run in which concentration measurements were made.

The radial position of the sampling probe was determined from the spacers used. Since a 0.75 inch spacer located the end of the probe at the centerline of the pipe, the radial position was obtained as the difference between 0.75 and the actual spacer used. The reduced radial position r/r_w was calculated assuming r_w to be 0.80 inches.

CHAPTER VI

CALIBRATIONS AND EXPERIMENTAL ERRORS

Calibration Procedures

Thermocouples

The thermocouples were calibrated by immersing them in an electrically heated, stirred water bath equipped with a standard thermometer and comparing the thermocouple outputs to the thermometer reading after thermal equilibrium had been established. The outputs of the thermocouples were measured on the recorder using an ice-water reference bath. As a check on the accuracy of the recorder, several output readings were also taken using a Leeds and Northup Model 8686 Millivolt Potentiometer. Agreement between the recorder and the potentiometer readings was found to be within 0.01 mv. The standard thermometer (minimum division $0.1^{\circ}C$) was calibrated against a similar thermometer certified by the National Bureau of Standards and found to be within $0.1^{\circ}C$ of the true temperature. Thermocouple calibrations were made at several points between $25^{\circ}C$ and $50^{\circ}C$.

At $30^{\circ}C$ all thermocouples gave the same output to within 0.01 mv.; at $38^{\circ}C$, one thermocouple was found to read lower than the others; and at $50^{\circ}C$, three thermocouples were found to read lower, the maximum deviation being 0.03 mv. Those thermocouples showing deviation were located near the exit of the test pipe. A calibration curve based on those thermocouples not showing deviation is presented in Figure 11.

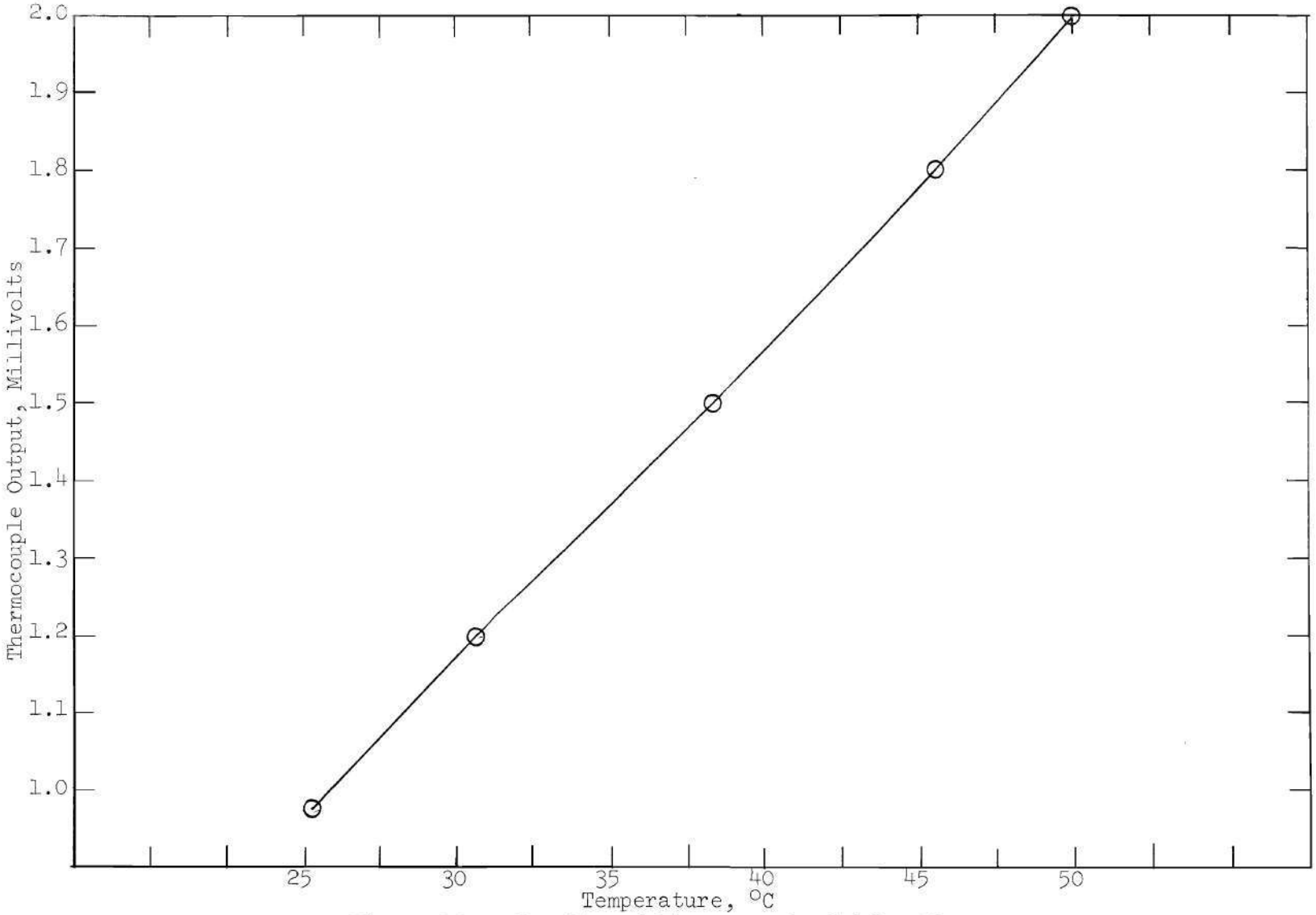

Figure 11. Results of Thermocouple Calibration

Dry Gas Meter

The dry gas meter was calibrated according to standard practices by the Meter Shop of the Atlanta Gas Light Company. Over the range of flow rates used in this study, the meter was found to give readings that were 1.5 per cent too low. A factor to correct actual meter readings by this amount was applied during reduction of the test data.

Concentration Measuring System

In order to determine the validity of using the chromatograph in the method previously described, it was necessary to establish that the output peak height was proportional to concentration over the range of interest and that the height was not affected by the amount of sample introduced.

Preliminary tests conducted using natural gas-air mixtures showed the method gave peaks reproducible to within about 2 per cent. Over the range from 1 cc/liter to 12 cc/liter, the output signal was linear with concentration and the peak height was not dependent on sample size over the range 0.6 to 1.2 cc. Tests using saturated naphthalene-air mixtures at room temperature showed the same independence of sample size but indicated somewhat poorer reproducibility than the natural gas samples.

A calibration of the chromatograph using naphthalene-air samples of varying concentration was made using a syringe heated to 180°C. A sampling bomb was constructed from a 6 inch section of 1 inch standard brass pipe capped at each end. The inside surface of the bomb was coated with naphthalene. A fitting containing a rubber septum was attached through a threaded hole tapped in one of the caps. The bomb was mounted

in a constant temperature water bath such that the fitting extended slightly above the surface. Gas samples were withdrawn through the septum at various temperatures between 22°C and 50°C. The system was allowed approximately 15 minutes to attain equilibrium at each new temperature and several samples were taken at each temperature. Bath temperature was measured with a calibrated thermometer accurate to ± 0.1°C.

Assuming the naphthalene-air mixture to be saturated at each temperature, the concentration of naphthalene was calculated from the vapor pressure equation in Appendix B assuming ideal gas behavior. Results of the calibration test are presented in Table 20 in Appendix C and are shown plotted in Figure 12. These results indicate the chromatograph output based on peak height to be linear over the range of concentrations measured during this study. The maximum deviation from a straight line fitted through the data is about 5 per cent.

Error Analysis

Mass Transfer Runs

It is difficult to determine an average error to be applied to all of the mass transfer runs because of the varying conditions at which the runs were made. It is felt that experimental accuracy improved for the higher Reynolds number runs and for the lower temperature runs due to better control of flow rates and temperatures. Results should also be more reliable for the test sections near the entrance of the pipe because the weight losses were larger for these sections and the effects of small errors in weighing would be diminished.

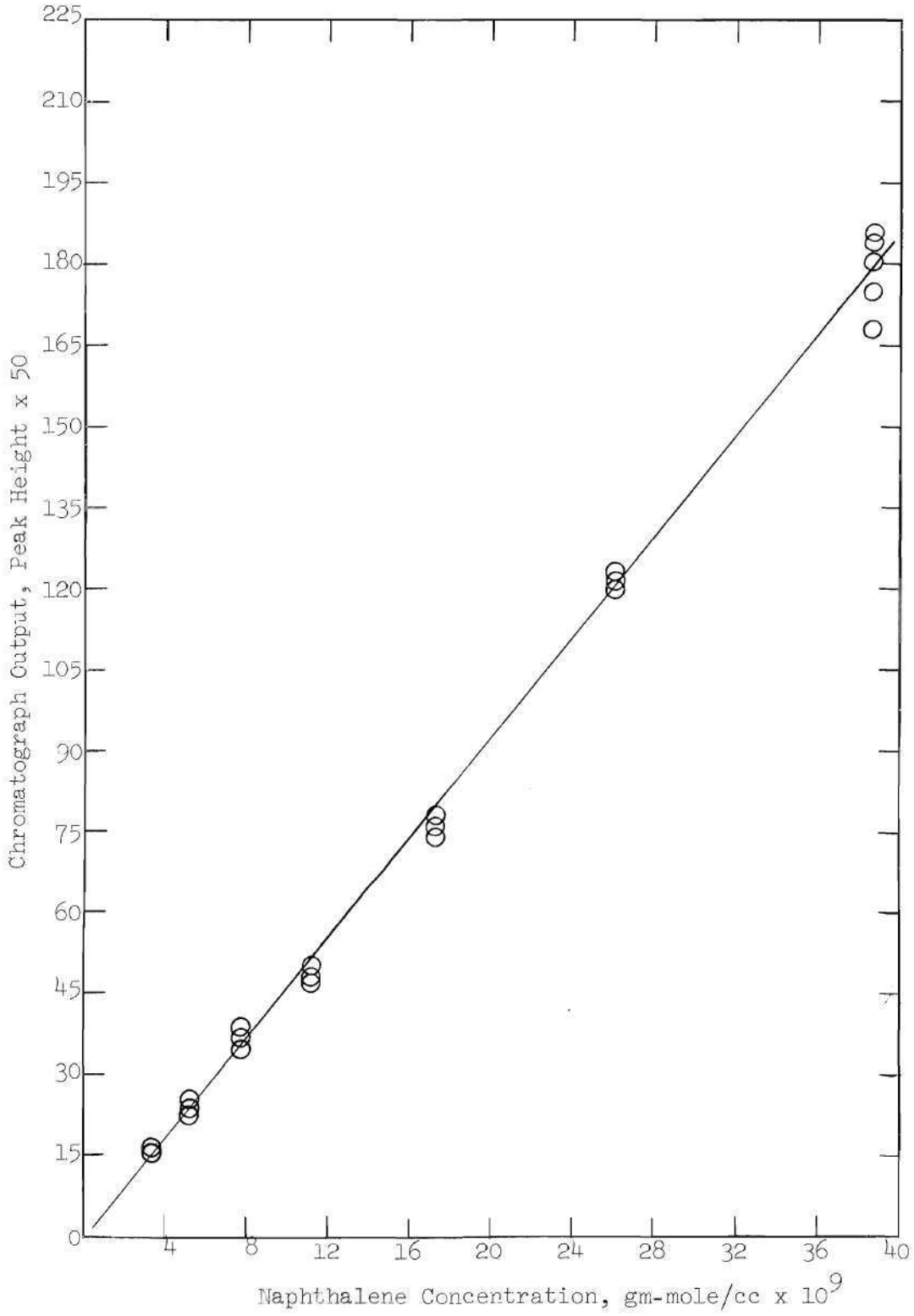

Figure 12. Results of Chromatograph Calibration

The average test temperature is believed to be accurate to ± 0.25°C., however, individual thermocouples varied about the average by as much as 0.75°C during the high temperature runs. The fact that heater adjustments were made periodically so that each thermocouple output was sometimes higher and sometimes lower than the average, should have the effect of smoothing out the temperature variations over the entire run. Flow rates determined at 1000 second intervals varied by a maximum of 3 per cent but these also are probably smoothed out by periodic adjustments.

Runs were timed so as to make the weight loss correction term less than 10 per cent of the smallest weight loss measured. In the case of the low temperature runs, this could not always be accomplished and the correction term was nearer 15 per cent of the weight loss. Since the measured weight losses varied by a factor of about 10 from the entrance to the exit end of the pipe, the correction term represented only a small percentage of the measured weight loss for most of the test sections.

Measured diameters at each end of the test pipe varied from the calculated average diameter by a maximum of about 2 per cent. For the majority of the runs the variation was 1 per cent or less.

A test in which weight losses were determined for assembly and disassembly of the test pipe at room temperature resulted in all test sections showing a weight loss of 0.002 ± 0.001 grams. The consistency of the results indicates that losses due to chipping or breaking of the coating present no problem, provided reasonable care is taken during handling of the test sections. The above mentioned loss is accounted for as part of the overall weight loss correction term at each test

temperature.

Considering all errors occur in the same direction and at the maximum estimated values with a 50 per cent error in the correction term, a maximum error of 15 to 20 per cent might be expected in measured values of the wall flux. Bosworth (6) estimates his maximum error for a similar system, except using profilometric techniques, to be about 24 per cent.

A more realistic appraisal of the errors attributable to experimental technique might be obtained by considering the six runs which were made repeating conditions of previously made runs. Five such runs were made for naphthalene and one for para-dichlorobenzene. In most cases, mass fluxes at the same locations agreed well within 20 per cent and usually better than 10 per cent. In some cases, mostly for high temperature, low Reynolds number runs at positions far down the pipe, the fluxes varied by more than 50 per cent. This is probably attributable to free convection effects which are difficult to duplicate in a flow system.

Concentration Measurements

The errors involved in these measurements may be generally divided into two categories. First, there are those errors in obtaining a sample and, second, those errors associated with the analysis of the sample. In the first category would be such items as the uncertainty in the exact position of the sampling probe, the effect of the probe on the flow pattern in the pipe, and the amount of material drawn in from surrounding areas during sampling. The second type of error would be such things as variations in injection technique and instability or lack of

reproducibility in the analyzing equipment.

Preliminary tests made by injecting a syringe through a sampling port in a short section similar to the test pipe indicated that the tip of the sampling needle could be located within about 1 mm. This represents about 5 per cent of the pipe radius. Obviously this uncertainty could have serious effects at locations where the concentration gradients are large. The measurements described in this study were made at positions far enough downstream so that this did not present a serious problem. Based on theoretical concentration gradients, it is estimated that the uncertainty in position could produce errors of the order of 10 per cent.

Other errors associated with sampling are more difficult to assess. From tests made, no effect of speed of withdrawal of the sample could be detected. Undoubtedly, the presence of the sampling probe would produce some distortion in the flow pattern, but these effects would be expected to be small at the low flow rates studied and to have more effect at positions downstream than at the end of the sampling needle. Therefore, it is estimated that the total error attributable to obtaining a sample is about 15 per cent.

The uncertainty involved in the analysis method is expected to be about 5 per cent. This is based primarily on the deviations obtained from successive samplings of standard naphthalene-air mixtures. Natural gas-air mixtures gave considerably better reproducibility than the samples involving naphthalene. Consequently, it is believed that the major factor contributing to the uncertainty in analysis was in the test material itself rather than in the operating characteristics of the chromatograph.

CHAPTER VII

DISCUSSION OF RESULTS

The results of the constant property theoretical solution are first discussed. Experimental mass transfer results are next presented and compared to the theoretical results. Finally, measured concentration profiles and their relation to the theoretical profiles are discussed.

Theoretical Results

Numerical solutions of the equations representing the mathematical model were obtained for each temperature and test material used in the experimental runs. These solutions are for naphthalene at 50.0°C, 38.2°C, and 30.9°C, and for para-dichlorobenzene at 30.9°C. The results of these solutions are summarized in Tables 3, 4, 5, and 6. The wall flux term N_{Aw} is based on a pipe diameter of 1.60 inches. Other values presented are not dependent on the diameter but only on the axial location ReScD/z and the Schmidt number. To obtain N_{Aw} for a pipe of different diameter, one would multiply the tabulated value by the ratio of 1.60 to the new diameter in inches.

The computer program was modified to obtain numerical solutions for the case of fully-developed laminar flow and for "rod-like flow" in which the velocity profile remains uniform throughout the pipe. Results for these cases for para-dichlorobenzene at 30.9°C are presented in Tables 7 and 8.

Table 3. Theoretical Results For Naphthalene-Air System At 50.0° C

Entrance Profile: Uniform

Diameter: 1.60 inches

C_{Aw}: 3.936×10^{-8} gm-mol/cc

Sc: 2.40

ReScD/z	$N_{Aw} \times 10^{10}$ gm-mol/cm^2 sec	$(Nu_{AB})_{loc}$	$(Nu_{AB})_{lm}$	Dimensionless Bulk Conc, C_b^*
5623	161.6	23.29	51.95	0.036
2483	114.3	16.78	34.04	0.053
1100	80.1	12.10	22.90	0.080
786	68.8	10.55	19.54	0.095
500	55.5	8.76	15.85	0.119
323	45.2	7.37	13.03	0.149
204	36.3	6.21	10.66	0.189
149	31.2	5.59	9.35	0.223
99.9	25.8	4.93	7.98	0.274
69.5	21.6	4.47	6.97	0.330
49.5	18.1	4.14	6.19	0.393
40.1	16.1	3.99	5.78	0.438

Table 4. Theoretical Results For Naphthalene-Air System At 38.2° C

Entrance Profile: Uniform

Diameter: 1.60 inches

C_{Aw}: 1.478×10^{-8} gm-mol/cc

Sc: 2.42

ReScD/z	$N_{Aw} \times 10^{10}$ gm-mol/cm^2 sec	$(Nu_{AB})_{loc}$	$(Nu_{AB})_{lm}$	Dimensionless Bulk Conc, C_b^*
5661	56.66	23.38	52.05	0.036
2500	40.09	16.84	34.10	0.053
1108	28.10	12.14	22.94	0.080
791	24.11	10.59	19.57	0.094
503	19.48	8.79	15.87	0.119
325	15.84	7.40	13.05	0.148
205	12.72	6.23	10.67	0.188
150	10.95	5.60	9.36	0.222
100.6	9.05	4.94	7.99	0.272
70.0	7.56	4.48	6.98	0.329
49.8	6.35	4.15	6.20	0.392
31.6	4.91	3.86	5.38	0.494

Table 5. Theoretical Results For Naphthalene-Air System At 30.9° C

Entrance Profile: Uniform — Diameter: 1.60 inches

C_{Aw}: 7.754×10^{-9} gm-mol/cc — Sc: 2.43

ReScD/z	$N_{Aw} \times 10^{10}$ gm-mol/cm^2 sec	$(Nu_{AB})_{loc}$	$(Nu_{AB})_{lm}$	Dimensionless Bulk Conc, C_b^*
5686	28.45	23.43	52.13	0.036
2511	20.13	16.87	34.15	0.053
1113	14.11	12.17	22.98	0.079
795	12.11	10.61	19.60	0.094
505	9.78	8.81	15.89	0.118
327	7.95	7.41	13.06	0.148
206	6.39	6.24	10.69	0.188
150	5.50	5.60	9.37	0.221
101.0	4.54	4.95	8.00	0.272
70.4	3.80	4.49	6.99	0.328
50.1	3.19	4.16	6.21	0.391
31.8	2.47	3.86	5.39	0.493

Table 6. Theoretical Results For Para-Dichlorobenzene-Air System At 30.9° C

Entrance Profile: Uniform

Diameter: 1.60 inches

C_{Aw}: 8.778×10^{-8} gm-mol/cc

Sc: 2.26

ReScD/z	$N_{Aw} \times 10^{10}$ gm-mol/cm^2 sec	$(Nu_{AB})_{loc}$	$(Nu_{AB})_{lm}$	Dimensionless Bulk Conc, C_b^*
5287	335.8	22.75	50.71	0.038
2335	237.4	16.39	33.27	0.055
1035	166.3	11.82	22.41	0.083
739	142.6	10.31	19.12	0.098
470	115.1	8.57	15.52	0.124
304	93.5	7.21	12.77	0.155
207	77.8	6.26	10.80	0.189
148	66.3	5.57	9.38	0.224
101.3	55.2	4.95	8.07	0.273
70.8	46.2	4.49	7.05	0.329
50.2	38.7	4.15	6.24	0.392
30.2	29.0	3.83	5.33	0.506

Table 7. Theoretical Results For Fully-Developed Flow (Para-Dichlorobenzene-Air System At 30.9° C)

Entrance Profile: Parabolic Diameter: 1.60 inches

C_{Aw}: 8.778×10^{-8} gm-mol/cc Sc: 2.26

ReScD/z	$N_{Aw} \times 10^{10}$ gm-mol/cm^2 sec	$(Nu_{AB})_{loc}$	$(Nu_{AB})_{lm}$	Dimensionless Bulk Conc, C_b^*
5287	285.0	18.97	26.72	0.020
2335	211.4	14.27	20.19	0.034
1035	156.0	10.79	15.27	0.057
739	136.7	9.60	13.63	0.071
470	113.5	8.18	11.74	0.095
304	94.3	7.03	10.18	0.125
207	79.7	6.18	8.98	0.160
148	68.6	5.56	8.07	0.196
101.3	57.6	4.98	7.17	0.246
70.8	48.4	4.54	6.42	0.304
50.2	40.5	4.20	5.84	0.371
30.2	30.2	3.86	5.08	0.490

Table 8. Theoretical Results For Rod-Like Flow
(Para-Dichlorobenzene-Air System At 30.9° C)

Entrance Profile: Uniform

Diameter: 1.60 inches

C_{Aw}: 8.778×10^{-8} gm-mol/cc

Sc: 2.26

ReScD/z	$N_{Aw} \times 10^{10}$ gm-mol/cm^2 sec	$(Nu_{AB})_{loc}$	$(Nu_{AB})_{lm}$	Dimensionless Bulk Conc, C_b^*
5287	687.7	47.60	78.63	0.058
2335	445.5	31.84	53.42	0.087
1035	288.6	21.66	36.38	0.131
739	239.5	18.48	31.12	0.155
470	184.1	14.90	25.37	0.194
304	142.2	12.21	20.91	0.241
207	112.7	10.35	17.67	0.290
148	91.7	9.05	15.31	0.339
101.3	72.3	7.91	13.10	0.404
70.8	57.1	7.08	11.37	0.474
50.2	44.9	6.42	10.00	0.550
30.2	29.9	5.98	8.47	0.674

Ulrichson and Schmitz (10) and Wilkins (9) have discussed the error introduced in entrance length solutions for heat transfer when the radial velocity term in the energy equation is neglected. In both of these studies, it was found that neglecting the radial velocity term resulted in higher local Nusselt numbers and lower bulk temperatures than for the case when the term is included in the solution. To determine the error caused by neglecting the radial velocity term at the conditions of the present mass transfer study, the computer program was modified such that the dimensionless radial velocity V was assigned the value of zero in the numerical solution of the concentration equation. Results of this solution for para-dichlorobenzene at 30.9°C are presented in Table 9.

As can be seen from a comparison of the data in Tables 6 and 9, local Nusselt numbers differ by over 25 per cent near the pipe entrance and the relative error diminishes with increasing distance down the pipe. At ReScD/z of 100, the difference in local Nusselt numbers is about 7 per cent. Tables 6 and 9 also show that significantly lower bulk concentrations are obtained when the radial velocity term is neglected.

The apparent anomaly of obtaining higher mass fluxes and local Nusselt numbers when the radial velocity term is neglected in the diffusion equation can be explained. The result of neglecting radial velocity is to obtain lower values of C^* in the solution of the diffusion equation. At the wall, however, C^* is fixed at unity by a boundary condition. Consequently, higher values of the term $\left.\frac{\partial C^*}{\partial R}\right|_{R = 1,Z}$ are obtained when the radial velocity term is neglected. N_{Aw} and $(Nu_{AB})_{loc}$ are both characterized by the term $\left.\frac{\partial C^*}{\partial R}\right|_{R = 1,Z}$ and are thus

Table 9. Theoretical Results For Para-Dichlorobenzene-Air System At 30.9° C Neglecting Radial Velocity Term

Entrance Profile: Uniform — Diameter: 1.60 inches

C_{Aw}: 8.778×10^{-8} gm-mol/cc — Sc: 2.26

ReScD/z	$N_{Aw} \times 10^{10}$ gm-mol/cm^2 sec	$(Nu_{AB})_{loc}$	$(Nu_{AB})_{lm}$	Dimensionless Bulk Conc, C_b^*
5287	431.0	28.80	32.26	0.024
2335	293.2	19.88	22.90	0.038
1035	200.0	13.89	16.33	0.061
739	169.8	11.96	14.25	0.074
470	135.3	9.77	11.92	0.096
304	108.5	8.08	10.11	0.125
207	89.2	6.89	8.79	0.156
148	75.0	6.05	7.82	0.191
101.3	61.7	5.29	6.92	0.239
70.8	50.9	4.72	6.20	0.296
50.2	42.0	4.30	5.63	0.362
30.2	30.8	3.88	4.97	0.482

calculated to be higher than their corresponding values when radial velocity effects are included. The net effect is that the calculated N_{Aw} indicates more material is entering the stream than would be calculated by considering the change in bulk concentration.

In the numerical solutions, a step-by-step mass balance of material A was made at each axial step down the tube. The procedure used in setting up the mass balance is discussed in Appendix A. Essentially, the step-by-step mass balance compares the amount of subliming material entering the stream calculated from the value of N_{Aw} with the amount calculated from the change in bulk concentration. With the radial velocity term included, the step-by-step mass balance shows agreement between N_{Aw} and the flux determined from the change in C_b^* to be within 3 per cent at ReScD/z of 5000. Further downstream the agreement is well within 1 per cent. Neglecting the radial velocity term results in much higher deviations in the mass balance. At corresponding axial locations, the percentage deviation was found to be about 20 times higher than for the case when the radial velocity term is included.

The fact that an overall mass balance of subliming material is not satisfied when radial velocity is neglected can be seen by considering the log mean Nusselt numbers in Tables 6 and 9. These Nusselt numbers were calculated from the change in bulk concentration from the entrance to the axial position under consideration. Thus the lower values of $(Nu_{AB})_{lm}$ in Table 9 result from lower bulk concentrations. However, should the log mean Nusselt numbers have been calculated by integrating the local Nusselt numbers, $(Nu_{AB})_{lm}$ in Table 9 would be higher than $(Nu_{AB})_{lm}$ in Table 6. Only when the overall mass balance is

satisfied will the results obtained by each method agree.

While agreement between the local Nusselt numbers calculated with and without the radial velocity term improves considerably with distance down the pipe, it is interesting to note that the deviation between the predicted wall fluxes does not diminish as rapidly. For instance, local Nusselt numbers agree within about 1.3 per cent at ReScD/z of 30.2 whereas the difference in mass fluxes is still about 6 per cent.

A comparison of the theoretical results of this study for naphthalene-air at 50° C to the theoretical results of Bosworth (6) for the same conditions shows his results for local Nusselt number to be approximately 50 per cent high at ReScD/z of 1000, 25 per cent high at ReScD/z of 400, and 10 per cent high at ReScD/z of 150. Much of the difference found in the two solutions is attributable to the radial velocity term being neglected in Bosworth's solution. In obtaining his numerical solution, Bosworth used a considerably larger mesh size than was used in this study and this factor may also account for some of the difference in the results.

To determine the adequacy of the numerical solution, comparisons were made of the calculated results with the solutions of Lévêque (13) and Graetz (14) for fully-developed flow, of Graetz for rod-like flow, and of Wilkins (9) for the case of Prandtl number (or, for mass transfer, Schmidt number) equaling unity in developing flow. In all cases, the agreement was quite good. It was also noted that the numerical solution closely approached the solution of Pohlhausen (15) for a flat plate at higher values of ReScD/z. These comparisons are summarized in

Appendix A in Tables 14, 15, and 16, and Figure 47.

Mass Transfer Results

General

A total of 39 experimental mass transfer runs were made during this study. Naphthalene was used as the subliming substance for 32 of these runs and p-dichlorobenzene was used for the remaining 7 runs. Air was used as the test fluid for all runs.

For the naphthalene runs, the following positions of the test pipe were employed:

(1) Horizontal.

(2) Vertical with upflow.

(3) 45° from horizontal with upflow.

For each position, runs were conducted at three different temperatures (30.9° C, 38.2° C, and 50.0° C) and at three different Reynolds numbers (approximately 500, 1000, and 1500).

For the p-dichlorobenzene runs, the same pipe positions as given above were used. For each position, runs were conducted at two different Reynolds numbers (approximately 750 and 1500) at a temperature of 30.9° C.

A summary of the experimental runs conducted during this study and the exact conditions for each run is presented in Table 10.

The experimental results for the mass transfer runs are presented in Tables 21 through 59 in Appendix C. For all test runs, the measured mass fluxes were higher than predicted by the theoretical solution. This is believed to be caused by free convection currents initiated by

Table 10. Summary of Test Runs Conducted

Run No.	Temp. °C	Pipe Position	Reynolds Number	D_m, Inches	Date of Run
		Naphthalene - Air Runs			
1	50.0	Horiz.	445	1.621	8-09-65
2	50.0	Horiz.	447	1.623	8-10-65
3	50.0	Horiz.	1015	1.612	8-04-65
4	50.0	Horiz.	1376	1.640	8-16-65
5	50.0	Vert.	441	1.631	8-12-65
6	50.0	Vert.	447	1.625	8-11-65
7	50.0	Vert.	1016	1.614	8-05-65
8	50.0	Vert.	976	1.618	8-06-65
9	50.0	Vert.	1358	1.645	8-18-65
10	50.0	45°	509	1.628	11-16-65
11	50.0	45°	909	1.616	11-05-65
12	50.0	45°	1356	1.622	11-11-65
13	38.2	Horiz.	461	1.604	10-05-65
14	38.2	Horiz.	935	1.653	8-25-65
15	38.2	Horiz.	948	1.644	8-23-65
16	38.2	Horiz.	1426	1.610	10-01-65
17	38.2	Vert.	459	1.600	10-08-65
18	38.2	Vert.	954	1.656	8-27-65
19	38.2	Vert.	958	1.653	8-30-65
20	38.2	Vert.	1440	1.599	10-07-65
21	38.2	45°	477	1.612	11-04-65
22	38.2	45°	953	1.610	11-02-65
23	38.2	45°	1432	1.615	11-03-65
24	30.9	Horiz.	468	1.611	10-15-65
25	30.9	Horiz.	990	1.601	10-12-65
26	30.9	Horiz.	1414	1.604	10-21-65
27	30.9	Vert.	456	1.606	10-27-65
28	30.9	Vert.	990	1.607	10-22-65
29	30.9	Vert.	1453	1.606	10-19-65
30	30.9	45°	485	1.627	11-12-65
31	30.9	45°	982	1.607	11-01-65
32	30.9	45°	1505	1.609	10-29-65

Table 10. (Continued)

Run No.	Temp. °C	Pipe Position	Reynolds Number	D_m, Inches	Date of Run
		Para-Dichlorobenzene - Air Runs			
33	30.9	Horiz.	751	1.604	12-08-65
34	30.9	Horiz.	729	1.620	12-21-65
35	30.9	Horiz.	1386	1.598	12-09-65
36	30.9	Vert.	742	1.604	12-10-65
37	30.9	Vert.	1425	1.610	12-20-65
38	30.9	45°	724	1.628	12-22-65
39	30.9	45°	1360	1.634	12-29-65

density differences between the inlet air and the air near the pipe wall which contains the heavier subliming material.

For the naphthalene runs, agreement with the theoretical was found to improve markedly with decreasing operating temperature. This seems reasonable since a decrease in temperature results in lower concentrations near the wall and consequently lower Grashof numbers. The maximum Grashof numbers for the runs conducted, which are based on inlet conditions and the pipe diameter, are presented in Table 11 below.

Table 11. Maximum Grashof Numbers

Temperature, °C	Material	Diameter, inches	Maximum Grashof No.
30.9	Naphthalene	1.60	1690
38.2	Naphthalene	1.60	3030
50.0	Naphthalene	1.60	7360
30.9	Para-Dichlorobenzene	1.60	22760

For the conditions covered in this study, very little difference was found in the overall results obtained for horizontal, vertical, and 45° angle runs. For all pipe inclinations, the log mean Nusselt numbers near the end of the pipe were found to be approximately 60 per cent above the theoretical for naphthalene at 50.0° C, 40 per cent above for naphthalene at 38.2° C, and 20 per cent above for naphthalene at 30.9° C. Para-dichlorobenzene at 30.9° C showed deviations of about 60 per cent.

The effect of pipe inclination is more readily seen by considering local results. Local mass fluxes and local Nusselt numbers for the

vertical and 45° angle runs showed generally less fluctuations and better agreement with theory than those for the horizontal case. Near the entrance, however, the horizontal runs were in better agreement with theory.

The test results also indicate a tendency for the runs at higher Reynolds number to show more deviation from the theoretical solution. This is somewhat surprising since one might expect better agreement at higher Reynolds numbers if free convection was the only effect involved. One possible explanation for the effect of Reynolds number might be that a small amount of turbulence is generated by surface irregularities at the higher Reynolds numbers and this causes an increase in the wall flux.

Another effect found in some of the test runs was a significant reduction in the wall mass flux at locations near the end of the pipe. This effect was usually limited to the last two test sections and was sometimes preceded by higher than normal fluxes occurring at the test section immediately upstream. While this effect is somewhat similar to one described by Bosworth (6), it occurred at much lower values of ReScD/z and, in no case did the mass flux approach zero or become negative. This effect was more prevalent for the high temperature, low Reynolds number runs, but was detected even in some of the runs at high Reynolds numbers.

Figures 13 and 14 present measured mass fluxes for horizontal runs with naphthalene at 50.0° C, along with the theoretical solution for a pipe of 1.60 inch diameter. These results are compared to those given by Bosworth (6) for the same operating conditions. In order to compare the flux values, it was necessary to put them on the same dia-

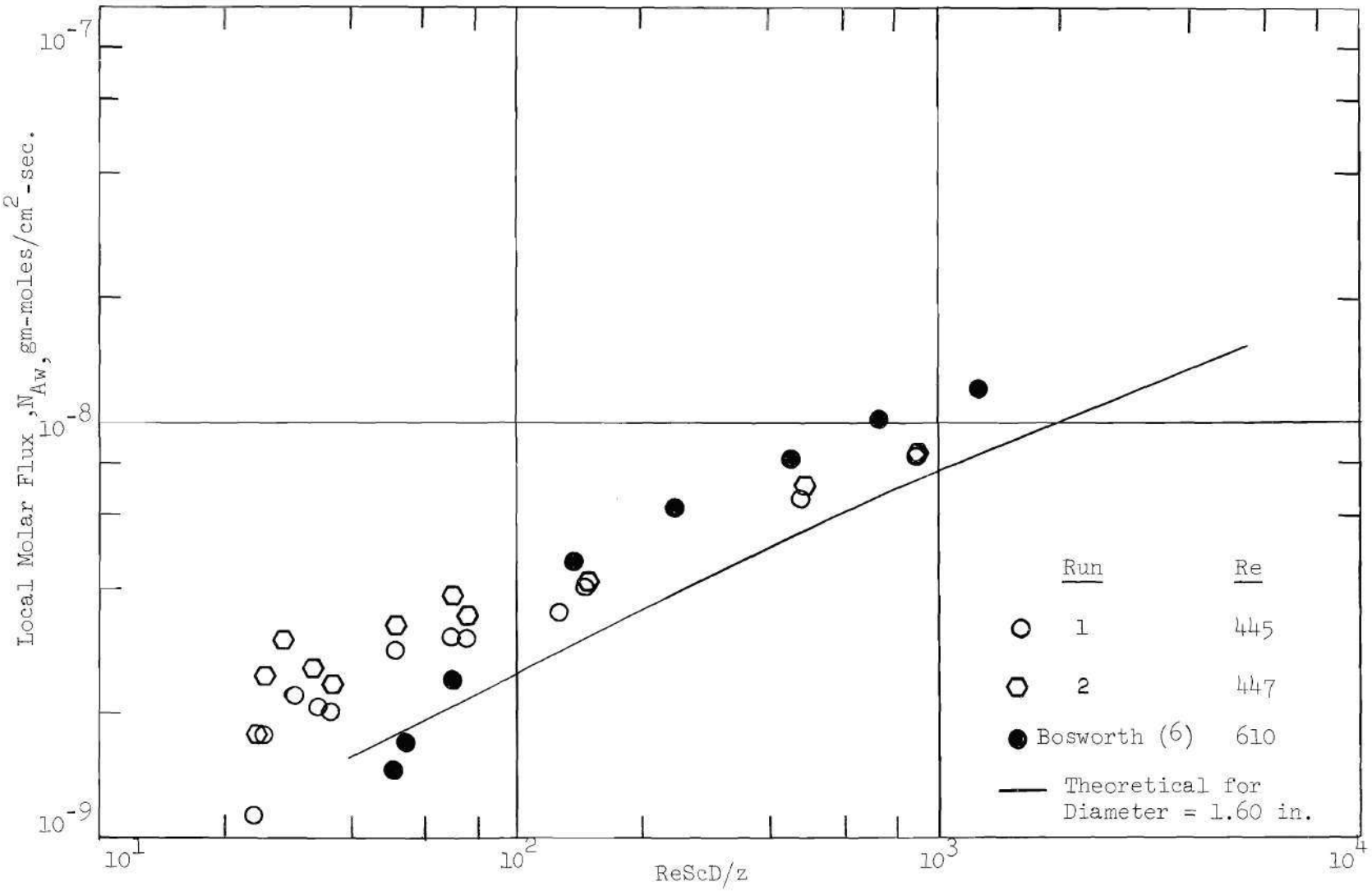

Figure 13. Local Molar Fluxes for Horizontal Runs with Naphthalene at 50.0°C (Low Re)

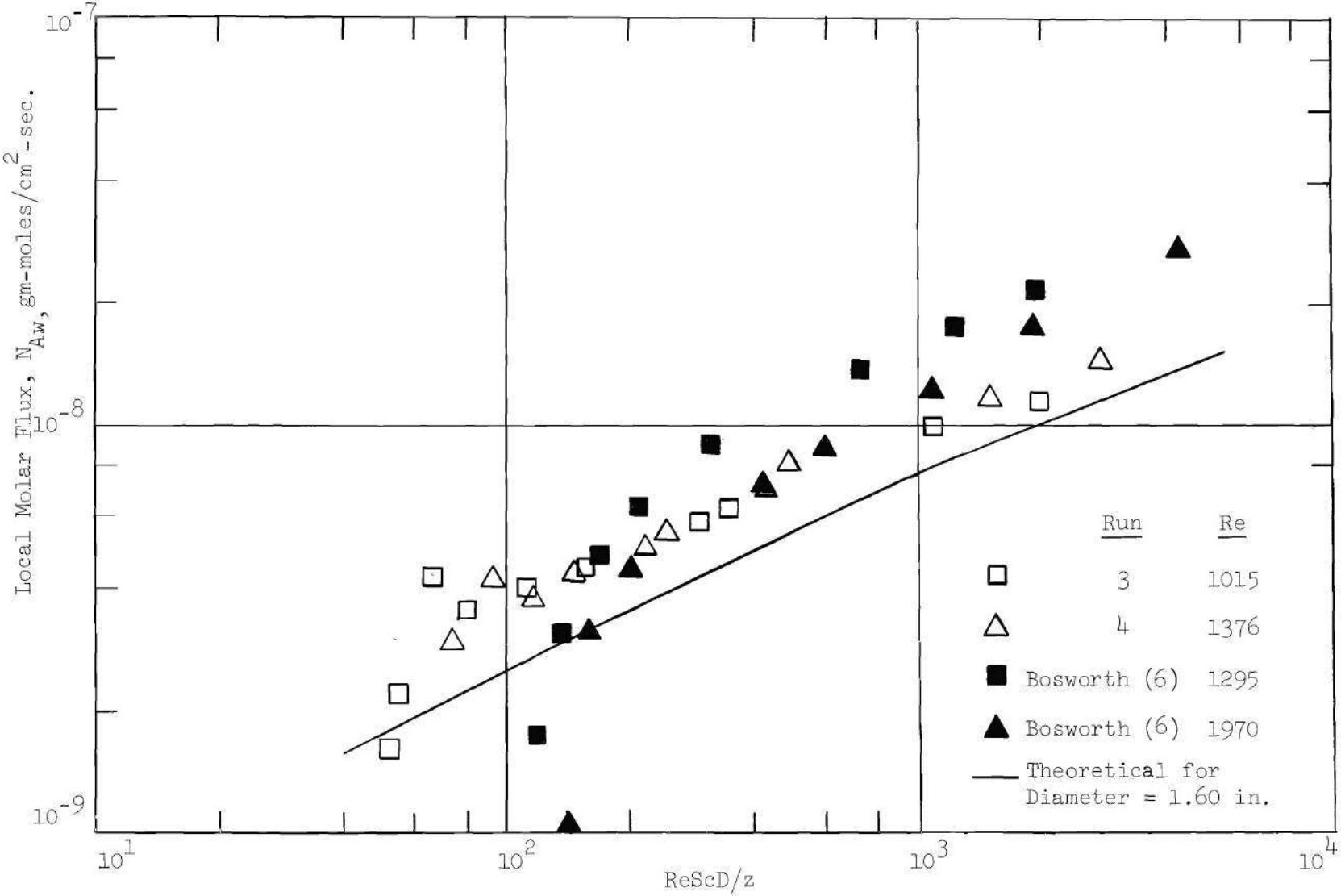

Figure 14. Local Molar Fluxes for Horizontal Runs with Naphthalene at 50.0°C (High Re)

meter basis. This was done by multiplying Bosworth's quoted fluxes by the ratio of the diameter used in his study to the one used in this study, i.e., 1.90/1.60. Such a comparison may not be entirely fair since free convection would be expected to play a more significant role for larger diameter pipes. Thus Bosworth's results might be expected to show higher mass fluxes than those of the present study.

As shown in the figures, the lower Reynolds number runs compare fairly well, with Bosworth's results being about 25 per cent high near the pipe entrance. Further down the pipe Bosworth's values drop below those of this study and finally become negative. For the higher Reynolds number runs, the agreement is much poorer, with Bosworth's results starting nearly twice as high at the entrance and showing a sharp drop off at about ReScD/z of 150. The disagreement in results at higher Reynolds number indicates some factor other than free convection is the cause of the discrepancy in the two sets of data.

Figure 15 shows experimental and theoretical mass fluxes for naphthalene in a horizontal pipe at 30.9° C. This figure is presented to illustrate the improved agreement with the theoretical results which were obtained for the lower Grashof number runs.

Horizontal Runs

The local and logarithmic mean Nusselt numbers for the horizontal runs are plotted against 1000z/ReScD and ReScD/z, respectively, in Figures 16 through 23. Also shown on these figures are curves representing the theoretical solution at the appropriate Schmidt number.

Experimental local Nusselt numbers show considerable deviation from the theoretical values as distance from the inlet was increased.

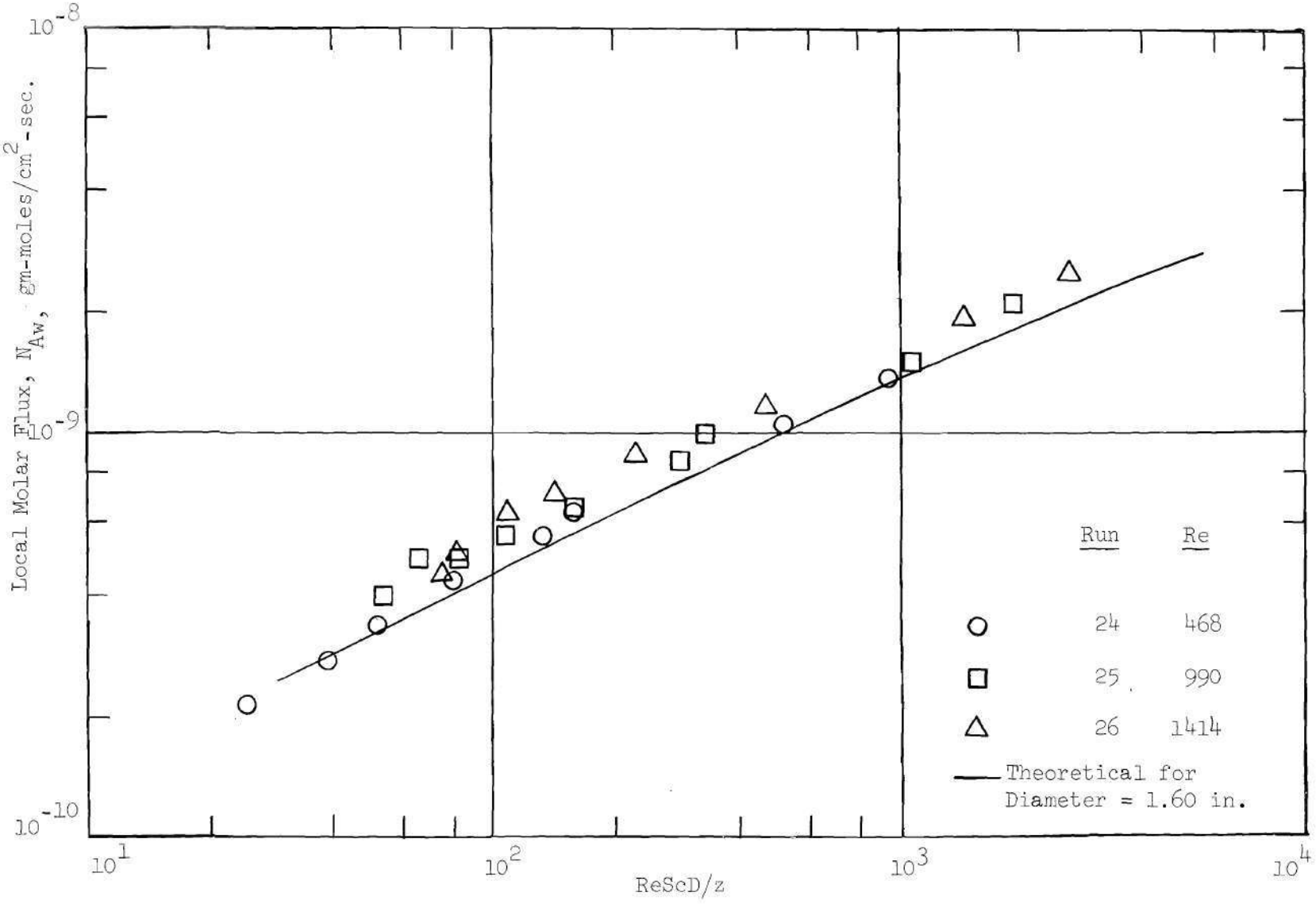

Figure 15. Local Molar Fluxes for Horizontal Runs with Naphthalene at 30.9°C

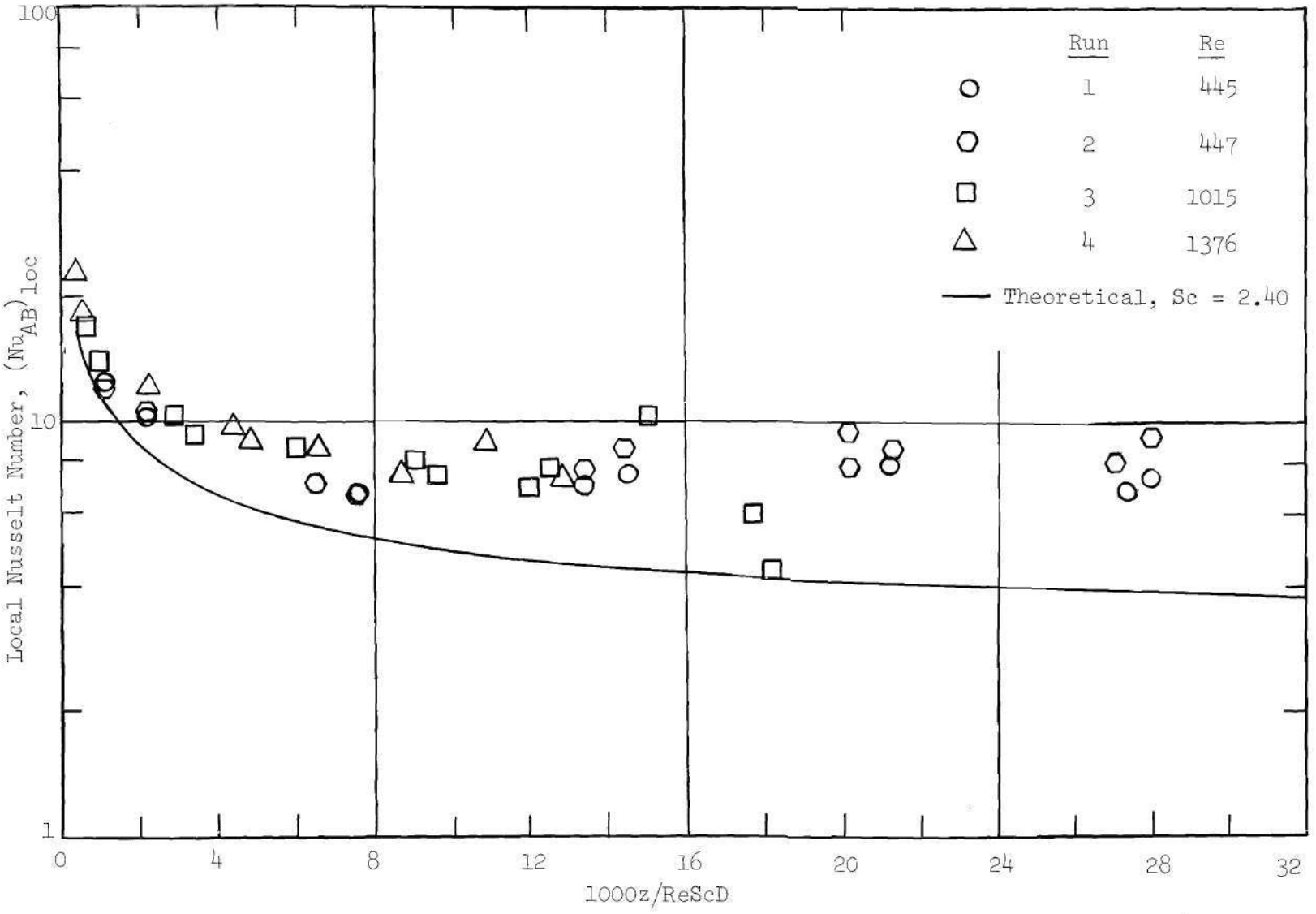

Figure 16. $(Nu_{AB})_{loc}$ for Horizontal Runs with Naphthalene at 50.0°C

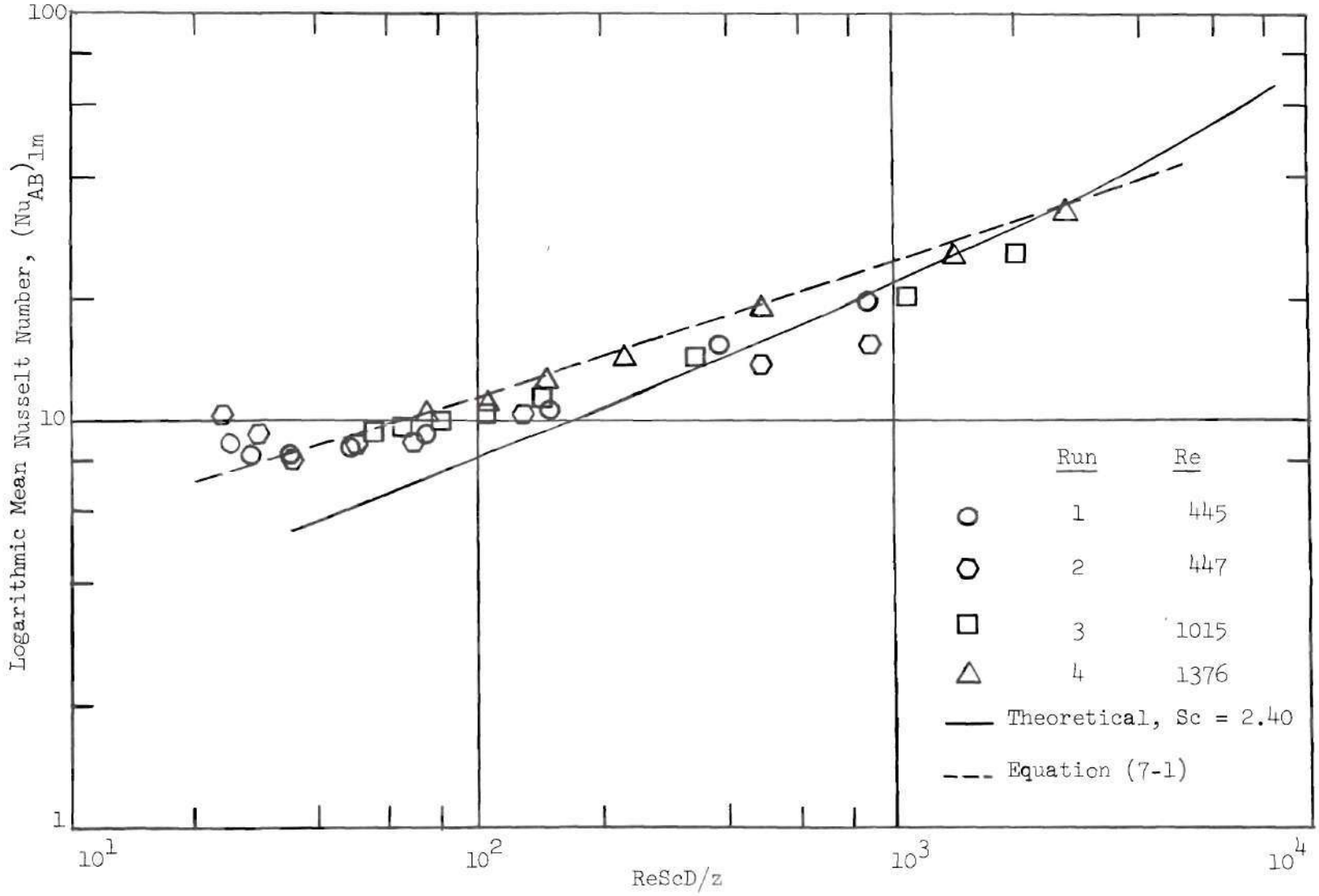

Figure 17. $(Nu_{AB})_{lm}$ for Horizontal Runs with Naphthalene at 50.0°C

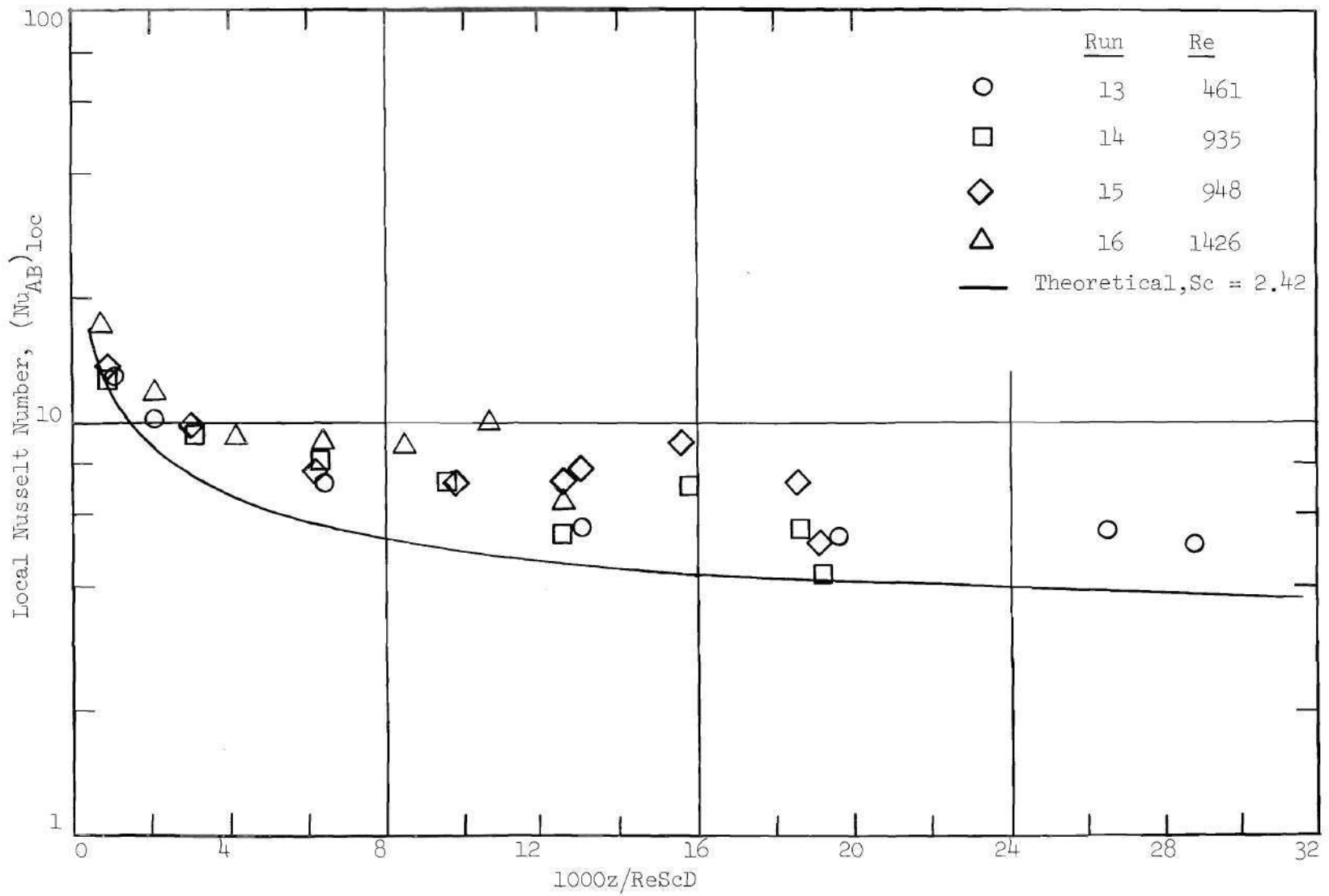

Figure 18. $(Nu_{AB})_{loc}$ for Horizontal Runs with Naphthalene at 38.2°C

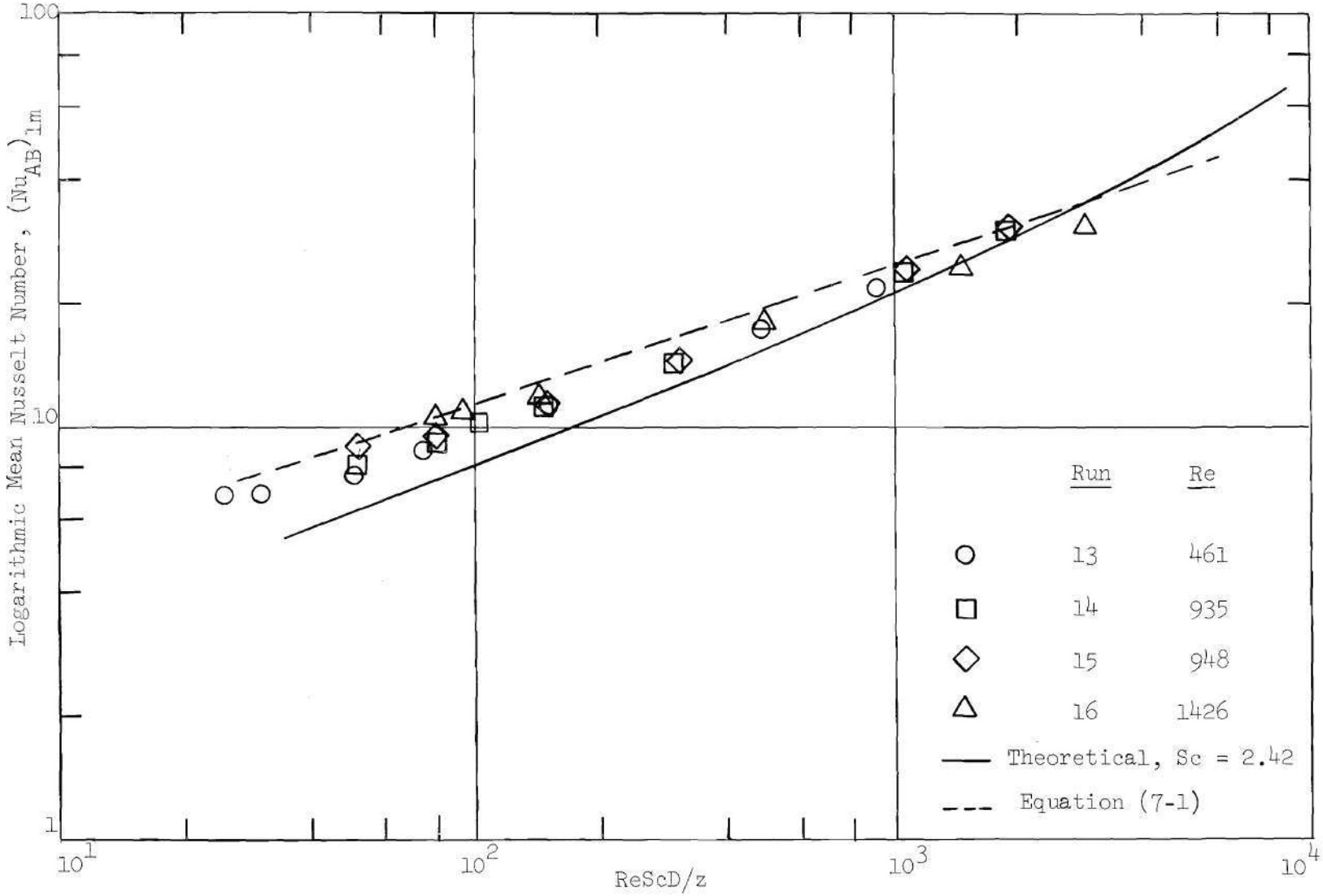

Figure 19. $(Nu_{AB})_{lm}$ for Horizontal Runs with Naphthalene at 38.2°C

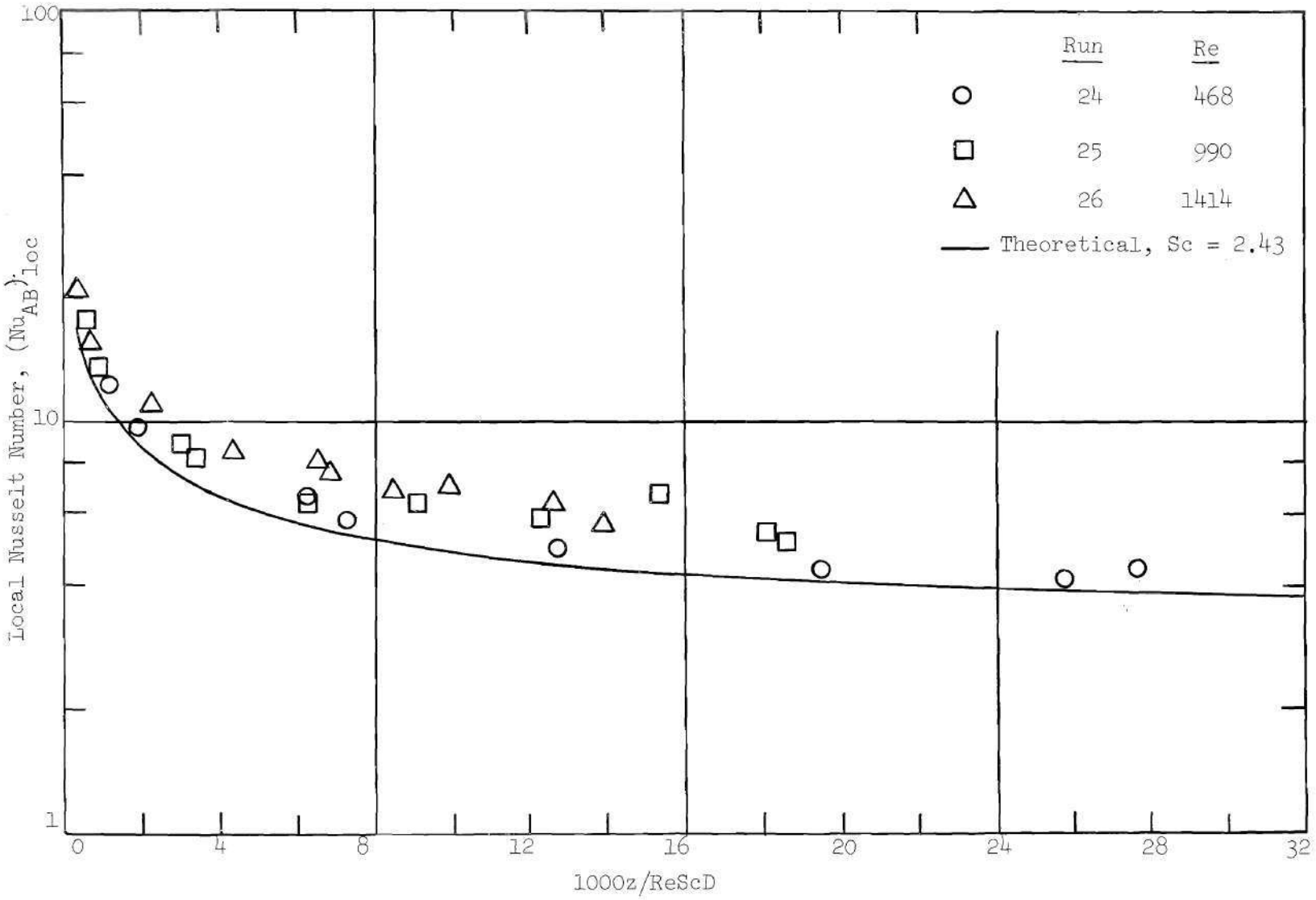

Figure 20. $(Nu_{AB})_{loc}$ for Horizontal Runs with Naphthalene at 30.9°C

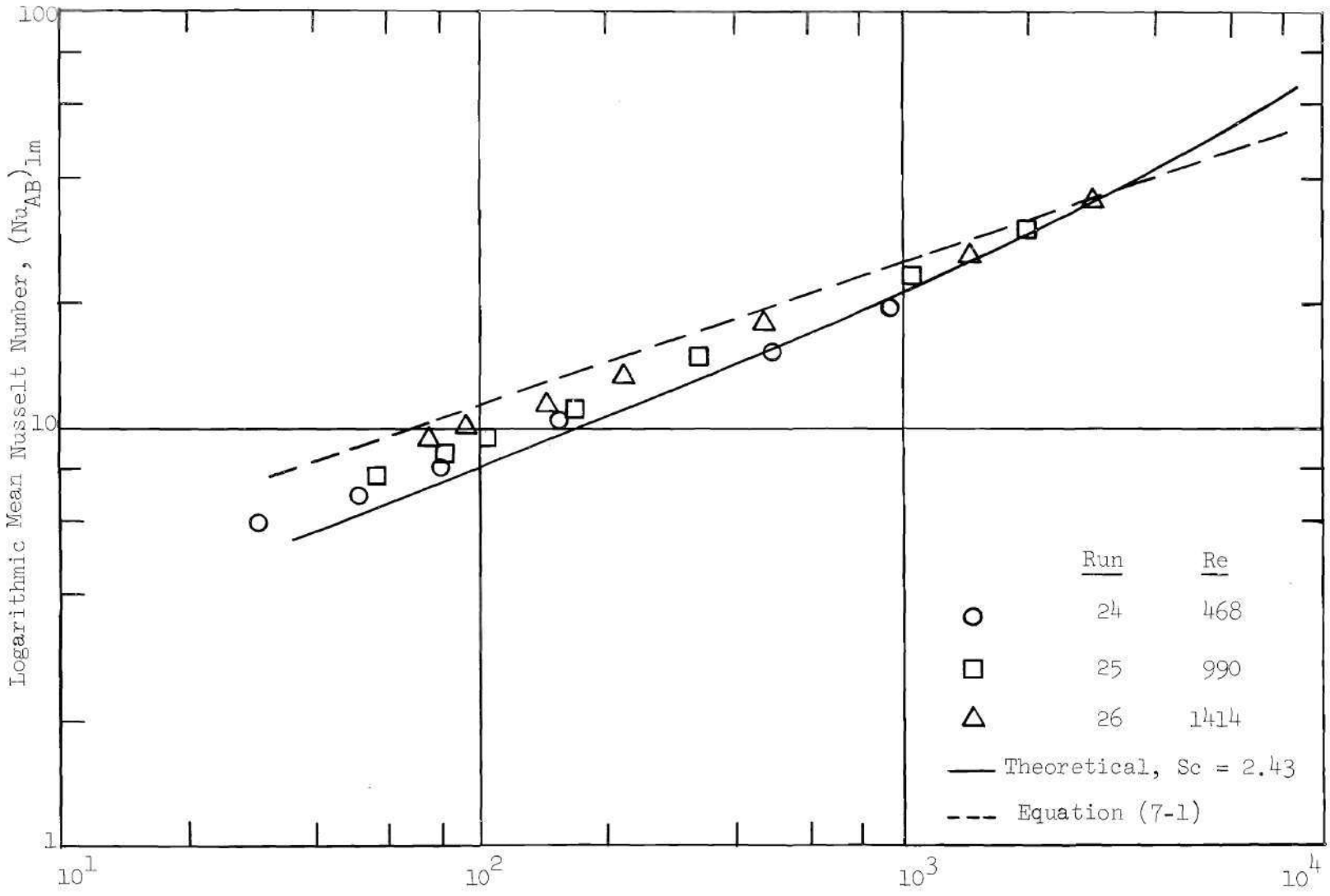

Figure 21. $(Nu_{AB})_{lm}$ for Horizontal Runs with Naphthalene at 30.9°C

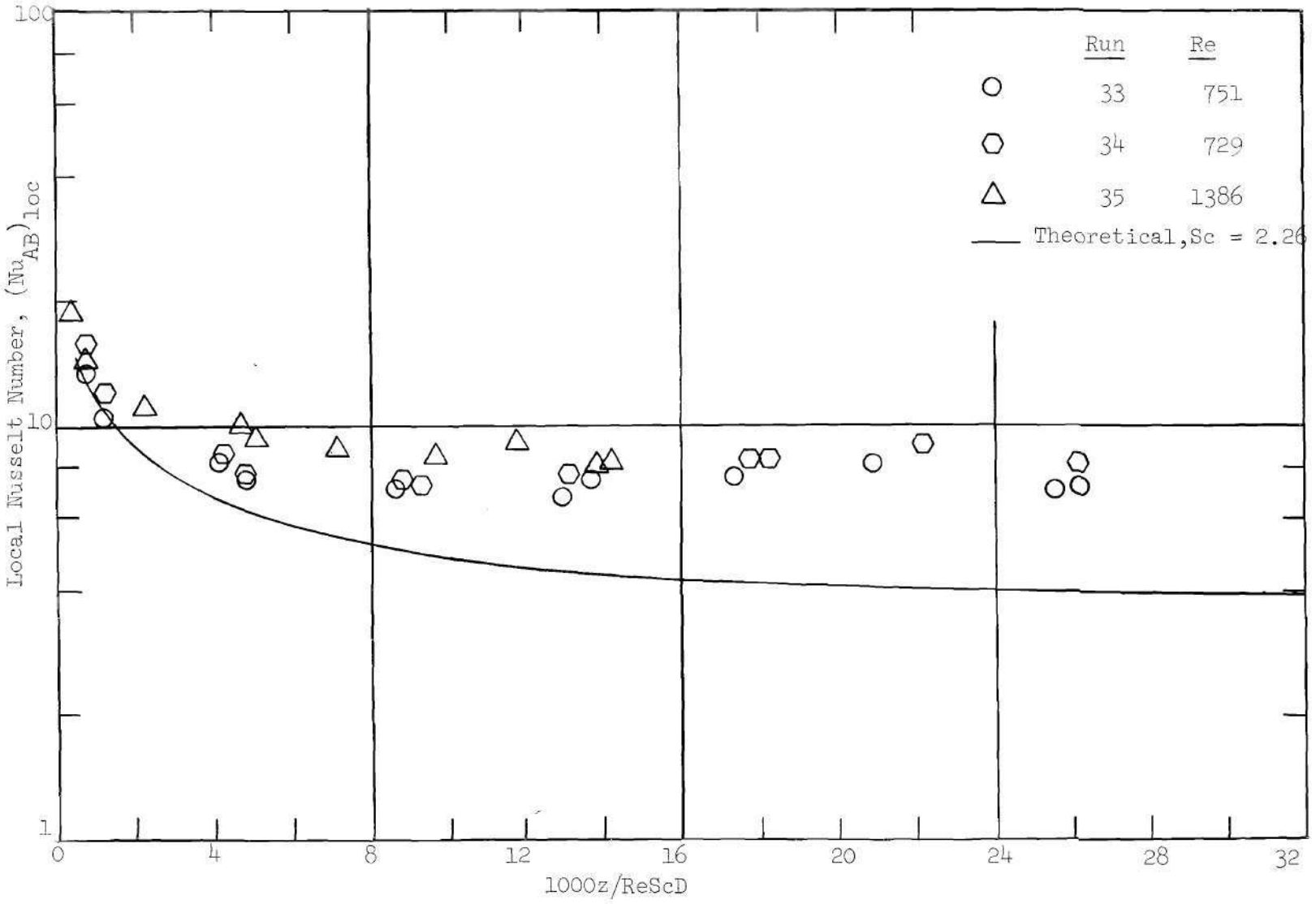

Figure 22. $(Nu_{AB})_{loc}$ for Horizontal Runs with Para-Dichlorobenzene at 30.9°C

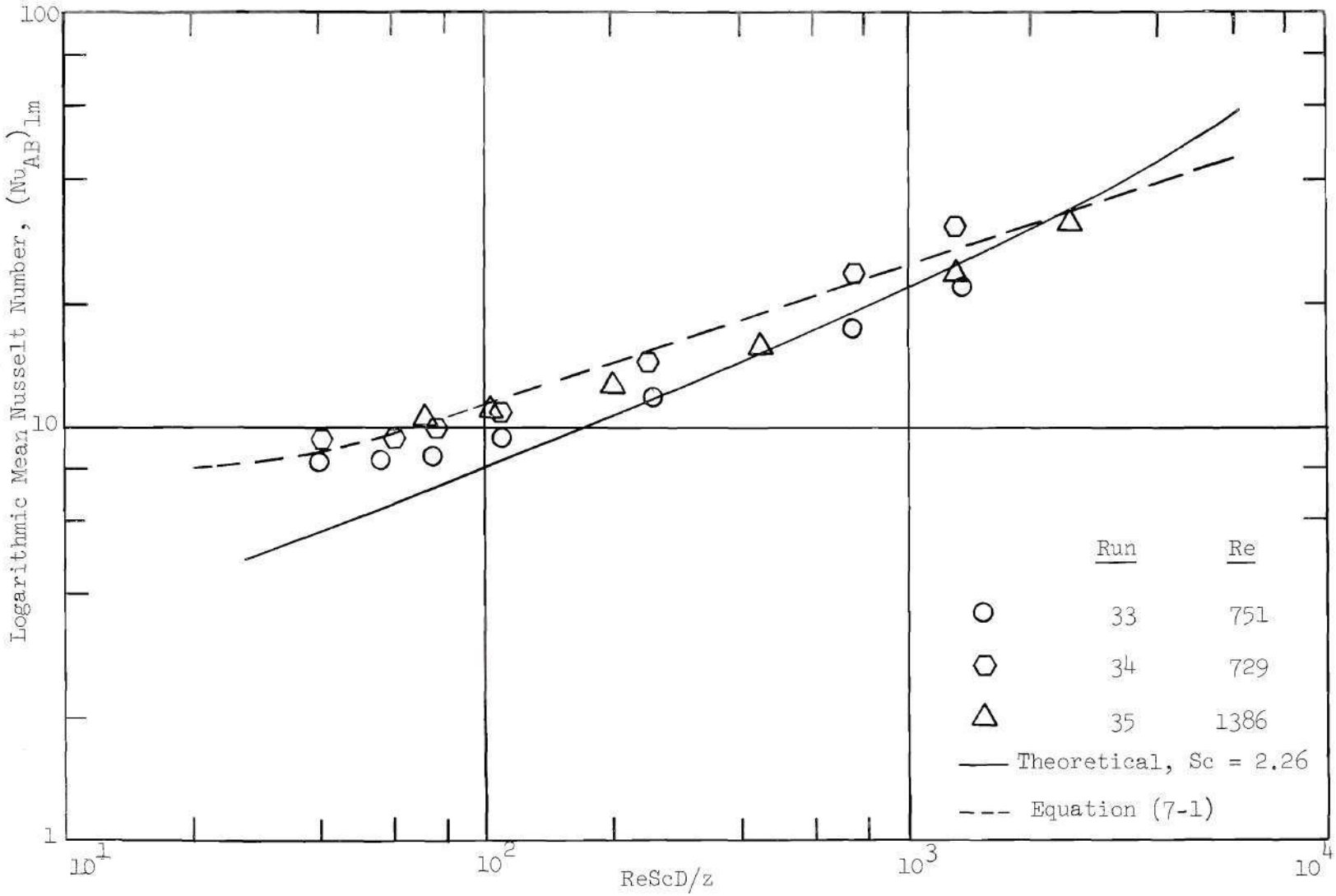

Figure 23. $(Nu_{AB})_{lm}$ for Horizontal Runs with Para-Dichlorobenzene at 30.9°C

Some measured values for para-dichlorobenzene at 30.9° C and naphthalene at 50.0° C are more than twice the value predicted by the theoretical solution. Best agreement in $(Nu_{AB})_{loc}$ occurs for naphthalene at 30.9° C, but, even for this case, local values are frequently over 30 per cent above the theoretical.

Plotted on the figures of logarithmic mean Nusselt number is an equation developed by Jackson, Spurlock and Purdy (16) for the heat transfer Nusselt number for air in laminar flow in the entrance region of a pipe. The equation is

$$Nu_{lm} = 2.67 \left[(Gz)_b^2 + (0.0087)^2 (Gr_w Pr_w)^{1.5} \right]^{1/6} \qquad (7\text{-}1)$$

where the Graetz number, Gz, is $(\pi/4)RePrD/z$. In plotting this equation, the Schmidt number was substituted for the Prandtl number. The Grashof number used was based on the log mean concentration difference obtained from the theoretical solution. As can be seen, the equation gives almost a straight line on the log-log plot indicating that, even for the highest Grashof number runs, the free convection term is relatively unimportant. This equation correlates the experimental data quite well for the higher Grashof number runs but gives results which are too high for the lower Grashof number runs.

Equation (7-1) was obtained by Jackson et al (16) by using experimental data near the pipe entrance to obtain the expression

$$Nu = 2.67(Gz)^{1/3} \qquad (7\text{-}2)$$

for the Nusselt number in the absence of free convection. A correction

term was obtained by considering free convection about a horizontal cylinder, converting this to an "equivalent Graetz number for free convection," and adding this vectorially to the Graetz number. The equation has the disadvantage that it does not reduce to the theoretical solution in the absence of free convection and also is probably strictly applicable only to the case of Prandtl numbers near 0.7.

Correlations of $(Nu_{AB})_{lm}$ were also attempted using modified forms of the equations of Proctor and Eubank, as given by McAdams (17) and Oliver (18). The original equations apply to heat transfer for fully-developed flow in horizontal tubes. Each equation contains an expression (different in the two equations) involving Gr and Pr which is added to the Graetz number to correct for free-convection effects. The procedure used here was to convert the expression to an equivalent ReScD/z by multiplying by $4/\pi$, replacing Pr by Sc, and replacing Gr by Gr_{AB} obtained from the theoretical solution.

To apply the correlations to developing flow, a value of ReScD/z near the end of the pipe was first selected. The equivalent ReScD/z at this location was calculated and added to the original ReScD/z. This resulted in a new value of ReScD/z for which $(Nu_{AB})_{lm}$ was obtained from the theoretical solution. The value of $(Nu_{AB})_{lm}$ thus obtained is considered to be the appropriate Nusselt number, corrected for free convection, to be assigned to the original ReScD/z.

Using the method described above, it was found that the correlations based on both equations resulted in increasing $(Nu_{AB})_{lm}$ only a few per cent above the theoretical, whereas, the experimental values of $(Nu_{AB})_{lm}$ near the end of the pipe were 20 to 60 per cent above the

theoretical solution.

Vertical Runs

The local and logarithmic mean Nusselt numbers for the vertical runs with upflow are presented in Figures 24 through 31. It should be pointed out that in the presence of free convection these results are only applicable to a pipe of the overall dimensions of that used in this study. This is because free convection effects at downstream positions will have an effect on the flow pattern and concentrations upstream.

The situation of subliming a high molecular weight material into a lower molecular weight gas flowing upward is analogous to the heat transfer situation of cooling a gas in upflow. In each case, the free and forced convection terms act in opposite directions. Constant wall temperature heat transfer correlations, such as those of Martinelli and Boelter (19) and Pigford (20) for fully developed laminar flow, and Wilkins (9) for developing laminar flow, predict the effect of opposing forced and free convection terms, is a reduction in Nusselt numbers from the predicted values assuming no free convection. Since the experimental data for this study lead to both local and log mean Nusselt numbers higher than the theoretical, it is apparent that the above mentioned correlations will not apply.

In an experimental study of diffusion of vapors into a fully-developed laminar air stream in a constant temperature wetted wall column, Gilliland and Sherwood (21) found their mass transfer data to be correlated much better by the Graetz equation for rod-like flow than by the equation representing fully-developed flow. These results

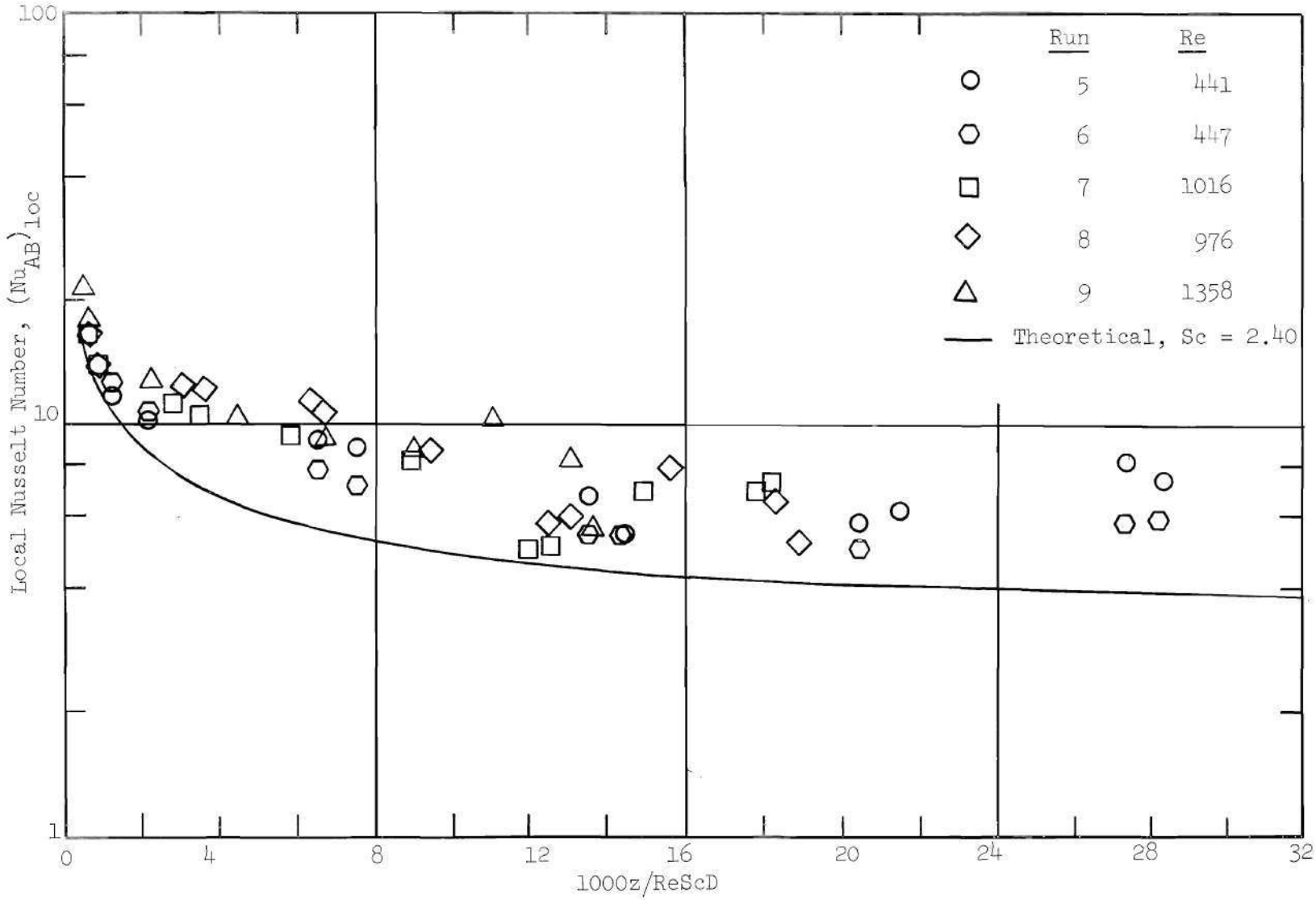

Figure 24. $(Nu_{AB})_{loc}$ for Vertical Runs with Naphthalene at 50.0°C

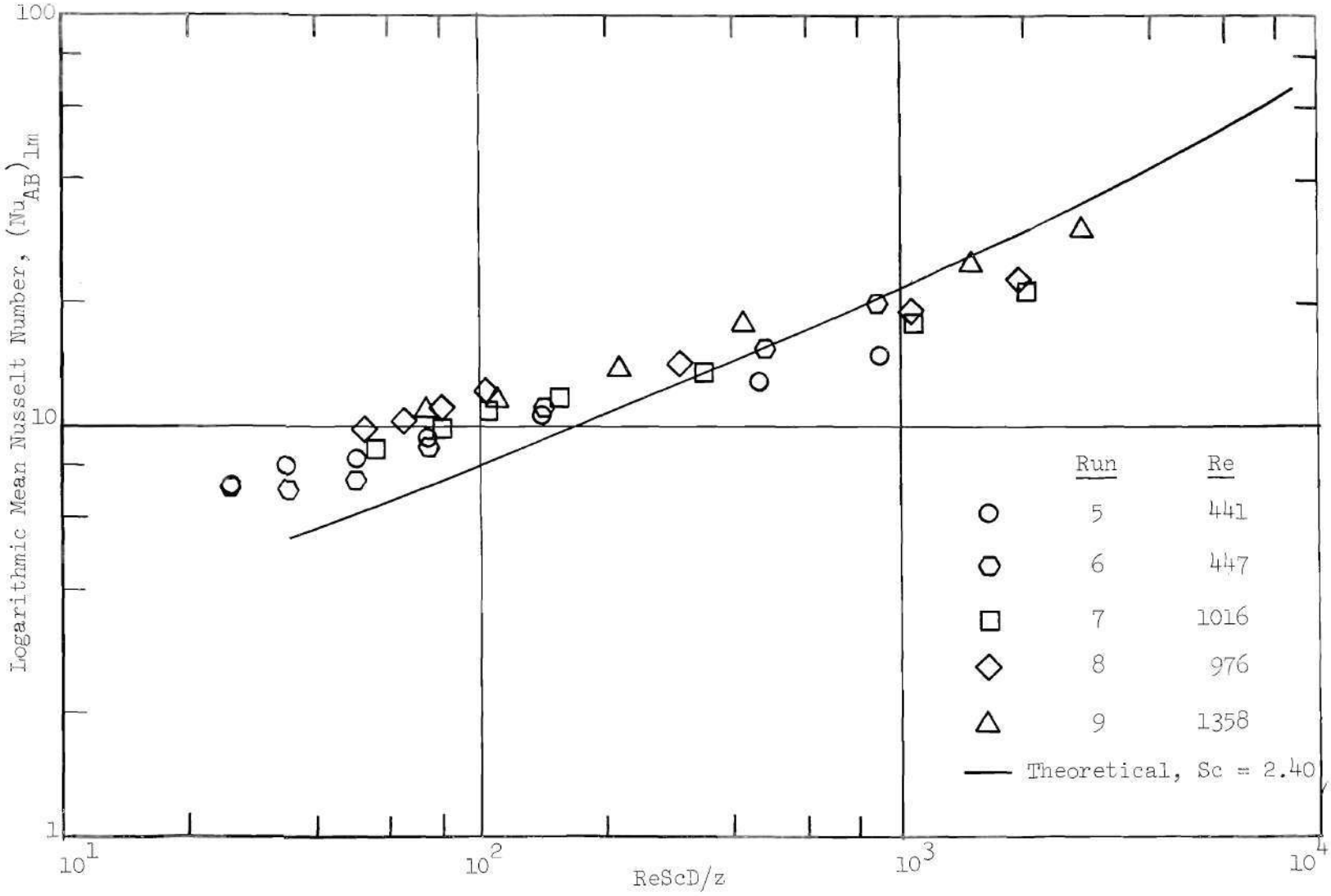

Figure 25. $(Nu_{AB})_{lm}$ for Vertical Runs with Naphthalene at 50.0°C

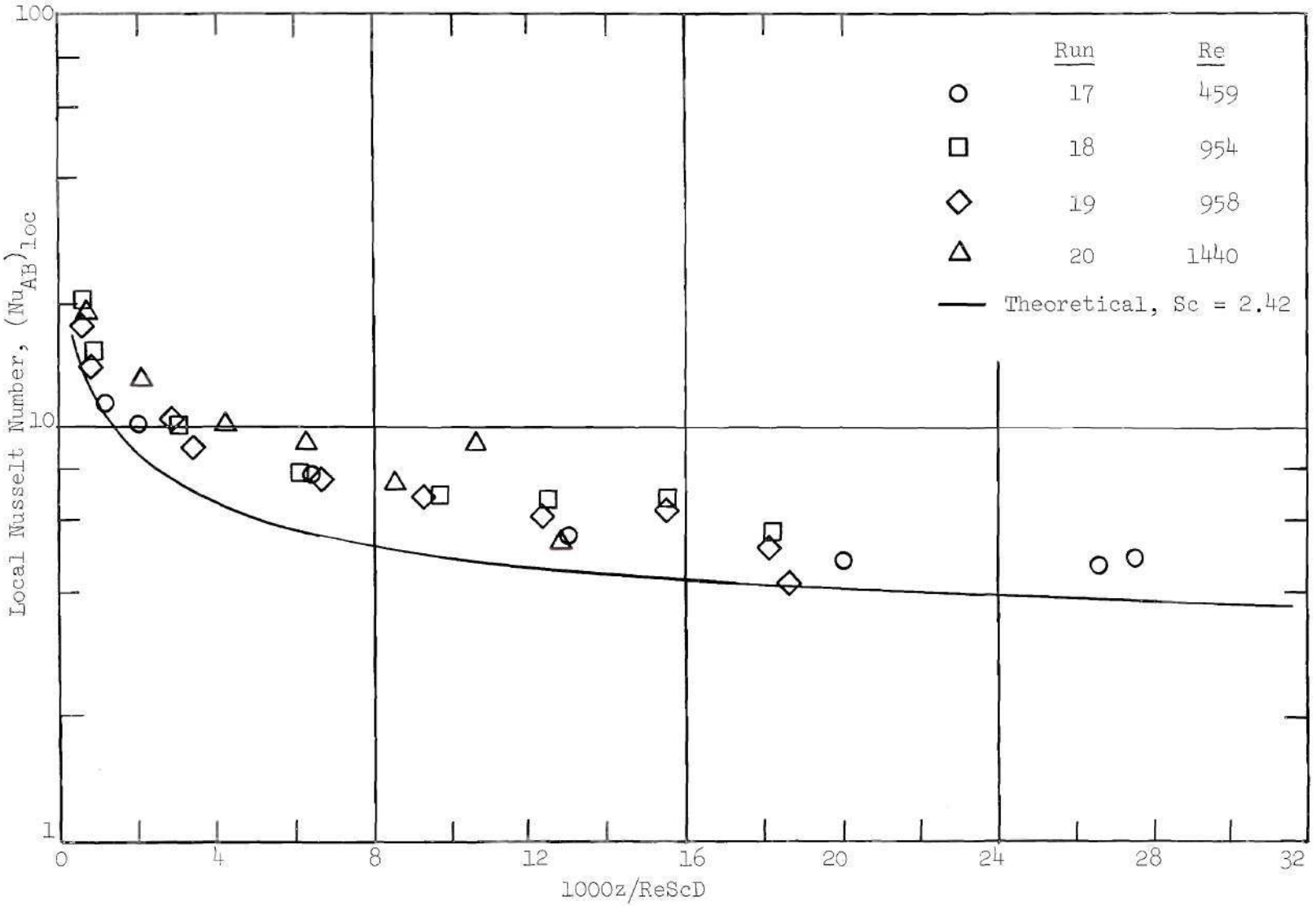

Figure 26. $(Nu_{AB})_{loc}$ for Vertical Runs with Naphthalene at 38.2°C

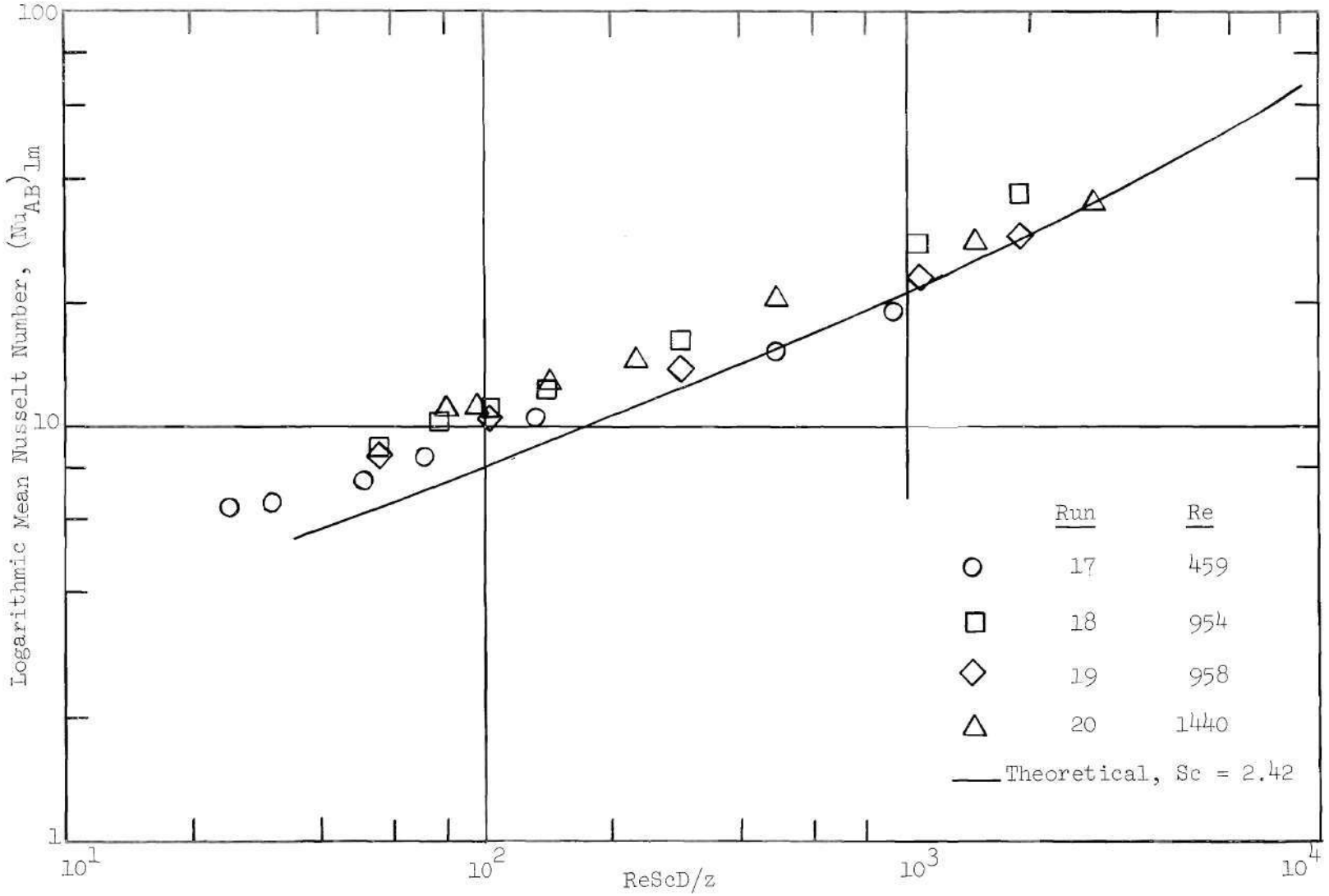

Figure 27. $(Nu_{AB})_{lm}$ for Vertical Runs with Naphthalene at 38.2°C

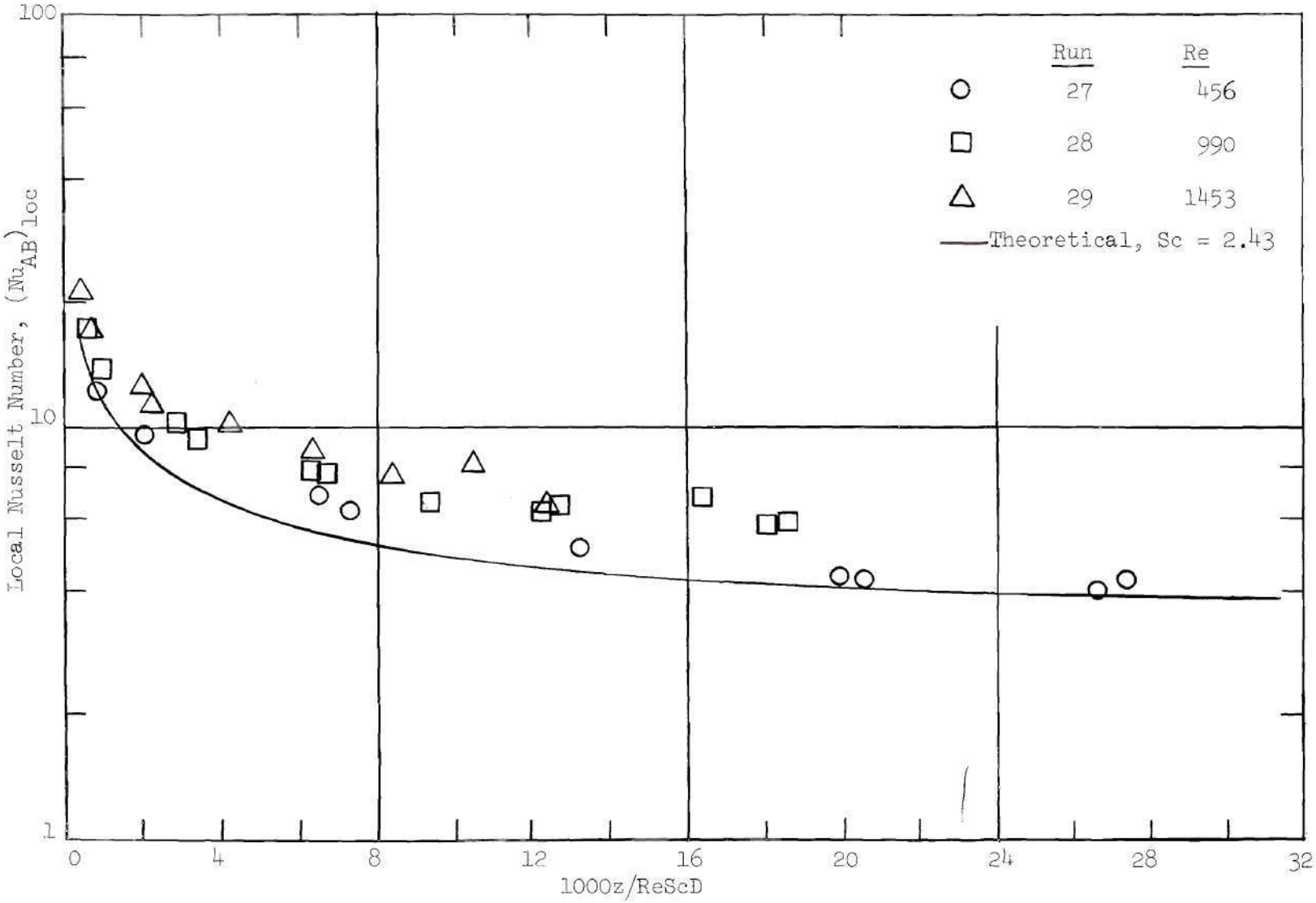

Figure 28. $(Nu_{AB})_{loc}$ for Vertical Runs with Naphthalene at 30.9°C

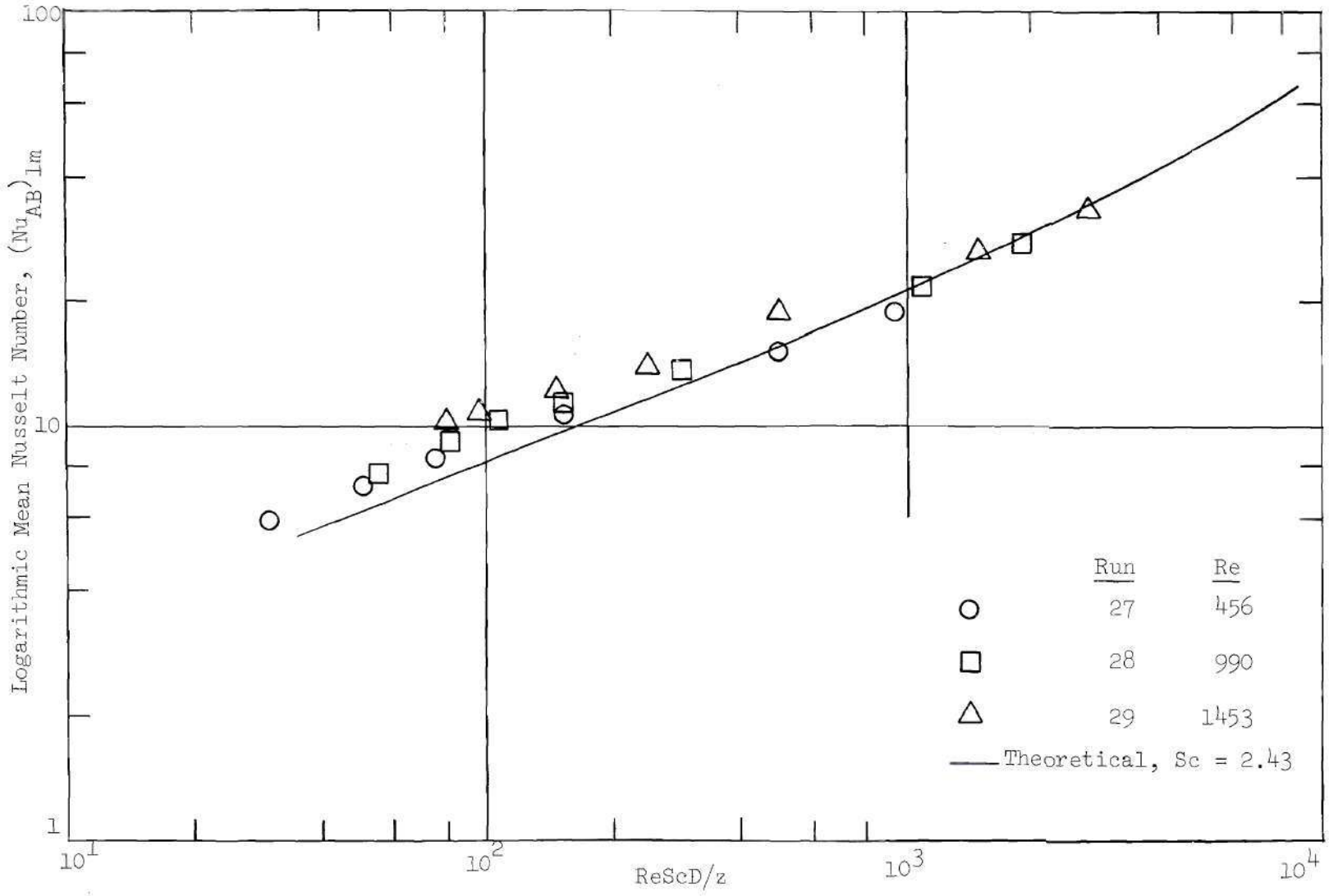

Figure 29. $(Nu_{AB})_{lm}$ for Vertical Runs with Naphthalene at 30.9°C

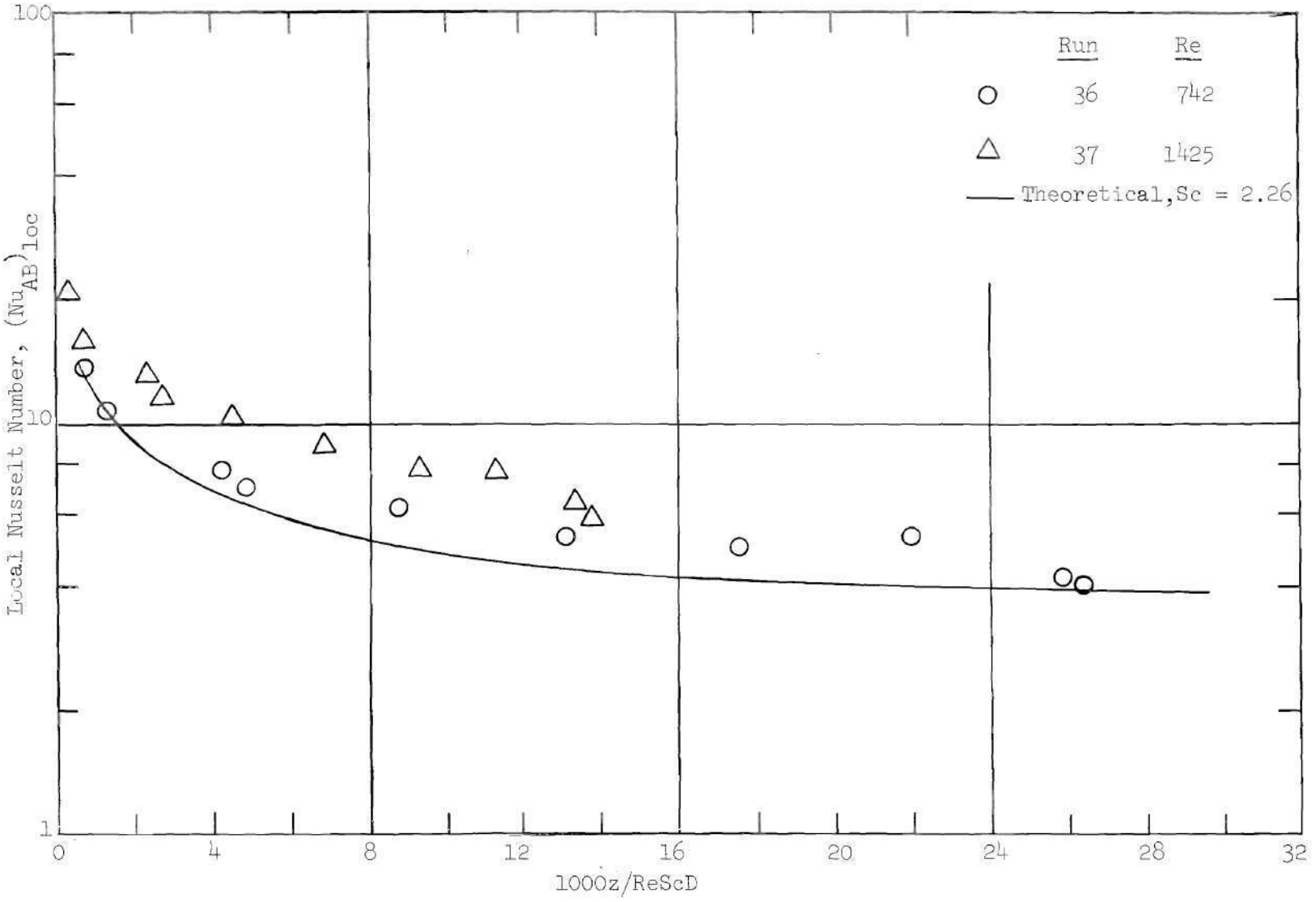

Figure 30. $(Nu_{AB})_{loc}$ Vertical Runs with Para-Dichlorobenzene at 30.9°C

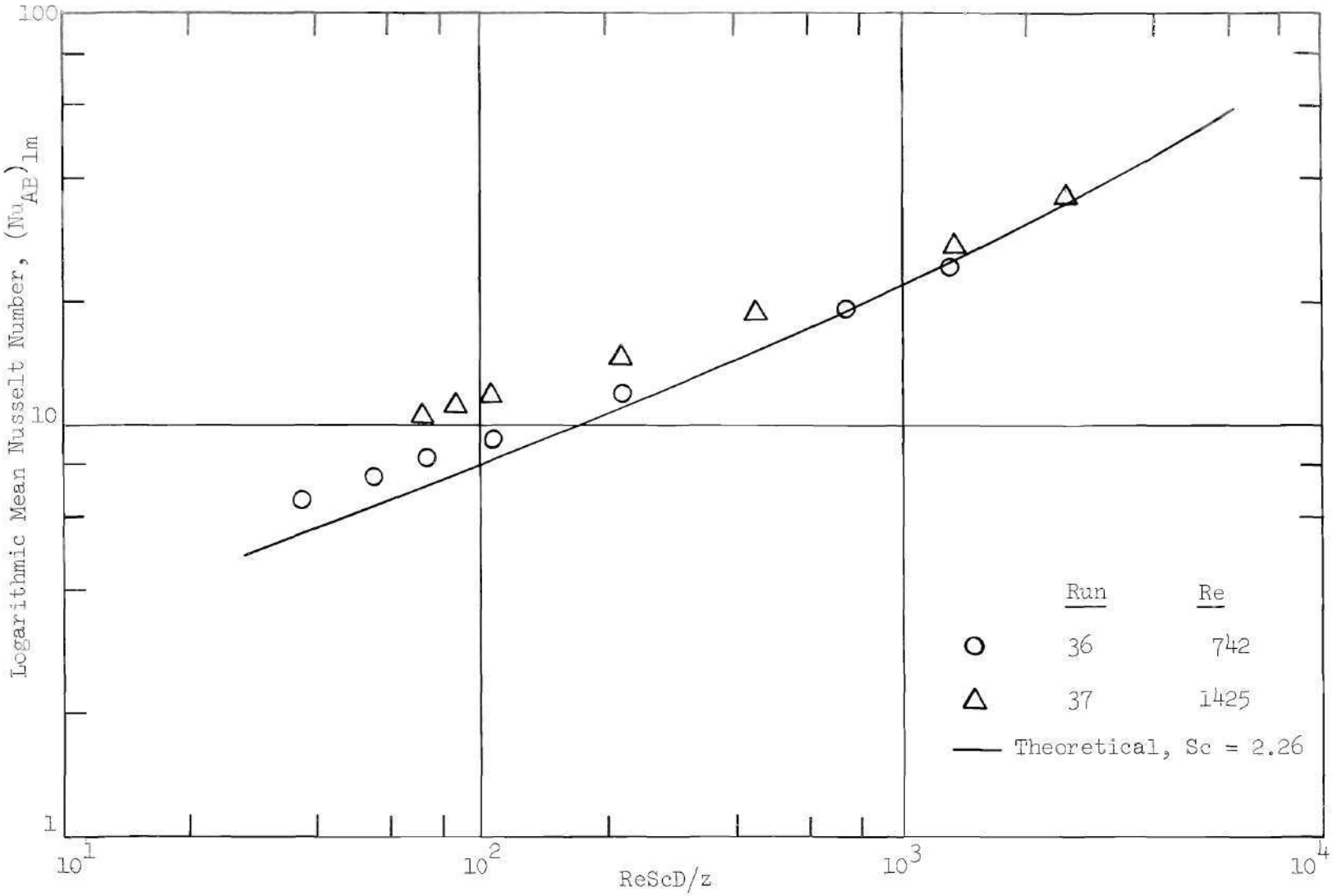

Figure 31. $(Nu_{AB})_{lm}$ for Vertical Runs with Para-Dichlorobenzene at 30.9°C

covered six organic liquids and water with air flowing both upward and downward. Boelter (22) showed that the above mentioned equation of Martinelli and Boelter (19) which takes free convection into account, could be used to obtain a correlation which is in fair agreement with the experimental data. While this represented a significant achievement, it did not explain why flow in both directions gives higher than theoretical results. For the results obtained in this study, the log mean Nusselt numbers for rod-like flow were found to correlate the experimental values near the end of the pipe quite well for the higher Grashof number runs. At lower Grashof numbers, the results fell between the rod-like and the developing flow solutions.

One explanation for the high Nusselt numbers found for the vertical runs might be a transition to turbulence caused by the natural convection forces. It has been established by several heat transfer investigations (23, 24, 25, 26) that a transition to turbulent flow occurs under certain conditions at Reynolds numbers considerably less than 2100. For heating in upflow, this phenomenon is associated with a reversal in flow at the center of the tube. For cooling in upflow, it is brought about by the velocity gradient at the wall becoming zero. Sheele, Rosen and Hanratty (25) also detected a certain asymmetry in the flow pattern for cooling water in upflow with constant wall temperature. The shift to asymmetric flow results in a region on one side of the tube in which there is essentially no flow, although occasionally backflow is observed. The appearance of either asymmetric or unstable flow could be correlated with the ratio of Grashof number to Reynolds number.

While the values of Gr_{AB}/Re covered in this study appear to be too low to result in a transition to turbulent flow, the fact that the flow is developing may change the picture considerably. Also, the fact that the test pipe almost certainly did not present as smooth an interior as those pipes used in heat transfer studies might have the effect of inducing disturbed or asymmetric regions to be formed.

45° Angle Runs

The local and logarithmic mean Nusselt numbers for the runs made at a 45° angle are presented in Figures 32 through 39. As in the vertical case, the measured Nusselt numbers would be expected to apply only to a pipe of similar dimensions to the one used in this study.

The free-convection forces encountered in this system might be expected to be a combination of those encountered for the vertical and horizontal cases. Although exceptions were found during many of the runs, the general trend appears to be that local values for the fluxes and Nusselt numbers agree more closely to the corresponding vertical values near the pipe entrance and more closely to the corresponding horizontal values further down the pipe. The considerable spread and overlapping found in the local results for the various pipe inclinations make it difficult to definitely establish this trend; however, the fact that it might occur does seem reasonable.

The overall results obtained for the 45° angle runs were essentially the same as those for the vertical and horizontal cases. Further data at higher Grashof numbers are required before any general conclusions can be reached as to the best way to predict entrance length Nusselt numbers for inclined pipes when free convection is a factor.

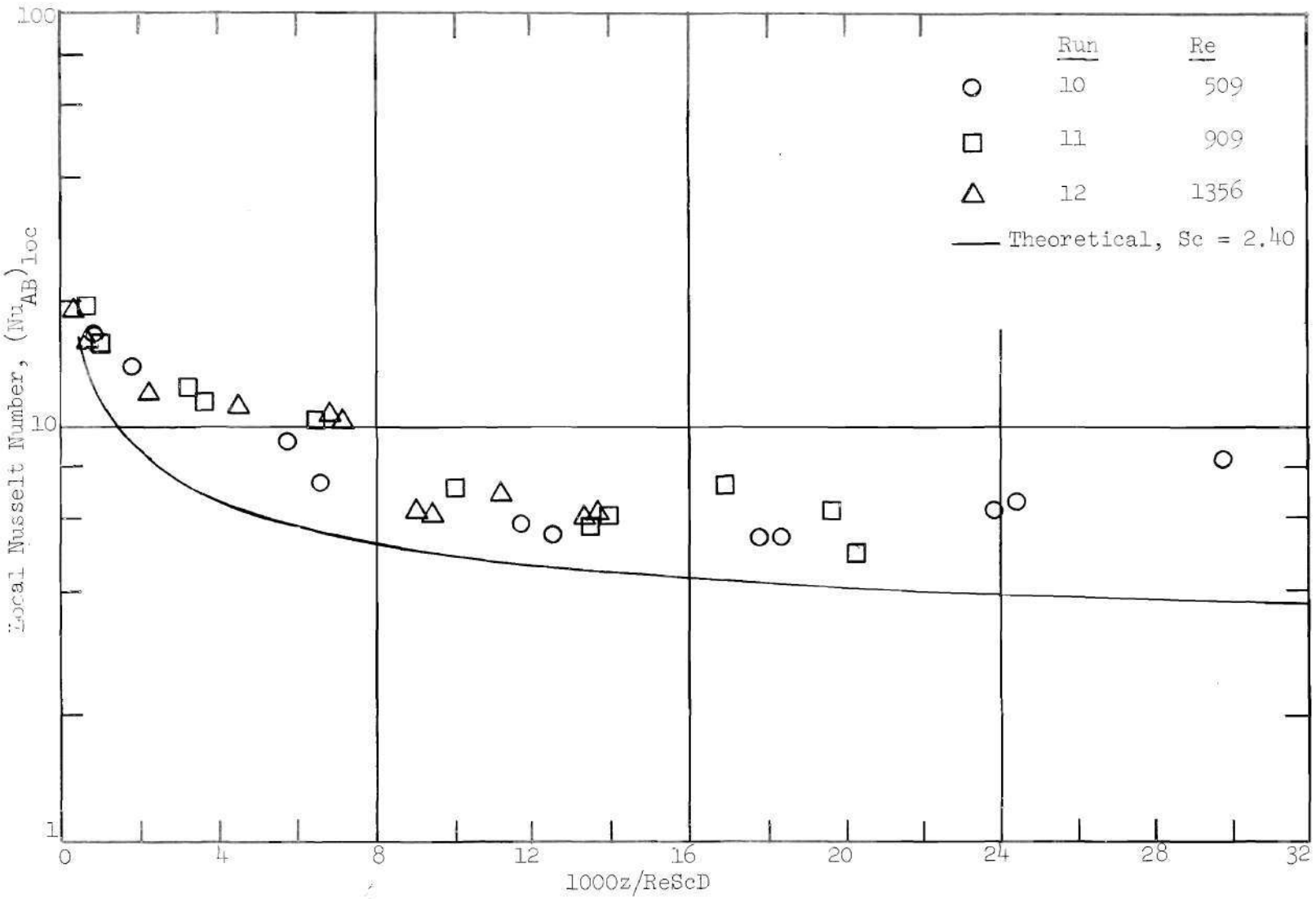

Figure 32. $(Nu_{AB})_{Loc}$ for 45° Angle Runs with Naphthalene at 50.0°C

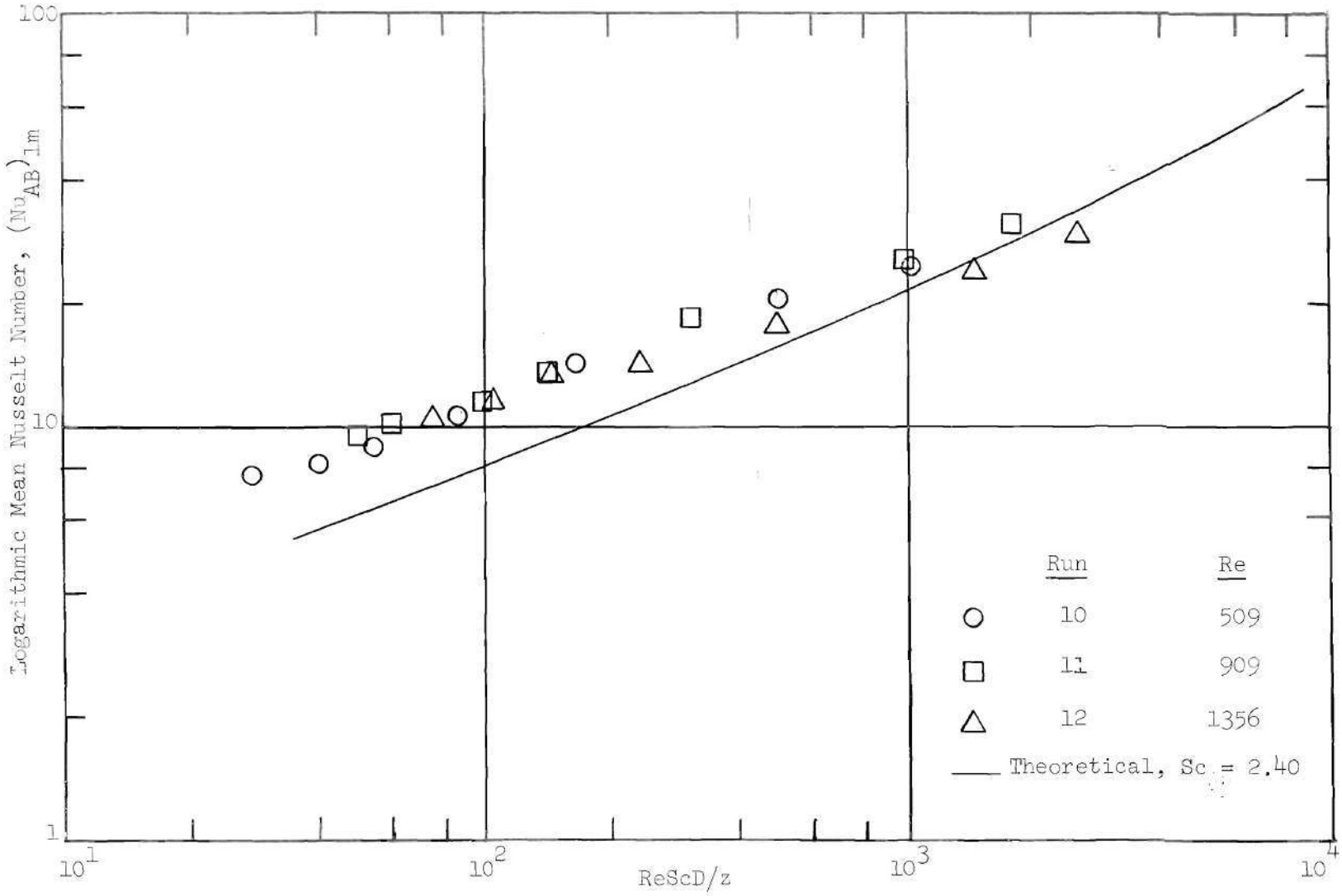

Figure 33. $(Nu_{AB})_{lm}$ for 45° Angle Runs with Naphthalene at 50.0°C

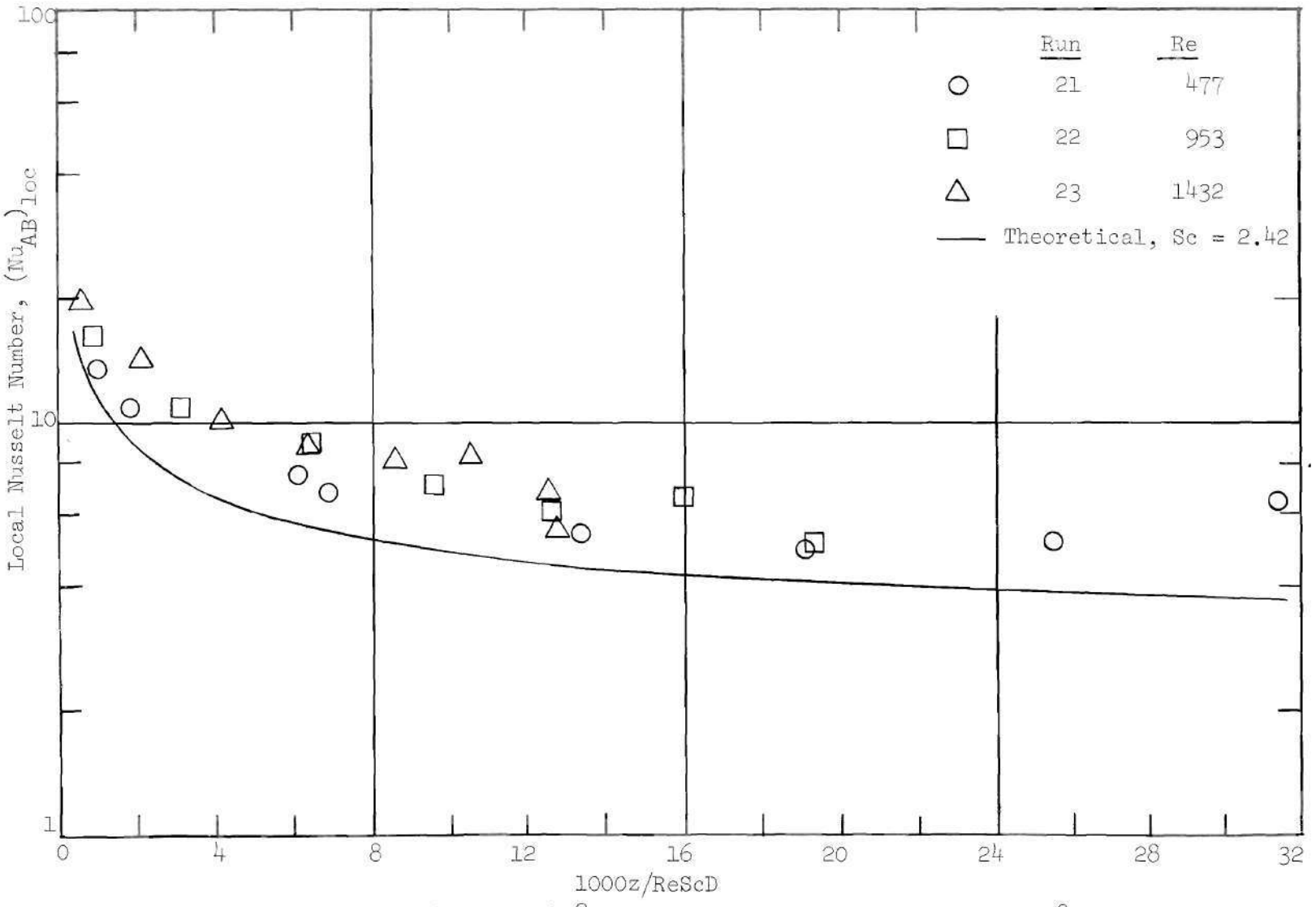

Figure 34. $(Nu_{AB})_{loc}$ for 45° Angle Runs with Naphthalene at 38.2°C

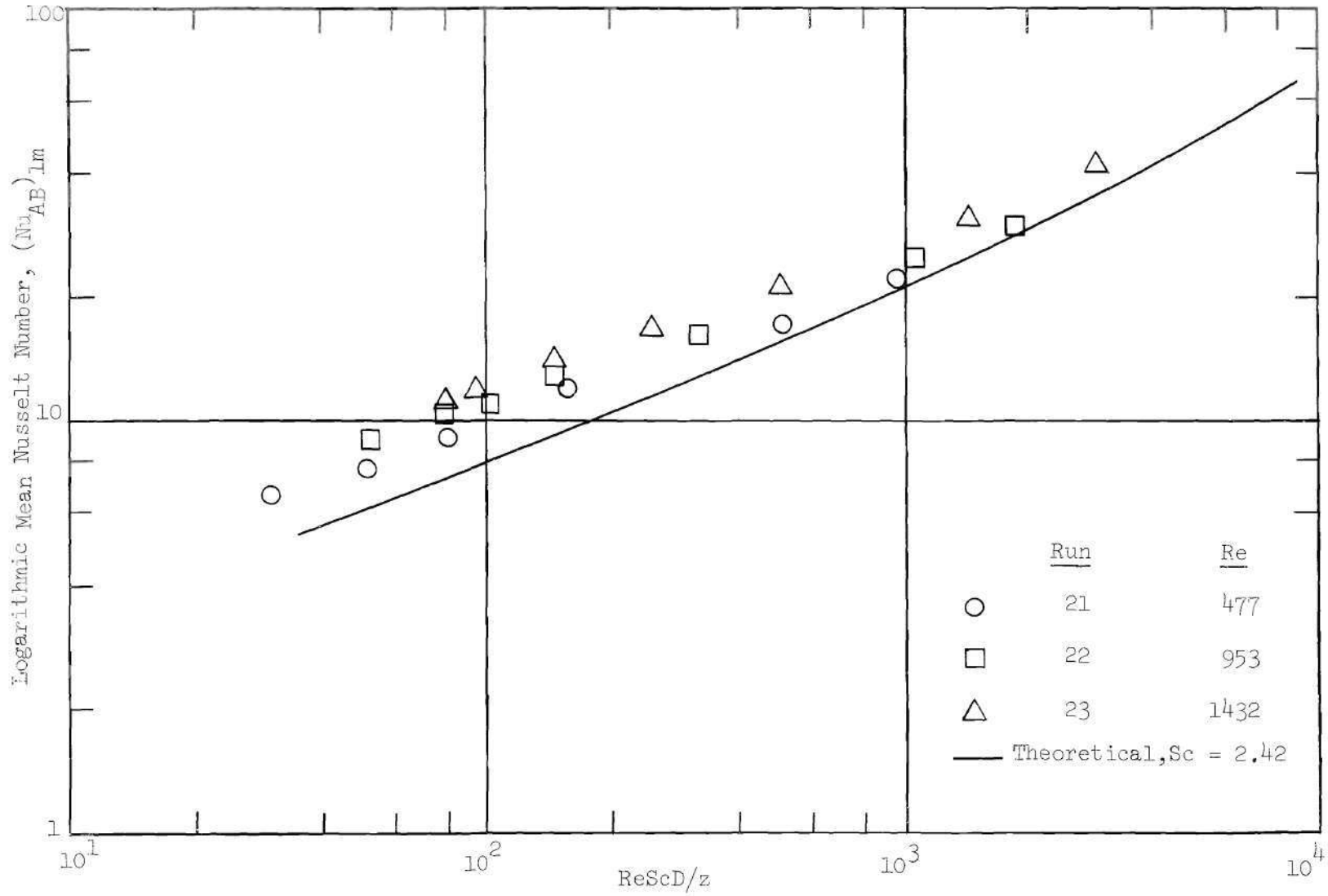

Figure 35. $(Nu_{AB})_{lm}$ for 45° Angle Runs with Naphthalene at 38.2°C

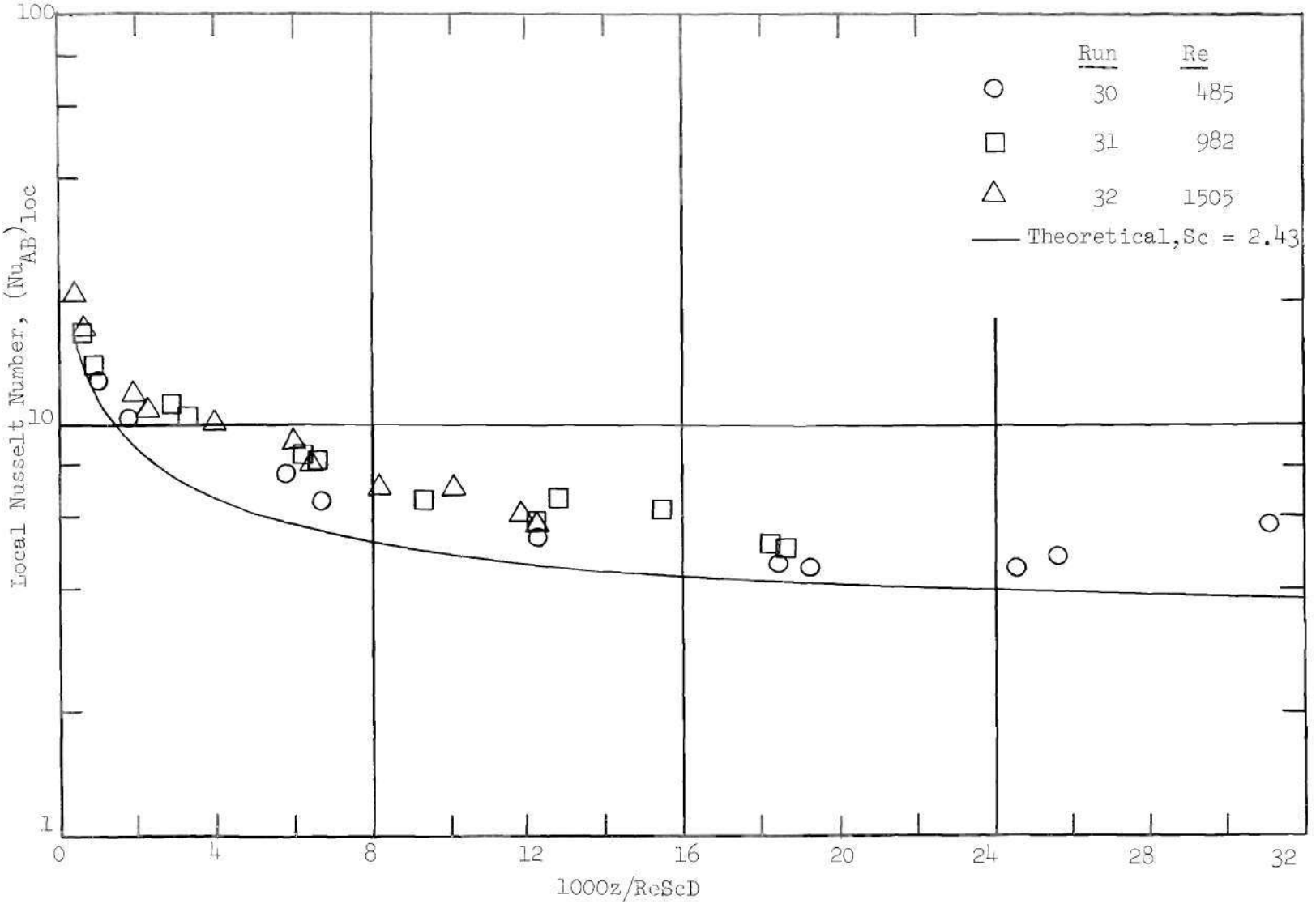

Figure 36. $(Nu_{AB})_{loc}$ for 45° Angle Runs with Naphthalene at 30.9°C

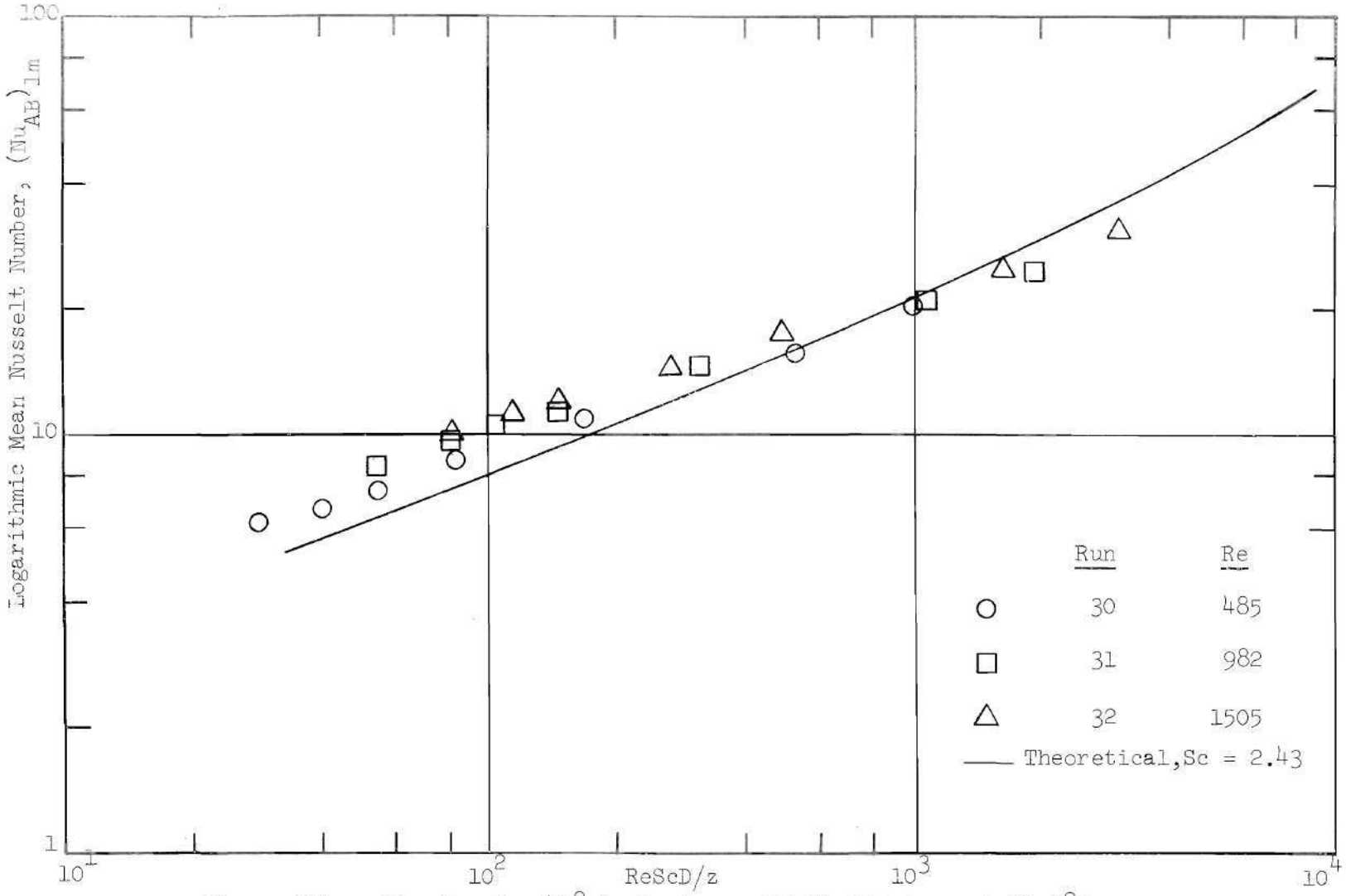

Figure 37. $(Nu_{AB})_{lm}$ for 45° Angle Runs with Naphthalene at 30.9°C

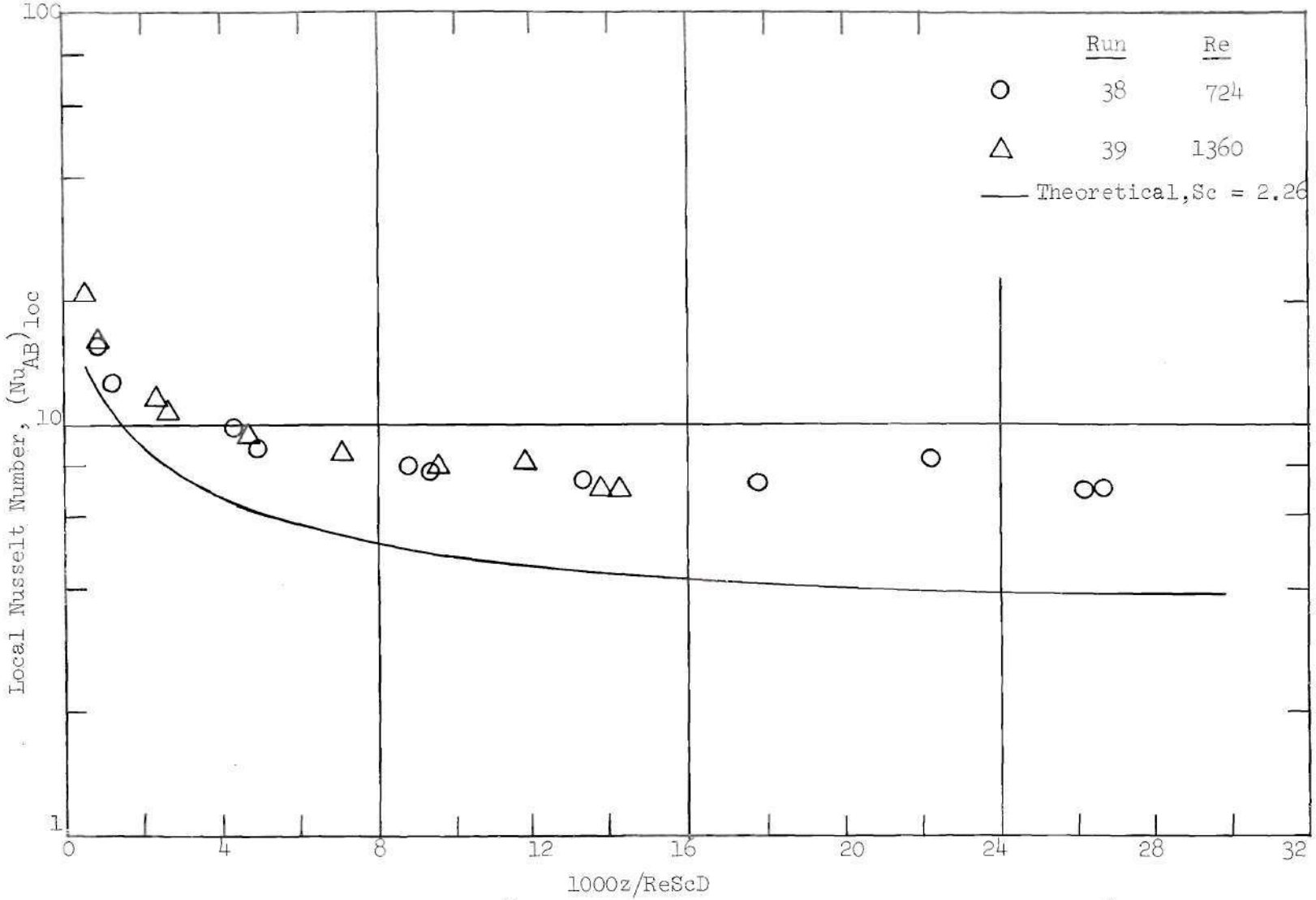

Figure 38. $(Nu_{AB})_{loc}$ 45° Angle Runs with Para-Dichlorobenzene at 30.9°C

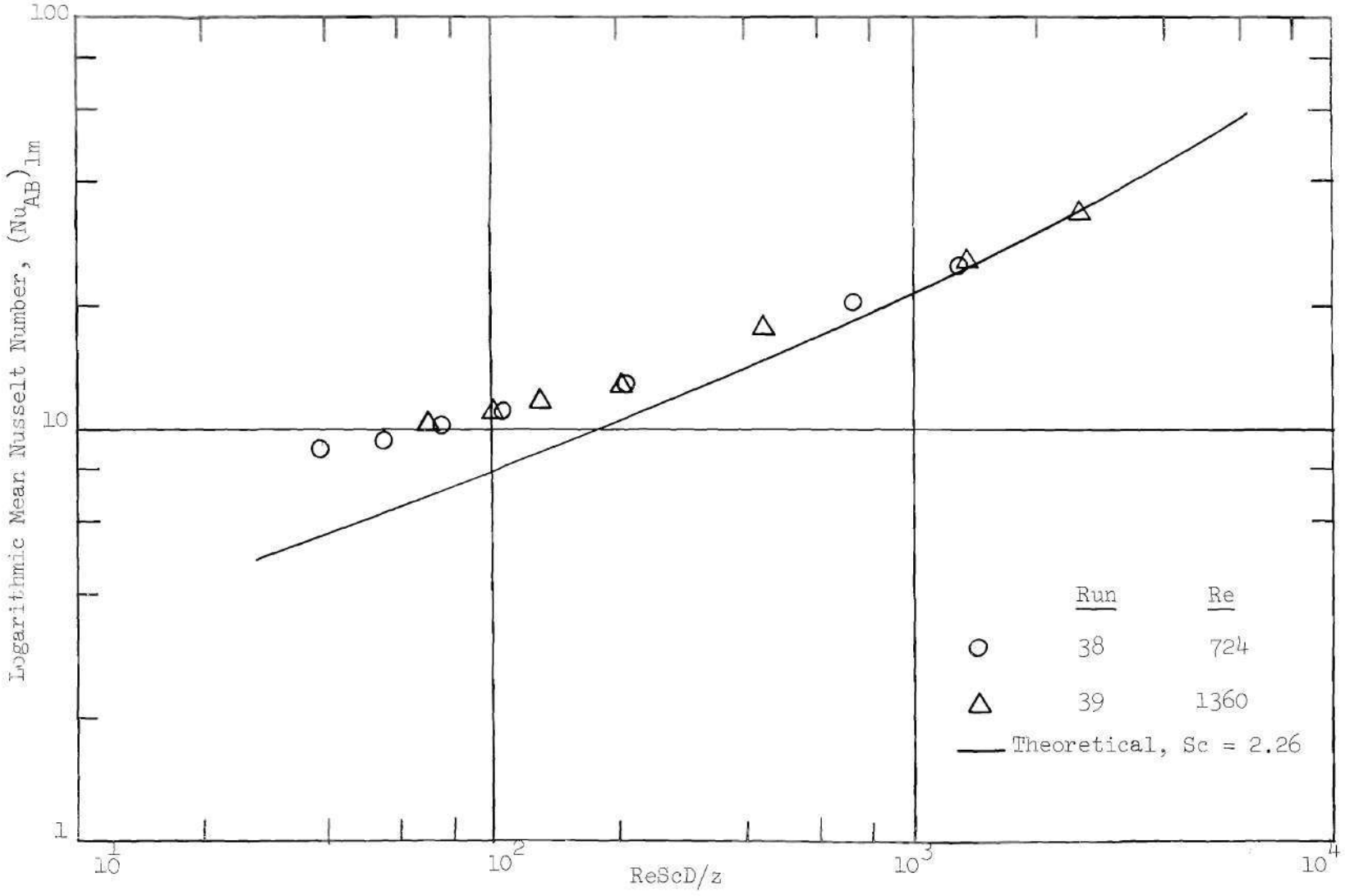

Figure 39. $(Nu_{AB})_{lm}$ for 45° Angle Runs with Para-Dichlorobenzene at 30.9°C

Over the limited range studied, it appears that any methods developed for use for the horizontal or the vertical cases could be used for the 45° inclination case without serious error.

Concentration Measurement Results

The experimental results are shown in Figures 40 through 45 and are presented in Table 60, Appendix C. Curves representing the theoretical concentration profile for the particular axial location are also shown on the figures.

Unfortunately, difficulties encountered in developing a reliable experimental technique did not allow the complete range of test conditions to be studied. However, from the limited results obtained, several interesting relations can be seen. All the profiles show considerably higher concentrations near the center of the pipe than predicted by theory. Agreement with the theoretical solution appears to be much better at positions near the wall. Runs at higher Reynolds numbers show more flattening of the profile than those for lower Reynolds numbers. This is in qualitative agreement with the results of the mass transfer runs, which showed higher deviations from theory for higher Reynolds numbers.

The data presented for the vertical run, No. 29, show an almost perfectly symmetrical profile while the 45° angle run, No. 30, shows slight asymmetry, having higher concentrations near the top wall. The horizontal runs exhibit somewhat more asymmetry, however, the direction of skewness is not always the same. Preliminary results obtained during the 50° C runs indicate the same flattening of the profile and much more skewness than the results reported here for 38.2° C and 30.9° C.

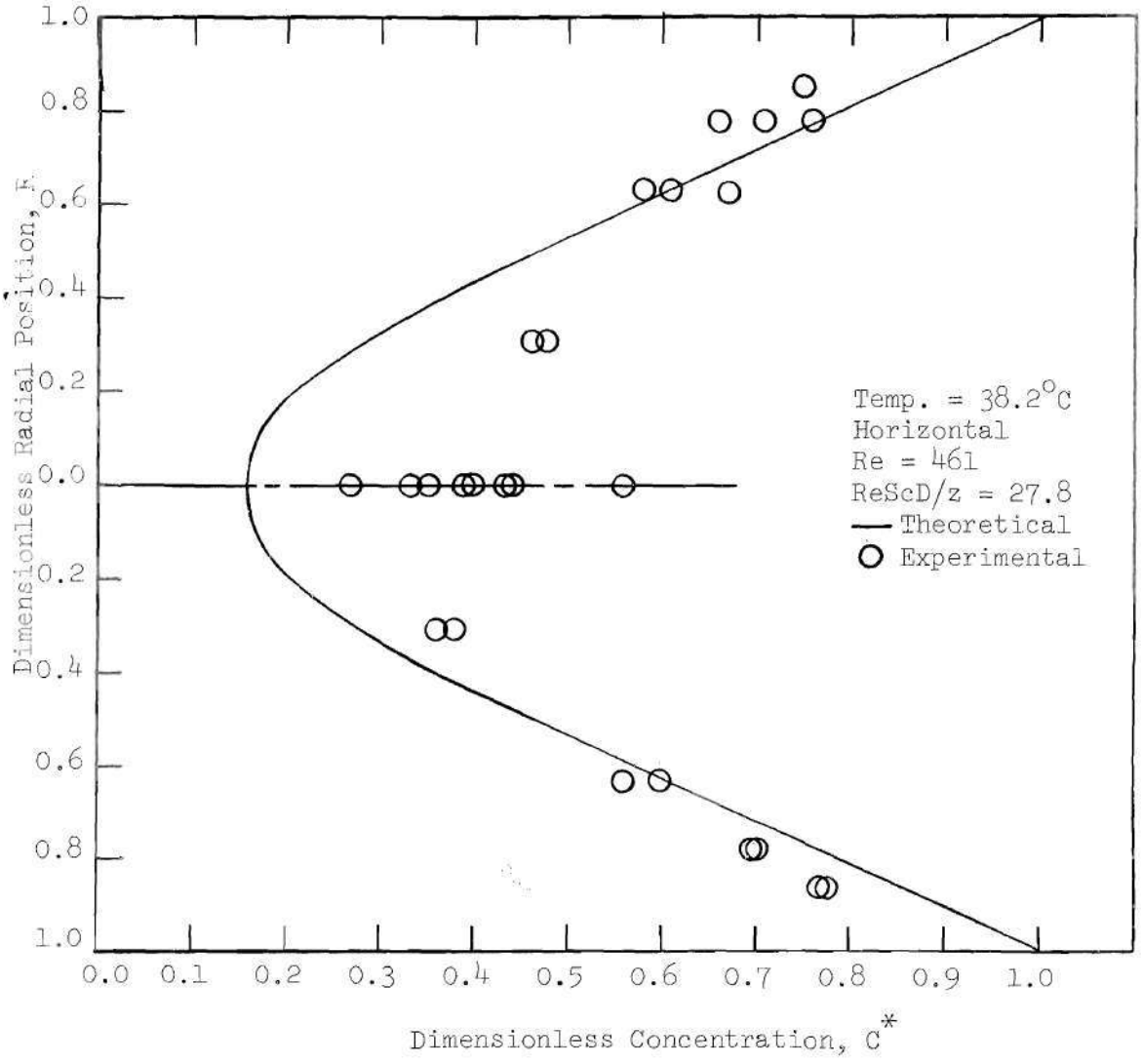

Figure 40. Concentration Profile for Run No. 13

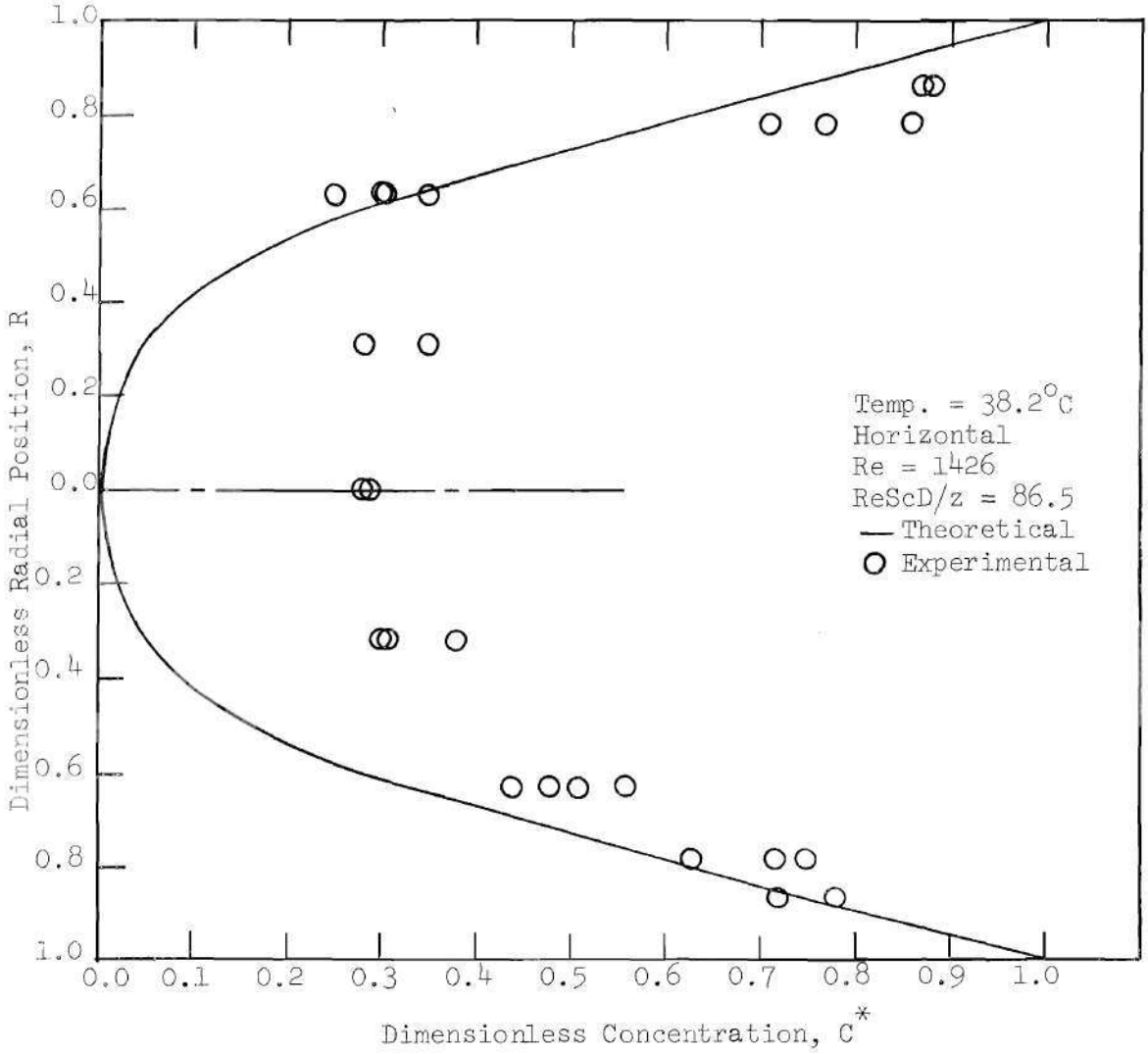

Figure 41. Concentration Profile for Run No. 16

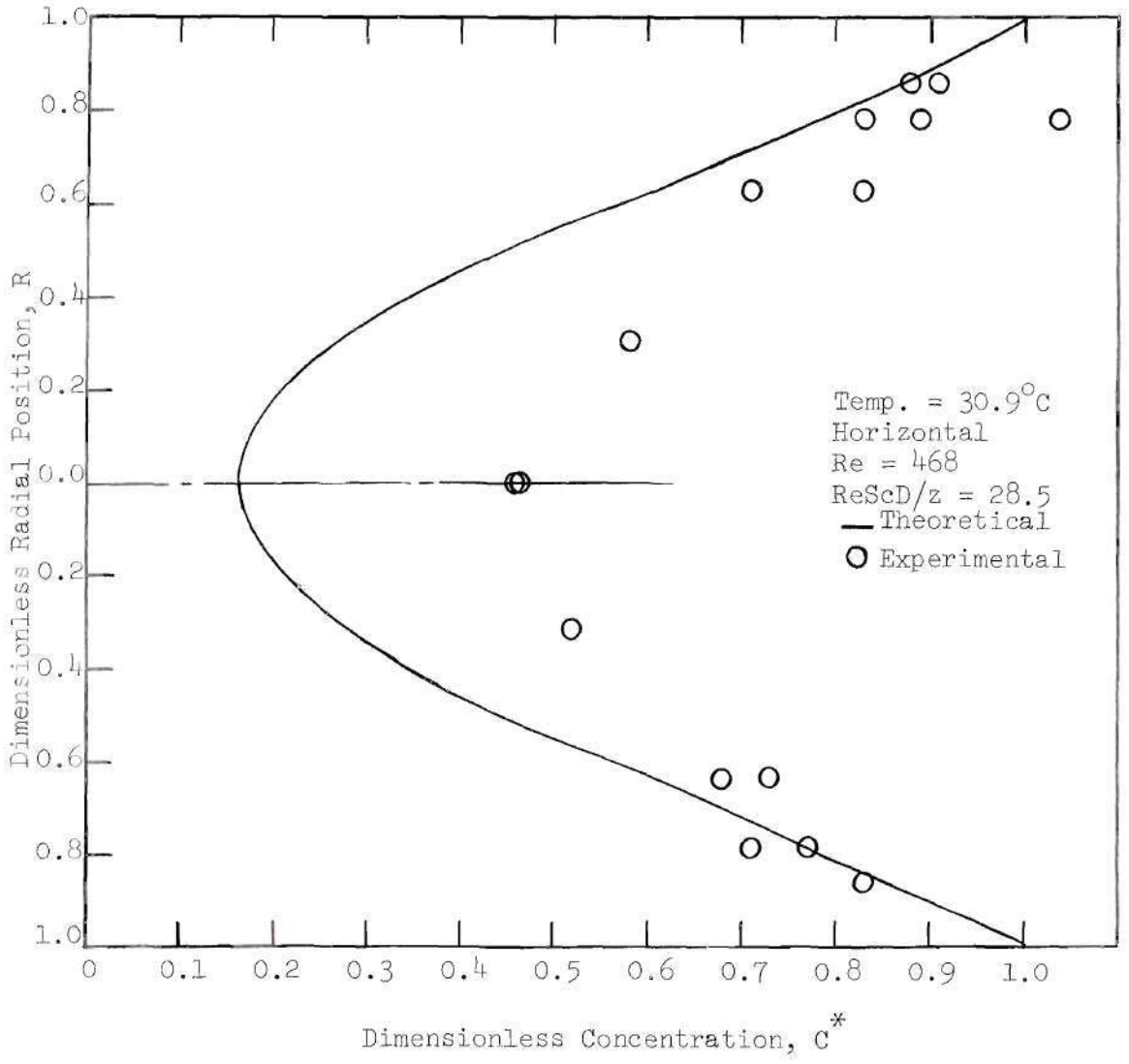

Figure 42. Concentration Profile for Run No. 24

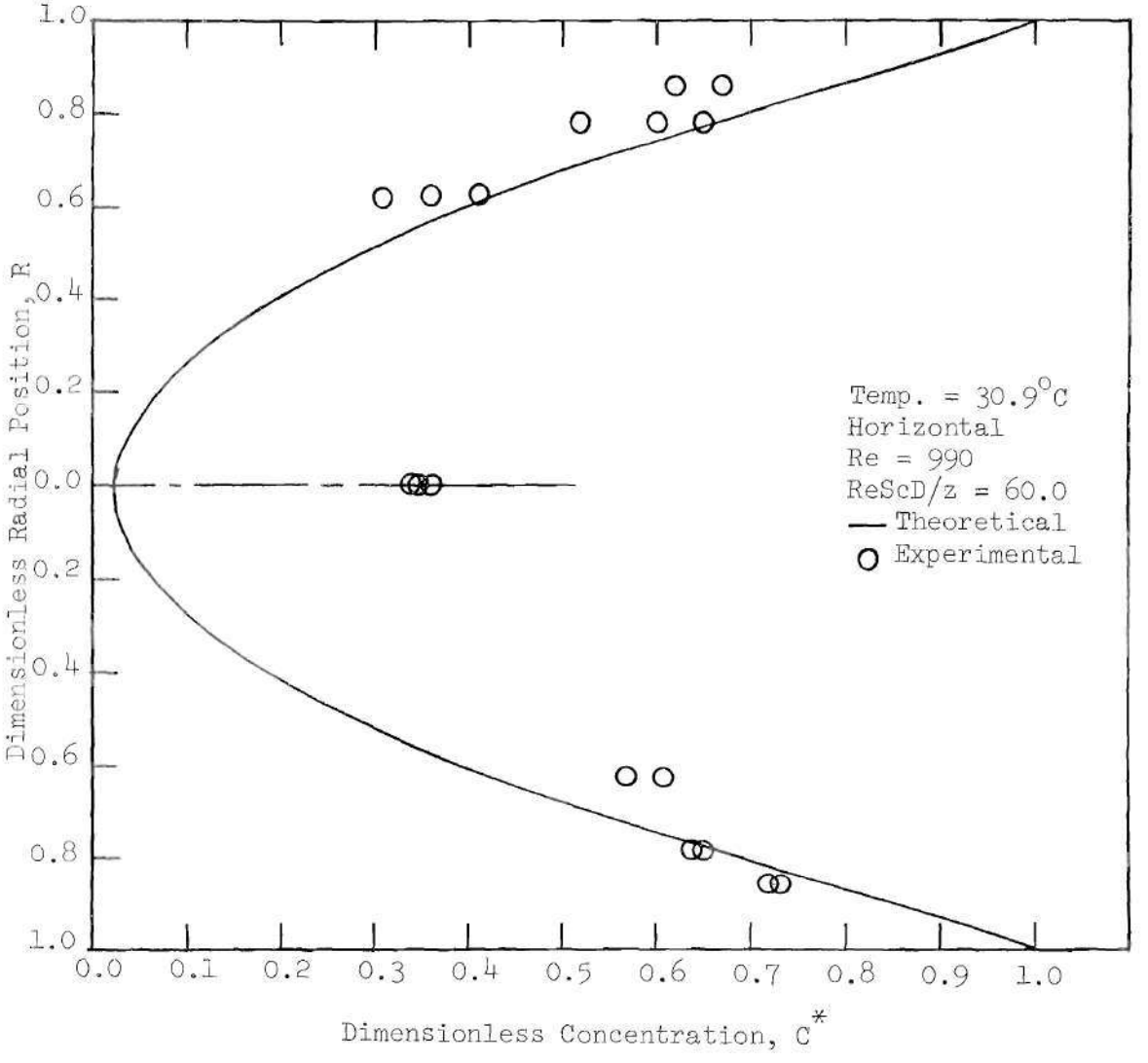

Figure 43. Concentration Profile for Run No. 25

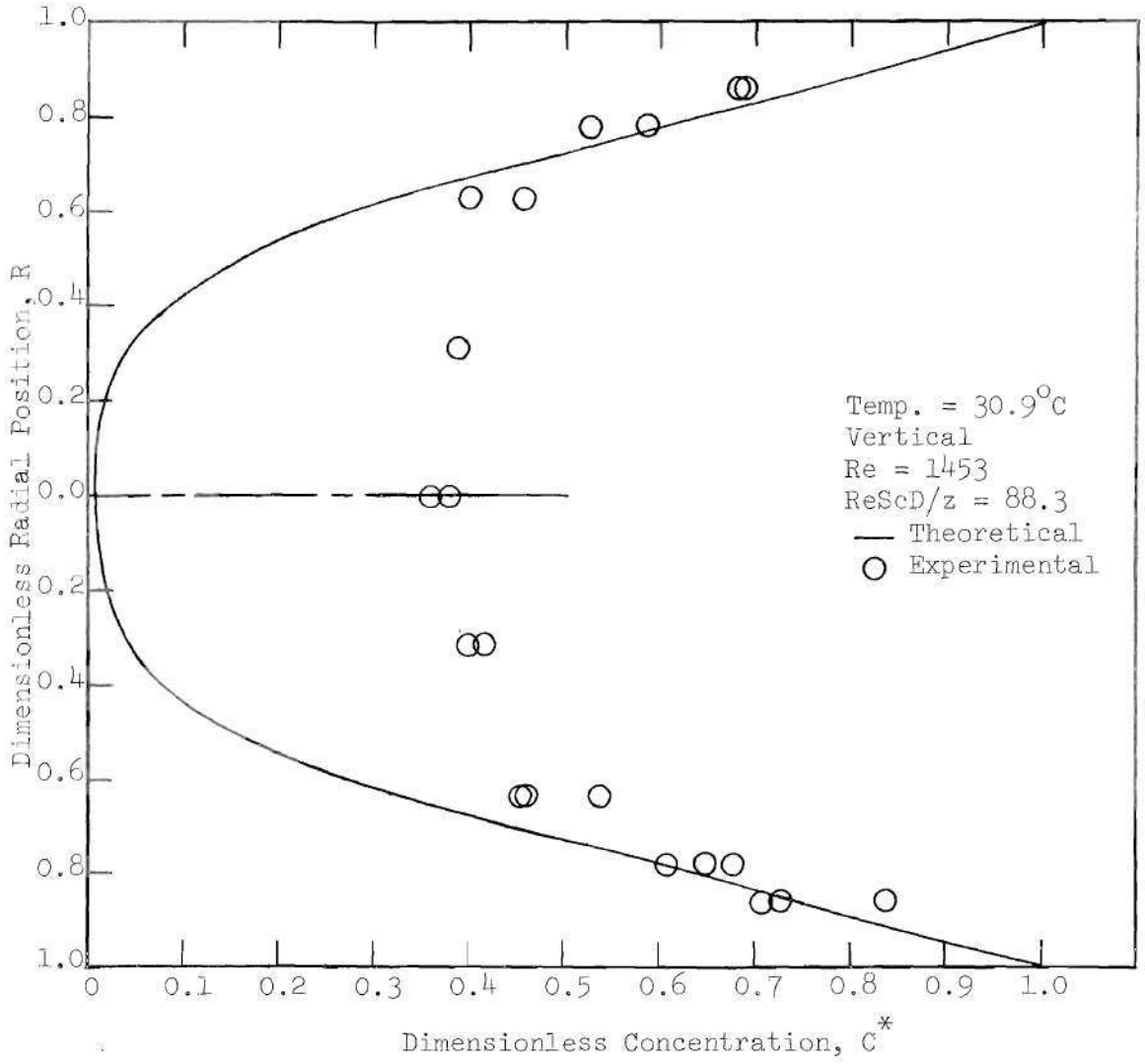

Figure 44. Concentration Profile for Run No. 29

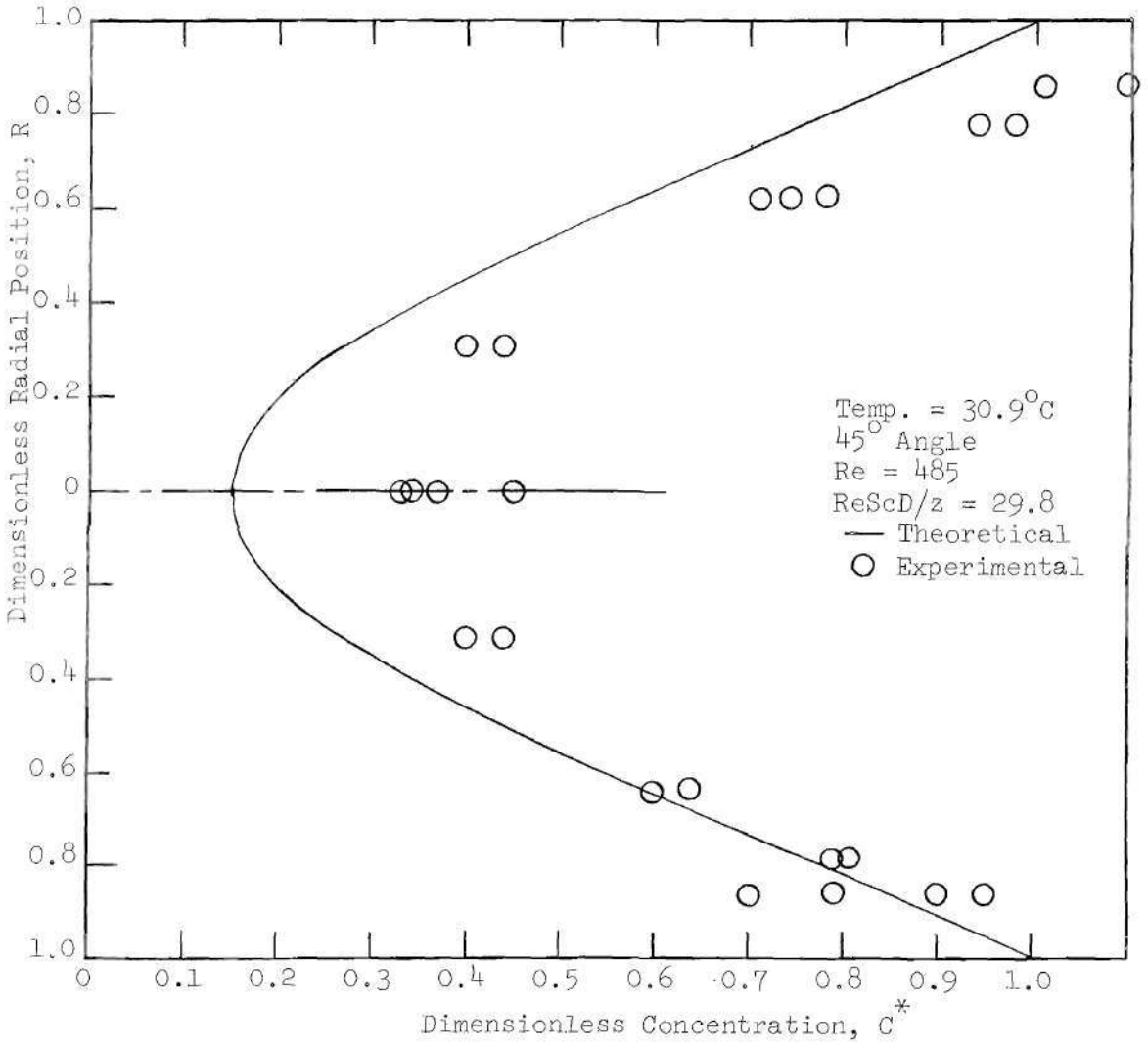

Figure 45. Concentration Profile for Run No. 30

The spread in the measured concentrations found at some locations appears to be much higher than would be expected even with the admittedly high experimental errors involved in the measurements. It is suggested that this is the result of slight variations with time in such operating parameters as air flow rate or pipe temperature which result in much larger changes in free convection currents at these locations.

For the run showing the symmetrical profile (Run No. 29), it was possible to obtain a value of the dimensionless bulk concentration C_b^*. This was done by first assuming the velocity profile at the appropriate ReScD/z to be that given by the theoretical solution. This velocity profile and the measured concentrations were then used in the numerical integration of an expression similar to equation (2-20). The C_b^* based on concentration measurements was compared to the C_b^* based on weight loss measurements at the same axial location. The results for C_b^* were 0.47 for the concentration measurements and 0.38 for the weight loss measurements. At the same location, the value of C_b^* from the theoretical solution was 0.29. The agreement in results for the two experimental techniques is within the estimated experimental errors and, considering the uncertainty in the velocity profile used, is felt to be quite adequate.

Since concentration measurements bear roughly the same relation to mass transfer experiments as temperature measurements do to heat transfer experiments, the need for more advanced methods for accurately determining concentration can be seen. The method described in this study, which is considered subject to much refinement, was an attempt to meet this need. Quite apart from the data taken on the particular system under study, it is felt that a major result of this work has been to demonstrate

the possibility of using concentration measuring techniques of this type to gain further insight into mass transfer processes.

CHAPTER VIII

CONCLUSIONS AND RECOMMENDATIONS

Based on the experimental results obtained during this study, the following conclusions are reached:

1. Measured mass transfer rates and Nusselt numbers for the entrance region are higher than predicted by a theoretical solution which assumes constant fluid properties.

2. More deviation from the theoretical solution was noted for runs having higher Grashof numbers indicating free convection is a major cause of the deviation.

3. The negative mass fluxes reported by Bosworth (6) for certain axial locations in the entrance region were not found to occur for any of the runs conducted during this study.

4. Over the range of variables studied, available heat transfer correlations which assume fully-developed flow give results which are too low when applied to mass transfer in the entrance length.

5. For Grashof numbers over 7000, the heat transfer correlation of Jackson, Spurlock and Purdy (16) represents the experimental mass transfer Nusselt numbers for horizontal flow quite well.

6. Over the range studied, very little difference in the overall mass transfer rate was noted for runs which were horizontal, vertical with upflow or at a 45° angle with upflow.

7. The method described to measure concentration profiles appears to work satisfactorily for the naphthalene-air system although

considerable room for improvement is noted.

8. Based on concentration profile measurements for the naphthalene-air runs, the concentrations near the center of the pipe were found to be considerably higher than predicted by the constant property theoretical solution.

Recommendations for future study in this area are:

1. The collection of more experimental data covering a wider range of Grashof numbers for entrance length heat and mass transfer. These results are necessary before meaningful correlations which include free convection effects can be made.

2. Further studies to determine if turbulence induced by free-convection effects is the cause of the higher mass transfer rates measured.

3. The extension of variable property theoretical solutions for heat and mass transfer to include the entrance region in horizontal flow.

4. Further work in the development of concentration measuring techniques. Refinements in the method described in this study which would lead to more reliable and more easily obtainable results would be most useful in future mass transfer studies.

APPENDICES

APPENDIX A

NUMERICAL SOLUTION OF THE MATHEMATICAL MODEL

General

The numerical solution of equations (2-4), (2-5) and (2-6) and their appropriate boundary conditions was accomplished by use of a Burroughs B-5500 digital computer. The equations were first put in finite difference form using an imaginary grid over the flow field. In a procedure advancing stepwise down the pipe, the system of linear difference equations resulting from equations (2-4) and (2-5) was first solved for values of axial and radial velocities at each grid point. These values were then used in the system of linear difference equations resulting from equation (2-6) to obtain a solution for the dimensionless concentration at each grid point.

Finite Difference Representation of Equations

The finite difference representation of the derivatives appearing in equations (2-4), (2-5) and (2-6) is similar to that used by Hornbeck, Rouleau and Osterle (27). If a grid is imposed on the flow field as shown in Figure 22, the following difference representations are used in equations (2-4) at any point $j+1,k(n < k < 1)$:

$$\frac{\partial U}{\partial Z} = \frac{U_{j+1,k} - U_{j,k}}{\Delta Z} \tag{A-1}$$

$$\frac{\partial U}{\partial R} = \frac{U_{j+1,k+1} - U_{j+1,k-1}}{2\Delta R} \tag{A-2}$$

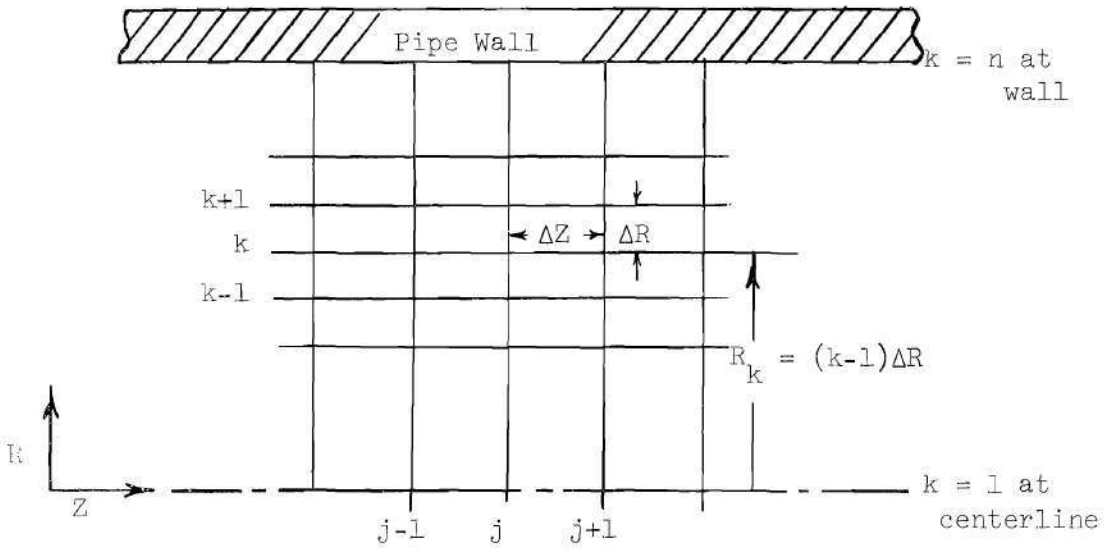

Figure 46. Grid Layout in Pipe

$$\frac{\partial^2 U}{\partial R^2} = \frac{U_{j+1,k+1} - 2U_{j+1,k} + U_{j+1,k-1}}{(\Delta R)^2} \tag{A-3}$$

$$\frac{\partial P}{\partial Z} = \frac{P_{j+1} - P_j}{\Delta Z} \tag{A-4}$$

This leads to the following finite difference equation

$$\alpha_{jk} U_{j+1,k-1} + \beta_{jk} U_{j+1,k} + \gamma_{jk} U_{j+1,k+1} + \eta_j P_{j+1} = \phi_{jk} \tag{A-5}$$

where

$$\alpha_{jk} = \frac{1}{2R_k \Delta R} - \frac{V_{jk}}{2\Delta R} - \frac{1}{(\Delta R)^2} \tag{A-6}$$

$$\beta_{jk} = \frac{2}{(\Delta R)^2} + \frac{U_{jk}}{\Delta Z} \tag{A-7}$$

$$\gamma_{jk} = \frac{V_{jk}}{2(\Delta R)} - \frac{1}{(\Delta R)^2} - \frac{1}{2R_k(\Delta R)} \tag{A-8}$$

$$\eta_{jk} = 1/\Delta Z \tag{A-9}$$

$$\phi_{jk} = \frac{U_{jk}^2 + P_j}{\Delta Z} \tag{A-10}$$

For any point j+1, 1, the following difference equation is used

$$\alpha_1 U_{j+1,0} + \beta_1 U_{j+1,1} + \eta_1 P_{j+1} = \phi_1 \tag{A-11}$$

where

$$\alpha_1 = \frac{U_{j,0}}{\Delta Z} + \frac{4}{(\Delta R)^2} \tag{A-12}$$

$$\beta_1 = \frac{-4}{(\Delta R)^2} \tag{A-13}$$

$$\eta_1 = \frac{1}{\Delta Z} \tag{A-14}$$

$$\phi_1 = \frac{U_{j,o}^2 + P_j}{\Delta Z} \tag{A-15}$$

For equation (2-5), the following difference representations are used for any point $j+1,k(n < k < 1)$:

$$R \frac{\partial U}{\partial Z} = \frac{R_k(U_{j+1,k} - U_{j,k}) + R_{k+1}(U_{j+1,k+1} - U_{j,k+1})}{2(\Delta Z)} \tag{A-16}$$

$$\frac{\partial(VR)}{\partial R} = \frac{V_{j+1,k+1}R_{k+1} - V_{j+1,k}R_k}{\Delta R} \tag{A-17}$$

where $R_k = (k - 1)\Delta R$

Substituting these values in equation (2-5) results in

$$\frac{R_k(U_{j+1,k} - U_{j,k})}{2(\Delta Z)} + \frac{R_{k+1}(U_{j+1,k+1} - U_{j,k+1})}{2\Delta Z}$$

$$+ \frac{V_{j+1,k+1}R_{k+1} - V_{j+1,k}R_k}{\Delta R} = 0 \tag{A-18}$$

For the point $j+1,1$ equation (2-5) is represented by

$$\frac{U_{j+1,2} + U_{j+1,1} - U_{j,2} - U_{j,1}}{2(\Delta Z)} + \frac{2V_{j+1,2}}{\Delta R} = 0 \tag{A-19}$$

Addition of equation (A-19) and equation (A-18) written for each k from

2 to (n-1) results in

$$\left(\frac{\Delta Z}{\Delta R}\right) V_w(Z) + \sum_{k=3}^{n} R_k U_{j+1,k} + \frac{3R_2}{4} U_{j+1,2} + \frac{1R_2}{4} U_{j+1,1}$$

$$= \sum_{k=3}^{n} R_k U_{j,k} + \frac{3R_2}{4} U_{j,2} + \frac{1R_2}{4} U_{j,1} \qquad \text{(A-20)}$$

since $V_w(Z) = V_{j+1,n}$.

Equation (A-20) may be rearranged to give

$$\sum_{k=3}^{n} R_k U_{j+1,k} + \frac{3R_2}{4} U_{j+1,2} + \frac{1R_2}{4} U_{j+1,1} = \Psi_{j+1} \qquad \text{(A-21)}$$

where

$$\Psi_{j+1} = \sum_{k=3}^{n} R_k U_{j,k} + \frac{3R_2}{4} U_{j+1,2} + \frac{1R_2}{4} U_{j+1,1} - \left(\frac{\Delta Z}{\Delta R}\right) V_w(Z) \qquad \text{(A-22)}$$

If the derivatives in equation (2-6) are represented by

$$\frac{\partial C^*}{\partial Z} = \frac{C^*_{j+1,k} - C^*_{j,k}}{Z} \qquad \text{(A-23)}$$

$$\frac{\partial C^*}{\partial R} = \frac{C^*_{j+1,k+1} - C^*_{j+1,k-1}}{(\Delta R)^2} \qquad \text{(A-24)}$$

$$\frac{\partial^2 C^*}{\partial R^2} = \frac{C^*_{j+1,k+1} - 2C^*_{j+1,k} + C^*_{j+1,k-1}}{(\Delta R)^2} \qquad \text{(A-25)}$$

for any point $j+1,k (n > k > 1)$, the following finite difference equation

is obtained:

$$\alpha'_{jk} C^{*}_{j+1,k-1} + \beta'_{jk} C^{*}_{j+1,k} + \gamma'_{jk} C^{*}_{j+1,k+1} = \phi'_{jk} \tag{A-26}$$

where

$$\alpha'_{jk} = \frac{1}{2R_k(\Delta R)} - \frac{1}{(\Delta R)^2} - \frac{(Sc)V_{j+1,k}}{2(\Delta R)} \tag{A-27}$$

$$\beta'_{jk} = \frac{(Sc)U_{j+1,k}}{\Delta Z} + \frac{2}{(\Delta R)^2} \tag{A-28}$$

$$\gamma'_{jk} = \frac{(Sc)V_{j+1,k}}{2(\Delta R)} - \frac{1}{(\Delta R)^2} - \frac{1}{2R_k(\Delta R)} \tag{A-29}$$

$$\phi'_{jk} = \frac{(Sc)U_{j+1,k}}{\Delta Z} C^{*}_{jk} \tag{A-30}$$

For the point j+1,1 the following difference equation is used:

$$\beta'_1 C^{*}_{j+1,1} + \gamma'_1 C^{*}_{j+1,2} = \phi'_1 \tag{A-31}$$

where

$$\beta'_1 = \frac{(Sc)U_{j+1,1}}{\Delta Z} + \frac{4}{(\Delta R)^2} \tag{A-32}$$

$$\gamma'_1 = \frac{-4}{(\Delta R)^2} \tag{A-33}$$

$$\phi_1' = \frac{(Sc)U_{j+1,1}}{\Delta Z} C^*_{j,1} \qquad (A\text{-}34)$$

In order to calculate the molal mass flux and the radial velocity at the wall, it is necessary to evaluate the concentration gradient at the wall, $\frac{\partial C^*}{\partial R}\Big|_{R=1,Z}$. The expression used to evaluate the gradient for the j+1 axial position was

$$\frac{\partial C^*}{\partial R}\Big|_{R=1} = \frac{-\ln C^*_{j+1,n-1}}{\Delta R} \qquad (A\text{-}35)$$

This expression is based on assuming a concentration profile near the wall of the form

$$C^* = Ae^{B(R-1)} \qquad (A\text{-}36)$$

A,B = functions of Z only

The concentration gradient at the wall, B, was evaluated from a knowledge of the concentration at a position ΔR away from the wall.

The use of an expression of the form of equation (A-36) was made in an effort to increase $\frac{\partial C^*}{\partial R}\Big|_{R=1}$, and thus N_{Aw}, near the pipe entrance. Earlier attempts to obtain the gradient by assuming a parabolic form for the concentration profile near the wall resulted in N_{Aw} being too low near the entrance. The effect of this was an inconsistency in a step-by-step mass balance. The mass balance is discussed later in this appendix. The expression for the gradient given in equation (A-35) resulted in improved agreement in the mass balance near the entrance. Further downstream, it gives results which are in close agreement to the results obtained using the parabolic form.

By combining equations (2-14) and (2-15), it may be shown that the radial velocity at the wall is

$$V_w(Z) = \frac{M_A(C_{Aw} - C_{Ao})}{\rho Sc} \frac{\partial C^*}{\partial R} \Bigg| R = 1,Z \qquad (A\text{-}37)$$

Thus for Z corresponding to the j+1 axial position

$$V_w = \frac{M_A(C_{Aw} - C_{Ao})(-\ln C^*_{j+1,n-1})}{\rho Sc \quad \Delta R} \qquad (A\text{-}38)$$

Solution of the Difference Equations

Let us assume that values are known for U, V, P and C^* for each radial position $k(n > k > 1)$ at the axial position j. It is desired to step down the pipe and solve for these values at the j+1 position which is a known distance, ΔZ, away.

Equation (A-5) for each k from k = 2 to k = n-1, equation (A-11) for k = 1, and equation (A-21), constitute a system of n equations in n unknowns, $U_{j+1,k}(n-1 > k > 1)$ and P_{j+1}. In applying equation (A-21), a first approximation is used by assuming V_w at j+1 is equal to V_w at j. This system of equations is solved by using Gauss elimination and back substitution.

Next, values of the radial velocity at j+1 are determined for k = 2, to k = n by direct substitution in equations (A-19) and (A-18) of the known values of axial velocity.

Using known values of U and V at the j+1 position, C^* at the j position, and the Schmidt number for the system, equation (A-26) may be written for each point j+1, $k(n > k > 1)$. At the point j+1, 1, equation

(A-31) is used. This results in a tridiagonal system of equations which may be solved for the unknowns $C^*_{j+1,1}$ to $C^*_{j+1,n-1}$ by the method outlined in reference (28).

The dimensionless concentration gradient at the wall $\left.\frac{\partial C^*}{\partial R}\right|_{R=1}$ is then determined using equation (A-35) and V_w at j+1 is calculated from equation (A-37). A test is then made to determine if the new value of V_w is within a required tolerance (in this study, 2 per cent) of the first approximation of V_w used. If not, the method is repeated using the new value of V_w as the next approximation in equation (A-22) until successive values of V_w are within the required tolerance. Since values of U, V, C^* and P are known at the j+1 axial position, one is now able to make the next step down the pipe.

Numerical Solution for Other Variables

At each step down the pipe, several other quantities were evaluated before moving on to the next step. The molal mass flux at the wall was determined from equation (2-15) with the derivative being represented by equation (A-35). The bulk concentration, C^*_b as defined in equation (2-20), was obtained from the known values of U and C^* using Simpson's Rule to perform the integration across the pipe cross-section. The local Nusselt number for mass transfer, $(Nu_{AB})_{loc}$, was determined from equation (2-22) using the numerically evaluated concentration gradient at the wall and the dimensionless bulk concentration.

The log mean Nusselt number, $(Nu_{AB})_{lm}$, was determined from

$$(Nu_{AB})_{lm} = (C_{Ab}-C_{Ao})\ Sc/(\Delta C)_{lm} Z \qquad (A-39)$$

where

$$(\Delta C)_{lm} = \frac{(C_{Aw}-C_{Ao}) - (C_{Aw}-C_{Ab})}{\ln \frac{C_{Aw}-C_{Ao}}{C_{Aw}-C_{Ab}}} \qquad (A\text{-}40)$$

In a similar manner, $(Nu_{AB})_{am}$ was calculated by replacing the logarithmic mean by the arithmetic mean concentration driving force in equation (A-39). Using a procedure similar to that used by Wilkins (9) to obtain a step by step energy balance, a step by step mass balance of subliming material was made. Between two successive axial locations a distance ΔZ apart, the average mass flux necessary to produce the calculated change in bulk concentration was found from the expression

$$(N_{Aw})_m = (\mu/2r_w\rho)(\Delta C_b/\Delta Z) \qquad (A\text{-}41)$$

This was compared with the arithmetic average of the mass fluxes at each end of the step, N_{Aw_1} and N_{Aw_2}, respectively, in an error expression

$$\text{Step Error} = 1 - \frac{N_{Aw_1} + N_{Aw_2}}{2(N_{Aw})_m} \qquad (A\text{-}42)$$

An overall error term, calculated in a similar manner, compared the overall change in bulk concentration from Z = 0 to the point in question with the change calculated by integrating the local flux values. The integration was performed numerically using the trapezoidal rule. At each axial location the distance parameter ReScD/z was calculated from

$$ReScD/z = 4Sc/Z \qquad (A\text{-}43)$$

The Grashof number based on the pipe diameter and the log mean concentration difference was calculated from

$$(Gr_{AB})_{lm} = 7844.8\, r_w^3\, \rho\, (M_A - M_B)(\Delta C)_{lm}/\mu^2 \qquad (A\text{-}44)$$

Notes on the Computer Program

The computer program was written in Algol for use on the Burroughs B-5500 digital computer. Values for eleven input variables are required to begin the program. These variables and the usual values used are given in Table 12. In general, the nomenclature of major variables is consistent with that used throughout this study within the limits imposed by the syntax of the computer language. The step error term discussed in the previous section is written as EQ1 in the program and the overall error term is EQ2. The term $(N_{Aw})_m$ is NAWC.

The program was written so as to allow flexibility in the selection of grid size. Several trials were made using different values of DELR and DELZ. These values ranged downward to DELR of 0.001 and DELZ of 10^{-7}. The values for these variables in Table 12 represent a compromise to obtain the highest accuracy possible and still cover the desired range in a reasonable amount of computer time, usually about fifteen minutes.

The initial step size was determined by the input value DELZ. After the first step, the step size was increased such that each step was 1.5 times the previous step until the step size reached a value of 0.0035. All subsequent steps were then of length 0.0035.

Several trial runs of the program were made before addition of

Table 12. Computer Input Variables

Variable	Explanatory Remarks	Usual Value
T	System temperature, ^{o}K	304.06, 311.36 or 323.16
MU	Viscosity of air, gm/cm-sec	See Appendix B
RHO	Density of air, gm/cc	See Appendix B
VBAR	Average dimensionless radial velocity at inlet	0.0
UBAR	Average dimensionless axial velocity at inlet	1.0
PRESS	Dimensionless pressure at inlet	0.0
CAO	Dimensionless concentration at inlet	0.0
I	An integer which signifies how many axial steps are taken	100
DELR	Number of radial divisions in the grid	0.00333
DELZ	Dimensionless length of first axial step	0.00001
RAD	Pipe radius in cm.	2.0320

the procedure of calculating the radial velocity at the wall from equation (A-37). For these runs, $V_w(Z)$ was assumed to be zero. Due to the relatively small mass fluxes encountered in this study, no significant effect on the calculated results was found by including the radial velocity at the wall in the solution. The procedure of evaluating $V_w(Z)$ was left in the computer program, however, to insure its applicability to systems involving higher mass transfer rates.

A typical program is given in Table 13. This program is written for the naphthalene-air system. To convert the program to para-dichlorobenzene-air, the expressions used to calculate vapor pressure, diffusivity and Schmidt number must be changed to coincide with the proper expressions as given in Appendix B.

Adequacy of the Numerical Solution

The question of stability and convergence of a numerical approach similar to that used in this study is discussed by Wilkins (9). He concludes that such a solution will be stable and convergent for non-negative axial velocities. Since axial velocities were always positive or zero in this study and due to the complexities of proving stability and convergence, it was decided to determine the adequacy of the solution by comparison to known solutions for fully-developed and for uniform flow and to Wilkins' solution for developing flow.

The numerically calculated log mean and local Nusselt numbers for a parabolic profile are presented in Table 7. This situation is the mass transfer analogy to the Graetz (14) problem in heat transfer which is discussed in detail by Jakob (29). Below ReScD/z of 1000, the

Table 13. Computer Program Used to Obtain Theoretical Solution

```
 LABEL  000000000PUNCHER00166033016613200000000000000000000000010000100000000000
BEGIN CARD B TIMM CARD LIST INTEGER I,J,K,N;REAL SC,T,DAB,MU,RHO,CAW,DEL00000100
R,VBAR,UBAR,ETA,DELZ,TERM2,TERM3,CHK,WVEL,GRAB,VP,CSTRB,T4,T5,T6,DELCA,D00000200
ELCL,NUAM,NULN,NAWC2,SUM,TERM1,PRESS,SLOPE,NAW,CAO,RAD,C1,C2,C3,C4,CAB,N00000300
UAB,NAWC,NAWC1,NAW1,CAB1,CABO,INT1,INT2,T1,T2,T3,EQ1,EQ2,Z,L,RESCDZ;ARRA00000400
Y ASTR,H,V,U,R,CSTR,A,B,C,D,E,F,Y,USC,VSC,AA,BB,CC,FF,W,G[0:1005];LABEL 00000500
REDO;LIST INPUT(T,MU,RHO,VBAR,UBAR,PRESS,CAO,I,DELR,DELZ,RAD);LIST LST1(00000600
T,MU,RHO,DAB,DELR,CAO,RAD,SC,CAW,DELZ);LIST LST2(Z,L,RESCDZ,NAW,CAB,SLOP00000700
E,NUAB,PRESS);LIST LST3(EQ1,EQ2,NAWC,GRAB);LIST LST4(CSTRB,NUAM,NULN);FI00000800
LE IN CARD(2,10);FILE OUT LINE 4(2,15);FORMAT FMT1("T = ",F7 .2,X4,"MU =00000900
 ",E12 .5,X4,"RHO = ",E12 .5,X4,"DAB = ",E12 .5,X4,"DELR = ",F8 .5//"CA00001000
 = ",F5 .2,X4,"RAD =",F7 .4,X8,"SC = ",F8 .5,X9,"CAW = ",E13 .6,X3,"DELZ00001100
 = ",F8 .5//),FMT2(//"Z = ",F9 .6,X4,"L = ",F8 .5,X4,"RESCD/Z = ",F11 .300001200
,X4,"NAW = ",E13 .6//"CAB = ",E13 .6,X4,"SLOPE = ",E13 .6,"NUAB = ",E13 00001300
.6,X4,"PRESSURE = ",E13 .6/),FMT3(X4,"RADIUS",X5,"AXIAL VELOCITY",X5,"RA00001400
DIAL VELOCITY",X5,"CONCENTRATION"),FMT5("EQ1 = ",F8 .5,X4,"EQ2 = ",F8 .500001500
,X4,"NAWC = ",E13 .6,X4,"GRAB = ",E13 .6/),FMT6("CSTRB=",F8 .5,X4,"NUAM 00001600
=",F8 .3,X4,"NULN = ",F8 .3/),FMT4(X3,F7 .4,X4,3(E14 .7,X6));READ(CARD,/00001700
,INPUT);CLOSE(CARD,RELEASE);SC←7.0×(T*(-0.185));RAD←0.80×RAD;DAB←MU/(RHO00001800
×SC);VP←EXP(2.303×(11.550-(3765/T)));CAW←VP/(82.06×760×T);N←1÷1/DELR;CAB00001900
0←0.0;CAB←0.0;INT1←0.0;FOR K←1STEP 1UNTIL(N-1)DO BEGIN V[K]←VBAR;U[K]←UB00002000
AR;CSTR[K]←0.0;R[K]←(K-1)×DELR;END;V[N]←U[N]←0.0;R[N]←CSTR[N]←1.0;TERM2←00002100
(2.0×DELR)*(-1.0);TERM3←(DELR)*(-2.0);WRITE(LINE,FMT1,LST1);FOR J←1STEP 00002200
1UNTIL I DO BEGIN ETA←1.0/DELZ;REDO;SUM←0.0;FOR K←2STEP 1UNTIL(N-1)DO BE00002300
GIN TERM1←(2.0×R[K]×DELR)*(-1.0);A[K]←TERM1-V[K]×TERM2-TERM3;B[K]←2.0×TE00002400
RM3+U[K]×ETA;C[K]←V[K]×TERM2-TERM1-TERM3;D[K]←R[K];E[K]←ETA;F[K]←((U[K]×00002500
U[K])+PRESS)×ETA;SUM←SUM+(R[K]×U[K])END;B[1]←4.0×TERM3+U[1]×ETA;C[1]←-4.00002600
0×TERM3;D[1]←R[2]/4.0;D[2]←3.0×D[1];D[N]←0.0;E[1]←ETA;F[1]←((U[1]×U[1])+00002700
PRESS)×ETA;F[N]←SUM+((U[1]-U[2])×R[2]/4.0);F[N]←F[N]-V[N]×DELZ/DELR;FOR 00002800
K←1STEP 1UNTIL(N-2)DO BEGIN F[K]←F[K]/B[K];E[K]←E[K]/B[K];C[K]←C[K]/B[K]00002900
;F[K+1]←F[K+1]-F[K]×A[K+1];E[K+1]←E[K+1]-E[K]×A[K+1];B[K+1]←B[K+1]-C[K]×00003000
A[K+1];D[K+1]←D[K+1]-D[K]×C[K];D[N]←D[N]-D[K]×E[K];F[N]←F[N]-D[K]×F[K]EN00003100
D;FOR K←(N-1)DO BEGIN F[K]←F[K]/B[K];E[K]←E[K]/B[K];D[N]←D[N]-D[K]×E[K];00003200
F[K+1]←F[K+1]-D[K]×F[K]END;Y[N]←F[N]/D[N];Y[N-1]←F[N-1]-E[N-1]×Y[N];FOR 00003300
K←(N-2)STEP(-1)UNTIL 1DO Y[K]←F[K]-E[K]×Y[N]-C[K]×Y[K+1];H[1]←0.0;H[2]←-00003400
(DELR×(Y[2]+Y[1]-U[2]-U[1]))/(4.0×DELZ);FOR K←2STEP 1UNTIL N-2DO H[K+1]←00003500
```

Table 13. (Continued)

```
(K=1)×H[K]/K=(DELR/(2×DELZ))×(((K=1)/K)×(Y[K]=U[K])+(Y[K+1]=U[K+1]))}H[N00003600
]+(N=2)×H[N=1]/(N=1)=(DELR/(2×DELZ))×(((N=2)/(N=1))×(Y[N=1]=U[N=1]))}FOR00003700
 K+1STEP 1UNTIL(N=1)DO BEGIN USC[K]+Y[K]×SC}VSC[K]+H[K]×SC}END}FOR K+2ST00003800
EP 1UNTIL(N=1)DO BEGIN TERM1+(2.0×R[K]×DELR)*(=1.0)}AA[K]+TERM1=VSC[K]×T00003900
ERM2=TERM3}BB[K]+2.0×TERM3+USC[K]×ETA}CC[K]+VSC[K]×TERM2=TERM1=TERM3}FF[00004000
K]+USC[K]×ETA×CSTR[K]END}BB[1]+4.0×TERM3+USC[1]×ETA}CC[1]+=4.0×TERM3}FF[00004100
1]+USC[1]×ETA×CSTR[1]}FF[N=1]+FF[N=1]=CC[N=1]}W[1]+BB[1]}G[1]+FF[1]/W[1]00004200
}FOR K+2STEP 1UNTIL(N=1)DO BEGIN W[K]+BB[K]=AA[K]×CC[K=1]/W[K=1]}G[K]+(F00004300
F[K]=AA[K]×G[K=1])/W[K]END}ASTR[N=1]+G[N=1]}FOR K+(N=2)STEP(=1)UNTIL 1D00004400
 ASTR[K]+G[K]=CC[K]×ASTR[K+1]/W[K]}SLOPE+=(LN(ASTR[N=1]))/DELR}NAW1+DAB×00004500
(CAW=CAO)×SLOPE/RAD}WVEL+=NAW1×128.17×RAD/MU}CHK+(WVEL=H[N])/WVEL}IF ABS00004600
(CHK)>0.02THEN BEGIN V[N]+WVEL}GO TO REDO}END}FOR K+1STEP 1UNTIL(N=1)DO 00004700
BEGIN U[K]+Y[K]}V[K]+H[K]}CSTR[K]+ASTR[K]}END}PRESS+Y[N]}V[N]+H[N]}C1+C200004800
+C3+C4+0.0}FOR K+2STEP 2UNTIL(N=1)DO BEGIN C1+C1+U[K]×CSTR[K]×(K=1)}C2+C00004900
2+U[K+1]×CSTR[K+1]×K}C3+C3+U[K]×(K=1)}C4+C4+U[K+1]×K END}CAB1+(CAW=CAO)×00005000
((2×C1)+C2)/((2×C3)+C4)}NAWC1+MU/(2×RAD×RHO)×(CAB1=CAB)/DELZ}CAB+CAB1}NU00005100
AB+2×SLOPE×(CAW=CAO)/(CAW=CAB)}Z+Z+DELZ}IF Z=DELZ THEN NAW+2×NAWC1=NAW1}00005200
T1+CAB=CABO}INT1+INT1+(NAW+NAW1)×DELZ/2}T2+(2×RAD×RHO/MU)×INT1}EQ1+1=(NA00005300
W+NAW1)/(2×NAWC1)}EQ2+1=T2/T1}NAW+NAW1}NAWC+NAWC1}L+Z/SC}RESCDZ+4.0/L}T400005400
+CAW=CAO}T5+CAW=CAB}DELCA+(T4+T5)/2}DELCL+(T4=T5)/LN(T4/T5)}GRAB+7844.8×00005500
RAD×RAD×RAD×RHO×99.19×(DELCL)/(MU×MU)}CSTRB+((2×C1)+C2)/((2×C3)+C4)}NUAM00005600
+T1×SC/(DELCA×Z)}NULN+T1×SC/(DELCL×Z)}WRITE(LINE,FMT2,LST2)}WRITE(LINE,F00005700
MT5,LST3)}WRITE(LINE,FMT6,LST4)}WRITE(LINE,FMT3)}FOR K+1STEP(N=1)/10UNTI00005800
L N DO WRITE(LINE,FMT4,R[K],U[K],V[K],CSTR[K])}DELZ+1.5×DELZ}IF DELZ≥0.000005900
035THEN DELZ+0.0035}END}TIMM(LINE,2)}END.                                    00006000
 LABEL  000000000PUNCHER00166033016613200000000000000000000010000100000000000
```

numerically calculated Nusselt numbers were compared to values calculated from the Graetz solution by Lee (30). The results of this comparison are presented in Table 14. The agreement between the two solutions was quite good with the maximum deviation occurring at ReScD/z near 1000 where the local Nusselt numbers for the Graetz solution were about 5 per cent lower than those obtained numerically.

In comparing mean Nusselt numbers, the question arises as to whether log mean or arithmetic mean values are being employed. For instance, Lee's (30) calculated Graetz solution values are based on the arithmetic mean driving force whereas the values used in this study are based on the logarithmic mean. Fortunately, this presents no problem in this study since above ReScD/z of 100 the difference between the two is less than 1 per cent. At ReScD/z of 30, which is about the minimum value covered here, the difference is only about 4 per cent.

Because of the large number of eigenvalues required to obtain accurate solutions to the Graetz problem near the entrance, the numerical solution for fully-developed flow was compared to the Lévêque solution for ReScD/z > 1000. The Lévêque solution represents an asymptotic solution to the Graetz problem and should apply at high values of ReScD/z. This solution, as given by (11), can be represented by

$$(Nu_{AB})_{lm} = 1.62(ReScD/z)^{1/3} \qquad (A\text{-}45)$$

Results of the comparison of $(Nu_{AB})_{lm}$ values calculated numerically to those calculated from equation (A-45) are presented in Table 15. At ReScD/z of 2000, the Lévêque values are about 6 per cent higher than the

Table 14. Comparison of Numerical Solution for Fully-developed Flow to the Graetz Solution

ReScD/z	Mean Nusselt Number**		Local Nusselt Number	
	Numerical	Graetz	Numerical	Graetz
980	15.0	15.2	10.5	10.0
746	13.6	13.9	9.6	9.17
435	11.5	11.6	8.0	7.68
220	9.22	9.21	6.30	6.18
97.1	7.08 (7.02)	7.04	4.93	4.88
64.9	6.26 (6.19)	6.19	4.44	4.41
43.3	5.58 (5.46)	5.47	4.08	4.06

* Graetz values calculated by Lee (30).

** Numerical values are log mean Nusselt numbers and Graetz values are arithmetic mean Nusselt numbers. For ReScD/z < 100, numerically calculated arithmetic mean Nusselt numbers are also presented following the log mean value.

Table 15. Comparison of Numerical Solution for Fully-developed Flow to the Lévêque Solution

ReScD/z	Logarithmic Mean Nusselt Number	
	Numerical	Lévêque*
12073	35.41	37.17
5287	26.72	28.22
2335	20.19	21.49
1035	15.27	16.39

* Calculated from $(Nu_{AB})_{lm} = 1.62(ReScD/z)^{1/3}$

numerical. At higher values of ReScD/z, the two solutions were found to slowly converge. A similar situation was found by Wilkins (9) in comparing bulk temperatures calculated numerically and by the Lévêque solution.

For the uniform velocity case, the numerically calculated log mean Nusselt numbers were compared to

$$(Nu_{AB})_{lm} = 1.128(ReScD/z)^{1/2} \qquad (A\text{-}46)$$

which is based on an equation given in (31), modified for mass transfer. For ReScD/z from 750 to 2000, agreement was within 2 per cent and, at ReScD/z of 5000, agreement was within 3 per cent. These results are presented in Table 16.

Wilkins (9) points out that comparison to the fully-developed

Table 16. Comparison of Numerical Solution to Solution for Rod-like Flow

ReScD/z	Logarithmic Mean Nusselt Number	
	Numerical	Theoretical*
5287	78.63	82.02
2335	53.42	54.51
1035	36.38	36.29
739	31.12	30.67

* Calculated from $(Nu_{AB})_{lm} = 1.128(ReScD/z)^{1/2}$

velocity solution may not be a strenuous test to apply to an entrance length solution. This is because radial velocities do not enter into the fully-developed velocity solution and inconsistencies in mass or heat balances caused by radial velocity terms will not show up. For this reason, it was felt desirable to compare the numerical solution used in this study to that of Wilkins for developing flow.

A numerical solution with Sc = 1 was obtained to compare with Wilkins' results for Pr = 1. The results of this solution are presented in Table 17. A comparison of the solution to that of Wilkins is shown in Figure 47. As can be seen the agreement between the two solutions is excellent. Deviations between the two solutions are usually less than 1 per cent over the range of interest in this study. Also, pressure drop terms and velocity profiles reported by Wilkins were compared to those calculated in this study. Again, the agreement was excellent.

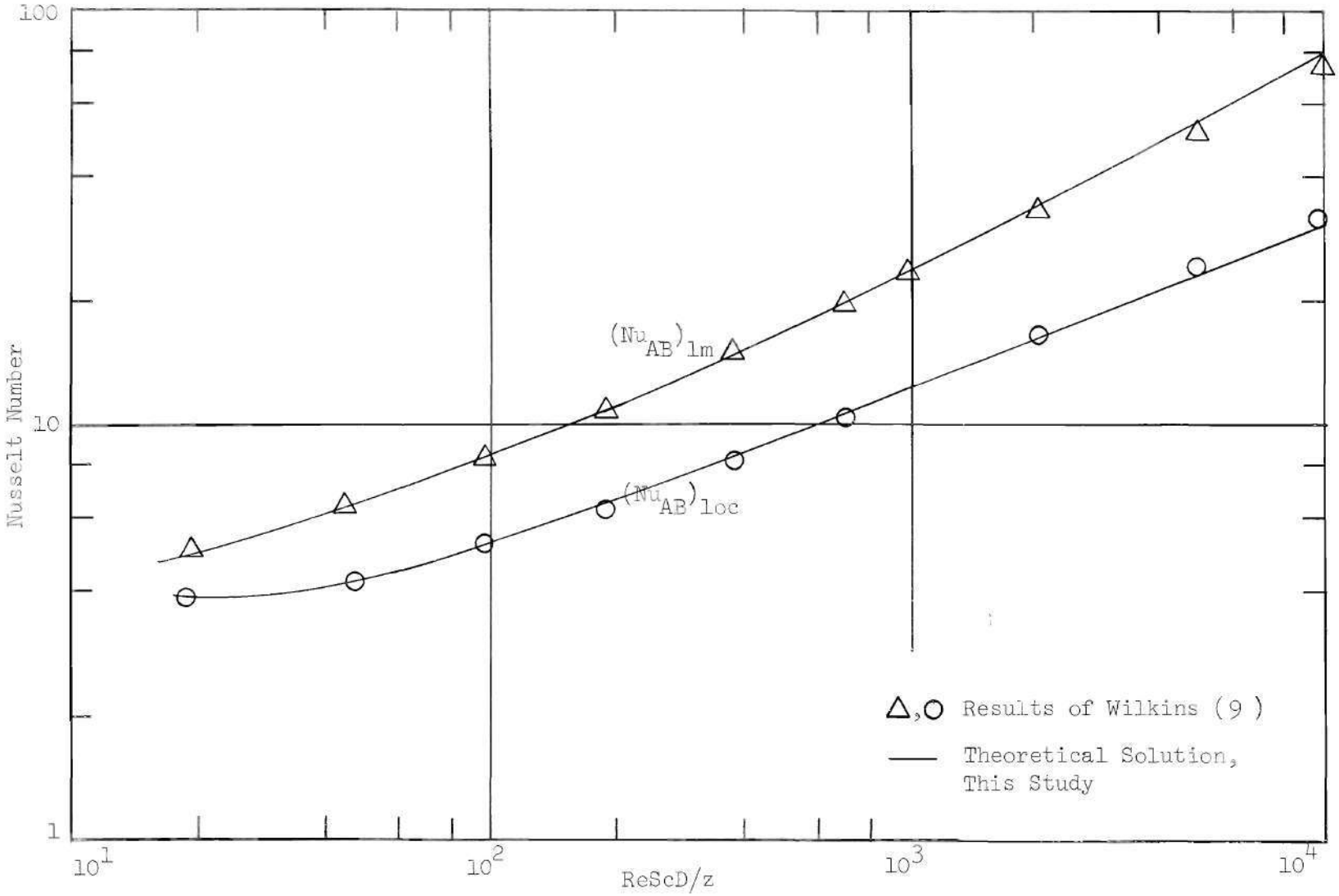

Figure 47. Comparison of Theoretical Results at Sc = 1

Table 17. Theoretical Results for Sc = 1 with Developing Flow

ReScD/z	$(Nu_{AB})_{loc}$	$(Nu_{AB})_{lm}$
12433	34.75	89.99
8121	29.07	70.22
5341	24.51	55.50
2339	17.58	35.87
1033	12.64	23.96
687	10.74	19.75
327	8.02	14.03
176	6.30	10.70
99.4	5.17	8.46
48.6	4.24	6.46
19.2	3.71	4.87
13.06	3.67	4.48

For developing flow, the approach to the Pohlhausen solution for a flat plate was investigated near the entrance. This solution can be represented by (7)

$$(Nu_{AB})_{lm} = .664\ Sc^{-0.167}(ReScD/z)^{1/2} \qquad (A-47)$$

It was found that by decreasing the grid size, the numerical solution at extremely high values of ReScD/z could be made to approach this solution as closely as desired. The reduction in grid size had no effect on the Nusselt numbers in the range of interest of this study.

The error term based on a step-by-step mass balance as defined in equation (A-42) was found to show deviations of up to 30 per cent at positions very near the pipe entrance. These errors rapidly diminished and were below 3 per cent at ReScD/z of 5000. Further down the pipe, they

approached zero. The overall error term showed deviations in the overall mass balance of approximately 30 per cent near the entrance, 10 per cent at ReScD/z of 5000, and 3 per cent at ReScD/z of 500.

Changing the grid size from 300 to 1000 radial divisions and the initial ΔZ from 10^{-5} to 10^{-7} was found to effect the results above ReScD/z of 10000. Below ReScD/z of 5000, the finer grid size had an insignificant effect on the calculated values or the magnitude of the error terms. Consequently, the coarser grid was used to conserve computing time.

APPENDIX B

PHYSICAL PROPERTIES

Density and Viscosity

The numerical values for the density and viscosity of air at one atmosphere pressure were obtained from tables given in reference (32). For purposes of interpolation, it was assumed that the viscosity was directly proportional to the absolute temperature and the density was inversely proportional to the absolute temperature.

Vapor Pressure

For naphthalene, the following vapor pressure equation of Sherwood and Bryant (33) was used:

$$\log_{10} VP = -(3765/T) + 11.55 \qquad \text{(B-1)}$$

VP in mm Hg, T in $^{\circ}K$

This expression is based on experimental data obtained by the authors using a flow method in which air was slowly passed through a tube packed with broken pieces of cast naphthalene. From measured weight loss and air volume, the vapor pressure was calculated assuming the leaving air saturated. This equation is recommended by the authors for use between $0^{\circ}C$ and $38^{\circ}C$.

Since the temperature range of interest in this study was from $30^{\circ}C$ to $50^{\circ}C$, several other vapor pressure expressions were also con-

sidered to determine the validity of using equation (B-1) to 50°C. An expression developed by Sogin (3) based on experimental measurements by Thomas (34) over the range 0°C to 80°C agrees within 2 per cent with equation (B-1) over the range of interest.

Bedingfield and Drew (35) report vapor pressures on reagent grade naphthalene at four temperatures between 50°C and 66°C. Their experimental method was of the flow type as described above. The reported vapor pressure at 50.0°C is 0.764 mm Hg. This is about 4 per cent lower than the value calculated at 50.0°C using equation (B-1).

A correlating equation for the vapor pressure of naphthalene based upon a literature survey and also some of their own experimental data is given by Christian and Kezios (12). Their equation gives vapor pressures which are approximately 5 per cent higher than those obtained from equation (B-1) over the temperature range of interest.

The vapor pressure of p-dichlorobenzene was determined from

$$\log_{10} VP = 11.347 - (3382.9/T) \qquad \text{(B-2)}$$

VP in mm Hg, T in °K

The equation was developed by Walsh and Smith (36) and is based on their measurements on highly purified p-dichlorobenzene by a direct pressure measurement technique.

Bedingfield and Drew (35) also made vapor pressure measurements on technical grade p-dichlorobenzene using a flow technique. Their results, represented by an equation developed by Sogin (3), appear to be about 3 per cent lower than the results obtained from equation (B-2).

An equation given in the International Critical Tables (37) for the vapor pressure of para-dichlorobenzene gave results approximately 40 per cent lower than equation (B-2).

Diffusivity and Schmidt Number

The Schmidt number for the naphthalene-air system was determined from the following equation recommended by Sherwood and Trass (38):

$$Sc = 7 \times T^{-0.185} \qquad \text{(B-3)}$$

T in $^{\circ}K$

This equation was developed according to the procedure recommended in (39) and gives agreement within about 2 per cent of experimental data (apparently the data of Mack (40) at 25°C). The diffusivity of naphthalene in air was evaluated from the known values of Schmidt number, viscosity, and density.

The diffusivity of p-dichlorobenzene in air at 30.9°C was calculated using Gilliland's method as given in (39). Sogin (3) has used this method and reports good agreement between his result and an experimental determination made by Kezios (41) at 77°F. Using Gilliland's equation, the diffusivity of p-dichlorobenzene at 30.9°C and one atmosphere was calculated to be 0.071 cm^2/sec. The diffusivity was also calculated by a method given in (11) which is based on the kinetic theory of gases. The Lennard-Jones force parameters were estimated from melting point data. The diffusivity at the above conditions was found to be 0.072 cm^2/sec by this method. The Schmidt number was calculated from known values of diffusivity, density, and viscosity.

The numerical values which were used for each of the physical properties at each test temperature during this study are presented in Table 18.

Table 18. Physical Properties of Test Materials

Temperature °C	Density of Air at 1 atm., gm/cc	Viscosity of Air, gm/cm-sec	Diffusivity, cm^2/sec	Schmidt Number at 1 atm.
		Naphthalene-Air System		
30.9	1.1612×10^{-3}	1.8635×10^{-4}	6.602×10^{-2}	2.430
38.2	1.1339×10^{-3}	1.8973×10^{-4}	6.913×10^{-2}	2.420
50.0	1.0925×10^{-3}	1.9520×10^{-4}	7.433×10^{-2}	2.403
		Para-Dichlorobenzene-Air System		
30.9	1.1612×10^{-3}	1.8635×10^{-4}	7.100×10^{-2}	2.260

APPENDIX C

EXPERIMENTAL RESULTS

Table 19. Individual Values Used in Obtaining Weight Loss Correction Term

Section Number	z in Inches	$C_{10}H_8$ at 30.9° C	$C_{10}H_8$ at 38.2° C	$C_{10}H_8$ at 50.0° C	$p\text{-}C_6H_4Cl_2$ at 30.9° C
		Weight Loss of Test Section in Grams			
2	1.97	0.006	0.007	0.008	0.026
3	3.59	0.007	0.007	0.012	0.024
5	11.31	0.006	0.006	0.002	0.020
6	12.88	0.007	0.007	0.007	0.035
8	23.34	0.005	0.006	0.010	0.013
9	24.91	0.006	0.005	0.004	0.026
11	35.35	0.005	0.009	0.005	0.020
12	36.88	0.006	0.007	0.017	0.036
14	47.28	0.005	0.006	0.005	0.018
15	48.94	0.005	0.006	0.004	0.018
17	59.28	0.006	0.006	0.004	0.018
18	69.72	0.006	0.007	0.005	0.019
19	71.41	0.005	0.006	0.007	0.017
Average Value		0.006	0.007	0.008	0.022

Table 20. Calibration of Chromatograph

Temperature °C	Chromatograph Output, Peak Height x 50	Naphthalene Concentration gm-mol/cc x 10^9
22.0	16, 16	3.15
26.1	22, 21, 22	5.20
31.2	38, 37, 36, 36	7.95
35.2	50, 52, 47	11.31
40.1	74, 77, 78	17.28
44.9	122, 120, 122	26.00
49.8	168, 186, 174, 181, 184	38.80

Table 21. Experimental Results of Test Run No. 1

Temperature, °C	50.0	Test Material	Naphthalene	Date	8-09-65
Pipe Position	Horizontal	Density, $g/cm^3 \times 10^3$	1.053	Duration of Run, sec	12300
Reynolds Number	445	Viscosity, $g/cm\text{-}sec \times 10^4$	1.952	Average Diameter, in.	1.62
Schmidt Number	2.40	Diffusivity, cm^2/sec	0.077		

Section Number	z in Inches	ReScD/z	$N_{Aw} \times 10^{10}$	$(Nu_{AB})_{loc}$	$(Nu_{AB})_{lm}$	C_b^*
2	1.97	881.8	83.9	12.47	19.85	0.086
3	3.59	483.0	66.0	10.23	16.02	0.124
5	11.31	153.4	40.4	7.34	11.17	0.253
6	12.88	134.8	36.9	6.89	10.68	0.272
8	23.34	74.3	32.4	7.16	9.04	0.385
9	24.91	69.7	33.8	7.67	8.94	0.401
11	35.35	49.1	28.9	7.92	8.61	0.504
12	36.88	47.1	28.2	7.93	8.58	0.518
14	47.28	36.7	20.4	6.88	8.34	0.597
15	48.94	35.5	21.0	7.25	8.29	0.608
17	59.28	29.3	22.0	9.25	8.27	0.677
18	69.72	24.9	17.4	9.16	8.42	0.742
19	71.41	24.3	11.5	6.21	8.40	0.749

Table 22. Experimental Results of Test Run No. 2

Temperature, °C	50.0	Test Material	Naphthalene	Date	8-10-65
Pipe Position	Horizontal	Density, $g/cm^3 \times 10^3$	1.054	Duration of Run, sec	10000
Reynolds Number	447	Viscosity, $g/cm\text{-}sec \times 10^4$	1.952	Average Diameter, in.	1.62
Schmidt Number	2.40	Diffusivity, cm^2/sec	0.077		

Section Number	z in Inches	ReScD/z	$N_{Aw} \times 10^{10}$	$(Nu_{AB})_{loc}$	$(Nu_{AB})_{lm}$	C_b^*
2	1.97	885.7	83.6	12.24	16.42	0.071
3	3.59	485.1	70.5	10.78	14.21	0.111
5	11.31	154.1	40.7	7.32	10.80	0.244
6	12.88	135.4	36.7	6.77	10.34	0.263
8	23.34	74.7	35.6	7.80	8.96	0.381
9	24.91	70.0	39.0	8.83	8.92	0.399
11	35.35	49.3	33.9	9.56	9.00	0.518
12	36.88	47.3	29.7	8.64	9.01	0.533
14	47.28	36.9	22.5	8.00	8.87	0.618
15	48.94	35.6	25.0	9.19	8.86	0.630
17	59.28	29.4	33.1	16.27	9.46	0.724
18	69.72	25.0	24.2	18.02	10.62	0.817
19	71.41	24.4	18.1	14.30	10.75	0.828

Table 23. Experimental Results of Test Run No. 3

Temperature, ^{o}C	50.0	Test Material	Naphthalene	Date	8-04-65
Pipe Position	Horizontal	Density, $g/cm^3 \times 10^3$	1.057	Duration of Run, sec	12537
Reynolds Number	1015	Viscosity, $g/cm\text{-}sec \times 10^4$	1.952	Average Diameter, in.	1.61
Schmidt Number	2.40	Diffusivity, cm^2/sec	0.077		

Section Number	z in Inches	ReScD/z	$N_{Aw} \times 10^{10}$	$(Nu_{AB})_{loc}$	$(Nu_{AB})_{lm}$	C_b^*
2	1.97	1998.8	119.4	16.94	23.54	0.046
3	3.59	1094.8	99.8	14.54	20.02	0.071
5	11.31	347.7	63.9	10.28	14.90	0.158
6	12.88	305.5	57.0	9.31	14.28	0.171
8	23.34	168.5	47.4	8.51	11.88	0.246
9	24.91	157.9	47.3	8.61	11.68	0.256
11	35.35	111.3	40.4	8.03	10.69	0.319
12	36.88	106.7	37.7	7.59	10.57	0.327
14	47.28	83.2	32.1	6.98	9.85	0.377
15	48.94	80.4	35.3	7.77	9.77	0.385
17	59.28	66.4	43.3	10.49	9.65	0.441
18	69.72	56.4	22.4	5.92	9.45	0.488
19	71.41	55.1	15.9	4.25	9.34	0.493

Table 24. Experimental Results of Test Run No. 4

Temperature, °C	50.0	Test Material	Naphthalene	Date	8-16-65
Pipe Position	Horizontal	Density, $g/cm^3 \times 10^3$	1.055	Duration of Run, sec	13000
Reynolds Number	1376	Viscosity, $g/cm\text{-}sec \times 10^4$	1.952	Average Diameter, in.	1.64
Schmidt Number	2.40	Diffusivity, cm^2/sec	0.077		

Section Number	z in Inches	ReScD/z	$N_{Aw} \times 10^{10}$	$(Nu_{AB})_{loc}$	$(Nu_{AB})_{lm}$	C_b^*
2	1.97	2756.7	153.6	22.19	33.81	0.048
3	3.59	1509.9	123.7	18.30	27.69	0.071
5	11.31	479.6	79.6	12.88	19.52	0.150
6	12.88	421.4	69.7	11.45	18.63	0.162
8	23.34	232.4	55.3	9.85	15.07	0.228
9	24.91	217.8	51.2	9.23	14.72	0.237
11	35.35	153.5	46.0	8.88	13.05	0.288
12	36.88	147.1	42.9	8.37	12.87	0.295
14	47.28	114.7	36.8	7.63	11.80	0.337
15	48.94	110.9	37.9	7.95	11.66	0.343
17	59.28	91.5	41.2	9.20	11.12	0.385
18	69.72	77.8	32.1	7.66	10.72	0.424
19	71.41	76.0	29.9	7.19	10.65	0.429

Table 25. Experimental Results of Test Run No. 5

Temperature, ^{o}C	50.0	Test Material	Naphthalene	Date	8-12-65
Pipe Position	Vertical	Density, $g/cm^3 \times 10^3$	1.059	Duration of Run, sec	11000
Reynolds Number	441	Viscosity, $g/cm\text{-}sec \times 10^4$	1.952	Average Diameter, in.	1.63
Schmidt Number	2.40	Diffusivity, cm^2/sec	0.0		

Section Number	z in Inches	ReScD/z	$N_{Aw} \times 10^{10}$	$(Nu_{AB})_{loc}$	$(Nu_{AB})_{lm}$	C_b^*
2	1.97	878.6	78.9	11.61	15.25	0.067
3	3.59	481.3	67.3	10.31	13.31	0.105
5	11.31	152.9	51.3	9.38	10.99	0.250
6	12.88	134.3	48.0	9.09	10.78	0.275
8	23.34	74.1	29.5	6.78	9.57	0.403
9	24.91	69.4	23.8	5.61	9.36	0.418
11	35.35	48.9	21.9	5.93	8.30	0.493
12	36.88	46.9	22.5	6.21	8.20	0.503
14	47.28	36.6	24.9	8.15	7.97	0.581
15	48.94	35.3	22.1	7.46	7.96	0.594
17	59.28	29.2	10.5	4.09	7.60	0.647
18	69.72	24.8	15.3	6.79	7.27	0.690
19	71.41	24.2	12.8	5.79	7.24	0.698

Table 26. Experimental Results of Test Run No. 6

Temperature, °C	50.0	Test Material	Naphthalene	Date	8-11-65
Pipe Position	Vertical	Density, $g/cm^3 \times 10^3$	1.057	Duration of Run, sec	10000
Reynolds Number	446	Viscosity, $g/cm\text{-}sec \times 10^4$	1.952	Average Diameter, in.	1.625
Schmidt Number	2.40	Diffusivity, cm^2/sec	0.077		

Section Number	z in Inches	ReScD/z	$N_{Aw} \times 10^{10}$	$(Nu_{AB})_{loc}$	$(Nu_{AB})_{lm}$	C_b^*
2	1.97	884.9	85.0	12.65	19.28	0.083
3	3.59	487.7	67.9	10.57	15.82	0.122
5	11.31	153.9	42.8	7.85	11.40	0.256
6	12.88	135.3	37.9	7.15	10.93	0.276
8	23.34	74.6	24.8	5.46	8.89	0.379
9	24.91	69.9	25.5	5.50	8.67	0.391
11	35.35	49.3	20.0	5.09	7.68	0.464
12	36.88	47.2	19.4	5.03	7.57	0.473
14	47.28	36.8	19.4	5.71	7.08	0.537
15	48.94	35.6	19.8	5.98	7.04	0.547
17	59.28	29.4	25.8	9.30	7.12	0.621
18	69.72	25.0	23.4	10.68	7.55	0.701
19	71.41	24.4	17.9	8.49	7.60	0.712

Table 27. Experimental Results of Test Run No. 7

Temperature, °C	50.0	Test Material	Naphthalene	Date	8-05-65
Pipe Position	Vertical	Density, $g/cm^3 \times 10^3$	1.059	Duration of Run, sec	12500
Reynolds Number	1016	Viscosity, $g/cm\text{-}sec \times 10^4$	1.952	Average Diameter, in.	1.614
Schmidt Number	2.40	Diffusivity, cm^2/sec	0.077		

Section Number	z in Inches	ReScD/z	$N_{Aw} \times 10^{10}$	$(Nu_{AB})_{loc}$	$(Nu_{AB})_{lm}$	C_b^*
2	1.97	2003.7	115.3	16.34	21.30	0.042
3	3.59	1097.5	99.3	14.43	18.63	0.066
5	11.31	348.6	69.8	11.23	14.73	0.156
6	12.88	306.3	63.0	10.30	14.25	0.170
8	23.34	168.9	52.0	9.46	12.31	0.253
9	24.91	158.3	51.5	9.50	12.13	0.264
11	35.35	111.5	40.3	8.18	11.17	0.330
12	36.88	106.9	36.7	7.53	11.03	0.338
14	47.28	83.4	22.3	4.90	9.98	0.380
15	48.94	80.6	23.3	5.14	9.81	0.386
17	59.28	66.5	29.8	7.01	9.16	0.423
18	69.72	56.6	27.5	6.97	8.83	0.465
19	71.41	55.2	28.7	7.37	8.79	0.471

Table 28. Experimental Results of Test Run No. 8

Temperature, ^{o}C	50.0	Test Material	Naphthalene	Date	8-06-65
Pipe Position	Vertical	Density, $g/cm^3 \times 10^3$	1.057	Duration of Run, sec	11000
Reynolds Number	976	Viscosity, $g/cm\text{-}sec \times 10^4$	1.952	Average Diameter, in.	1.618
Schmidt Number	2.40	Diffusivity, cm^2/sec	0.077		

Section Number	z in Inches	ReScD/z	$N_{Aw} \times 10^{10}$	$(Nu_{AB})_{loc}$	$(Nu_{AB})_{lm}$	C_b^*
2	1.97	1929.2	116.1	16.56	22.72	0.046
3	3.59	1056.7	97.6	14.29	19.43	0.071
5	11.31	335.6	81.5	13.35	15.63	0.170
6	12.88	294.9	78.5	13.15	15.34	0.188
8	23.34	162.6	62.9	12.12	14.15	0.294
9	24.91	152.4	57.8	11.35	14.00	0.307
11	35.35	107.4	39.1	8.58	12.83	0.380
12	36.88	103.0	36.9	8.21	12.65	0.388
14	47.28	80.3	24.1	5.79	11.42	0.434
15	48.94	77.6	24.7	6.00	11.23	0.440
17	59.28	64.0	30.5	7.99	10.49	0.481
18	69.72	54.5	22.9	6.48	10.00	0.520
19	71.41	53.2	17.9	5.14	9.91	0.525

Table 29. Experimental Results of Test Run No. 9

Temperature, ^{o}C	50.0	Test Material	Naphthalene	Date	8-18-65
Pipe Position	Vertical	Density, $g/cm^3 \times 10^3$	1.053	Duration of Run, sec	10000
Reynolds Number	1358	Viscosity, $g/cm\text{-}sec \times 10^4$	1.952	Average Diameter, in.	1.645
Schmidt Number	2.40	Diffusivity, cm^2/sec	0.077		

Section Number	z in Inches	ReScD/z	$N_{Aw} \times 10^{10}$	$(Nu_{AB})_{loc}$	$(Nu_{AB})_{lm}$	C_b^*
2	1.97	2728.6	148.6	21.39	30.61	0.044
3	3.59	1494.6	122.8	18.10	25.71	0.066
5	11.31	474.7	82.7	13.36	18.98	0.148
6	12.88	417.1	74.6	12.24	18.23	0.160
8	23.34	230.0	57.9	10.37	15.15	0.232
9	24.91	215.6	56.5	10.23	14.84	0.241
11	35.35	151.9	47.3	9.24	13.34	0.296
12	36.88	145.6	46.2	9.13	13.17	0.304
14	47.28	113.6	41.3	8.75	12.24	0.350
15	48.94	109.7	42.6	9.13	12.13	0.357
17	59.28	90.6	45.2	10.44	11.72	0.404
18	69.72	77.0	33.5	8.31	11.37	0.446
19	71.41	75.2	22.3	5.60	11.27	0.451

Table 30. Experimental Results of Test Run No. 10

Temperature, °C	50.0	Test Material	Naphthalene	Date	11-16-65
Pipe Position	45°	Density, $g/cm^3 \times 10^3$	1.052	Duration of Run, sec	13000
Reynolds Number	509	Viscosity, $g/cm\text{-}sec \times 10^4$	1.952	Average Diameter, in.	1.628
Schmidt Number	2.40	Diffusivity, cm^2/sec	0.077		

Section Number	z in Inches	ReScD/z	$N_{Aw} \times 10^{10}$	$(Nu_{AB})_{loc}$	$(Nu_{AB})_{lm}$	C_b^*
2	1.97	1012.5	114.5	17.15	24.09	0.091
3	3.59	554.6	94.4	14.90	20.45	0.137
5	11.31	176.2	48.4	9.26	14.95	0.288
6	12.88	154.8	37.6	7.38	14.14	0.306
8	23.34	85.4	26.1	5.88	10.80	0.397
9	24.91	80.0	24.2	5.58	10.49	0.408
11	35.35	56.4	21.1	5.46	9.02	0.473
12	36.88	54.0	20.3	5.33	8.87	0.481
14	47.28	42.1	21.0	6.20	8.18	0.540
15	48.94	40.7	21.9	6.63	8.12	0.550
17	59.28	33.6	23.2	8.18	7.99	0.614
18	69.72	28.6	14.9	6.12	7.88	0.668
19	71.41	27.9	13.9	5.80	7.83	0.675

Table 31. Experimental Results of Test Run No. 11

Temperature, ^{o}C	50.0	Test Material	Naphthalene	Date	11-05-65
Pipe Position	45^{o}	Density, $g/cm^3 \times 10^3$	1.066	Duration of Run, sec	11000
Reynolds Number	909	Viscosity, $g/cm\text{-}sec \times 10^4$	1.952	Average Diameter, in.	1.616
Schmidt Number	2.40	Diffusivity, cm^2/sec	0.077		

Section Number	z in Inches	ReScD/z	$N_{Aw} \times 10^{10}$	$(Nu_{AB})_{loc}$	$(Nu_{AB})_{lm}$	C_b^*
2	1.97	1795.0	134.6	19.73	30.57	0.066
3	3.59	983.2	107.3	16.26	24.90	0.096
5	11.31	312.3	76.5	13.20	18.04	0.206
6	12.88	274.4	70.3	12.41	17.41	0.224
8	23.34	151.3	50.2	10.14	14.70	0.322
9	24.91	141.8	45.2	9.29	14.39	0.334
11	35.35	99.9	31.6	7.16	12.58	0.396
12	36.88	95.8	29.1	6.68	12.35	0.403
14	47.28	74.7	23.5	5.79	11.01	0.445
15	48.94	72.2	24.3	6.07	10.84	0.451
17	59.28	59.6	27.0	7.28	10.11	0.493
18	69.72	50.7	21.4	6.24	9.61	0.532
19	71.41	49.5	16.9	4.99	9.52	0.537

Table 32. Experimental Results of Test Run No. 12

Temperature, ^{o}C	50.0	Test Material	Naphthalene	Date	11-11-65
Pipe Position	45^{o}	Density, $g/cm^3 \times 10^3$	1.061	Duration of Run, sec	10500
Reynolds Number	1356	Viscosity, $g/cm\text{-}sec \times 10^4$	1.952	Average Diameter, in.	1.622
Schmidt Number	2.40	Diffusivity, cm^2/sec	0.077		

Section Number	z in Inches	ReScD/z	$N_{Aw} \times 10^{10}$	$(Nu_{AB})_{ioc}$	$(Nu_{AB})_{lm}$	C_b^*
2	1.97	2686.2	137.6	19.64	28.68	0.042
3	3.59	1471.3	112.8	16.47	23.88	0.063
5	11.31	467.3	83.8	13.34	17.81	0.141
6	12.88	410.6	75.6	12.22	17.20	0.154
8	23.34	226.5	65.8	11.70	14.86	0.231
9	24.91	212.3	65.4	11.80	14.66	0.241
11	35.35	149.5	57.0	11.25	13.74	0.308
12	36.88	143.4	51.8	10.36	13.62	0.316
14	47.28	111.8	29.8	6.37	12.48	0.360
15	48.94	108.0	28.6	6.15	12.27	0.365
17	59.28	89.2	30.7	6.95	11.27	0.397
18	69.72	75.8	25.5	6.09	10.56	0.427
19	71.41	74.0	26.0	6.27	10.46	0.432

Table 33. Experimental Results of Test Run No. 13

Temperature, °C	38.2	Test Material	Naphthalene	Date	10-05-65
Pipe Position	Horizontal	Density, $g/cm^3 \times 10^3$	1.099	Duration of Run, sec	12000
Reynolds Number	461	Viscosity, $g/cm\text{-}sec \times 10^4$	1.897	Average Diameter, in.	1.604
Schmidt Number	2.42	Diffusivity, cm^2/sec	0.071		

Section Number	z in Inches	ReScD/z	$N_{Aw} \times 10^{11}$	$(Nu_{AB})_{loc}$	$(Nu_{AB})_{lm}$	C_b^*
2	1.97	908.7	309.8	13.20	22.07	0.093
3	3.59	497.7	239.1	10.64	17.49	0.131
5	11.31	158.1	135.9	7.07	11.70	0.256
6	12.88	138.9	121.7	6.48	11.11	0.274
8	23.34	76.6	89.9	5.51	8.83	0.369
9	24.91	71.8	91.4	5.72	8.63	0.382
11	35.35	50.6	74.9	5.33	7.72	0.457
12	36.88	48.5	73.7	5.34	7.62	0.467
14	47.28	37.8	64.4	5.29	7.11	0.529
15	48.94	36.5	67.3	5.63	7.06	0.538
17	59.28	30.2	71.9	6.95	6.92	0.600
18	69.72	25.6	57.9	6.56	6.90	0.659
19	71.41	25.0	53.3	6.19	6.89	0.667

Table 34. Experimental Results of Test Run No. 14

Temperature, °C	38.2	Test Material	Naphthalene	Date	8-25-65
Pipe Position	Horizontal	Density, $g/cm^3 \times 10^3$	1.094	Duration of Run, sec	12200
Reynolds Number	935	Viscosity, $g/cm\text{-}sec \times 10^4$	1.897	Average Diameter, in.	1.653
Schmidt Number	2.42	Diffusivity, cm^2/sec	0.072		

Section Number	z in Inches	ReScD/z	$N_{Aw} \times 10^{11}$	$(Nu_{AB})_{loc}$	$(Nu_{AB})_{lm}$	C_b^*
2	1.97	1900.6	399.8	16.91	30.49	0.062
3	3.59	1041.0	302.6	13.14	23.51	0.086
5	11.31	330.7	195.2	9.31	15.19	0.168
6	12.88	290.5	175.8	8.51	14.43	0.180
8	23.34	160.2	152.9	8.12	11.69	0.253
9	24.91	150.2	150.2	8.09	11.47	0.253
11	35.35	105.8	121.2	7.10	10.33	0.263
12	36.88	101.4	99.4	5.89	10.17	0.323
14	47.28	79.1	83.9	5.29	9.17	0.330
15	48.94	76.4	88.4	5.63	9.04	0.371
17	59.28	63.1	104.0	7.11	8.57	0.419
18	69.72	53.6	75.5	5.54	8.24	0.459
19	71.41	52.4	57.9	4.29	8.16	0.464

Table 35. Experimental Results of Test Run No. 15

Temperature, ^{o}C	38.2	Test Material	Naphthalene	Date	8-23-65
Pipe Position	Horizontal	Density, $g/cm^3 \times 10^3$	1.095	Duration of Run, sec	12000
Reynolds Number	948	Viscosity, $g/cm\text{-}sec \times 10^4$	1.897	Average Diameter, in.	1.644
Schmidt Number	2.42	Diffusivity, cm^2/sec	0.072		

Section Number	z in Inches	ReScD/z	$N_{Aw} \times 10^{11}$	$(Nu_{AB})_{loc}$	$(Nu_{AB})_{lm}$	C_b^*
2	1.97	1916.8	414.9	17.49	31.10	0.063
3	3.59	1049.9	315.4	13.65	24.09	0.088
5	11.31	333.3	203.5	9.70	15.69	0.172
6	12.88	293.0	180.9	8.76	14.91	0.184
8	23.34	161.6	146.1	7.75	11.94	0.256
9	24.91	151.5	140.0	7.52	11.67	0.265
11	35.35	106.7	128.6	7.15	10.39	0.323
12	36.88	102.3	117.7	6.94	10.25	0.330
14	47.28	79.8	112.4	7.16	9.55	0.380
15	48.94	77.1	120.1	9.07	9.48	0.389
17	59.28	63.6	128.1	9.07	9.29	0.442
18	69.72	54.1	92.2	7.14	9.12	0.490
19	71.41	52.8	64.0	5.02	9.05	0.496

Table 36. Experimental Results of Test Run No. 16

Temperature, ^{o}C	38.2	Test Material	Naphthalene	Date	10-01-65
Pipe Position	Horizontal	Density, $g/cm^3 \times 10^3$	1.096	Duration of Run, sec	12000
Reynolds Number	1426	Viscosity, $g/cm\text{-}sec \times 10^4$	1.897	Average Diameter, in.	1.610
Schmidt Number	2.42	Diffusivity, cm^2/sec	0.072		

Section Number	z in Inches	ReScD/z	$N_{Aw} \times 10^{11}$	$(Nu_{AB})_{loc}$	$(Nu_{AB})_{lm}$	C_b^*
2	1.97	2823.3	516.2	20.87	31.35	0.043
3	3.59	1546.4	418.4	17.30	25.81	0.065
5	11.31	491.2	274.9	12.35	18.39	0.139
6	12.88	431.6	243.6	11.09	17.58	0.150
8	23.34	238.0	189.4	9.32	14.29	0.214
9	24.91	223.1	182.2	9.05	13.97	0.222
11	35.35	157.2	168.3	8.95	12.50	0.273
12	36.88	150.7	160.7	8.63	12.35	0.280
14	47.28	117.5	151.8	8.70	11.54	0.325
15	48.94	113.5	159.4	9.23	11.45	0.332
17	59.28	93.7	161.7	10.06	11.13	0.378
18	69.72	79.7	95.3	6.31	10.70	0.416
19	71.41	77.8	82.7	5.51	10.59	0.420

Table 37. Experimental Results of Test Run No. 17

Temperature, $^{\circ}C$	38.2	Test Material	Naphthalene	Date	10-08-65
Pipe Position	Vertical	Density, $g/cm^3 \times 10^3$	1.087	Duration of Run, sec	13000
Reynolds Number	459	Viscosity, $g/cm\text{-}sec \times 10^4$	1.897	Average Diameter, in.	1.600
Schmidt Number	2.42	Diffusivity, cm^2/sec	0.072		

Section Number	z in Inches	ReScD/z	$N_{Aw} \times 10^{11}$	$(Nu_{AB})_{loc}$	$(Nu_{AB})_{lm}$	C_b^*
2	1.97	902.8	299.6	12.47	19.74	0.084
3	3.59	494.5	236.1	10.25	15.96	0.121
5	11.31	157.1	153.7	7.82	11.31	0.250
6	12.88	138.0	136.6	7.14	10.85	0.270
8	23.34	76.1	89.2	5.41	8.83	0.371
9	24.91	71.3	88.1	5.45	8.62	0.383
11	35.35	50.3	69.3	4.84	7.60	0.454
12	36.88	48.2	67.0	4.75	7.48	0.463
14	47.28	37.6	59.6	4.73	6.88	0.519
15	48.94	36.3	62.3	5.03	6.81	0.528
17	59.28	30.0	60.47	5.55	6.55	0.583
18	69.72	25.5	49.2	5.10	6.37	0.632
19	71.41	24.9	43.6	4.60	6.33	0.639

Table 38. Experimental Results of Test Run No. 18

Temperature, ^{o}C	38.2	Test Material	Naphthalene	Date	8-27/65
Pipe Position	Vertical	Density, $g/cm^3 \times 10^3$	1.097	Duration of Run, sec	12000
Reynolds Number	954	Viscosity, $g/cm\text{-}sec \times 10^4$	1.897	Average Diameter, in.	1.656
Schmidt Number	2.42	Diffusivity, cm^2/sec	0.071		

Section Number	z in Inches	ReScD/z	$N_{Aw} \times 10^{11}$	$(Nu_{AB})_{loc}$	$(Nu_{AB})_{lm}$	C_b^*
2	1.97	1942.4	468.6	20.17	37.53	0.074
3	3.59	1064.5	350.4	15.55	28.65	0.102
5	11.31	338.1	211.4	10.43	18.06	0.192
6	12.88	297.1	185.4	9.29	17.07	0.205
8	23.34	163.8	142.6	7.85	13.28	0.277
9	24.91	153.6	140.2	7.83	12.94	0.286
11	35.35	108.2	115.6	7.00	11.31	0.342
12	36.88	103.7	110.7	6.77	11.13	0.349
14	47.28	80.9	99.6	6.55	10.15	0.395
15	48.94	78.2	99.6	6.63	10.03	0.401
17	59.28	64.5	92.4	6.61	9.43	0.443
18	69.72	54.9	74.4	5.69	8.94	0.479
19	71.41	53.6	67.2	5.19	8.86	0.484

Table 39. Experimental Results of Test Run No. 19

Temperature, ^{o}C	38.2	Test Material	Naphthalene	Date	8-30-65
Pipe Position	Vertical	Density, $g/cm^3 \times 10^3$	1.099	Duration of Run, sec	12000
Reynolds Number	958	Viscosity, $g/cm\text{-}sec \times 10^4$	1.897	Average Diameter, in.	1.653
Schmidt Number	2.42	Diffusivity, cm^2/sec	0.071		

Section Number	z in Inches	ReScD/z	$N_{Aw} \times 10^{11}$	$(Nu_{AB})_{loc}$	$(Nu_{AB})_{lm}$	C_b^*
2	1.97	1947.9	418.9	17.77	30.55	0.061
3	3.59	1066.9	322.2	14.04	23.94	0.086
5	11.31	338.9	211.8	10.19	15.94	0.172
6	12.88	297.7	186.8	9.13	15.18	0.184
8	23.34	164.2	149.1	8.00	12.23	0.258
9	24.91	153.9	142.9	7.77	11.96	0.267
11	35.35	108.4	114.6	6.74	10.57	0.323
12	36.88	104.0	113.3	6.74	10.42	0.330
14	47.28	81.1	97.4	6.21	9.55	0.376
15	48.94	78.3	98.6	6.36	9.44	0.383
17	59.28	64.7	92.6	6.40	8.91	0.424
18	69.72	55.0	73.4	5.41	8.46	0.460
19	71.41	53.4	56.5	4.20	8.37	0.464

Table 40. Experimental Results of Test Run No. 20

Temperature, ^{o}C	38.2	Test Material	Naphthalene	Date	10-07-65
Pipe Position	Vertical	Density, $g/cm^3 \times 10^3$	1.084	Duration of Run, sec	15000
Reynolds Number	1440	Viscosity, $g/cm\text{-}sec \times 10^4$	1.897	Average Diameter, in.	1.599
Schmidt Number	2.42	Diffusivity, cm^2/sec	0.072		

Section Number	z in Inches	ReScD/z	$N_{Aw} \times 10^{11}$	$(Nu_{AB})_{loc}$	$(Nu_{AB})_{lm}$	C_b^*
2	1.97	2832.9	579.7	23.23	36.91	0.051
3	3.59	1551.7	459.2	18.86	29.75	0.074
5	11.31	492.8	297.4	13.36	20.53	0.153
6	12.88	433.0	264.4	12.05	19.58	0.165
8	23.34	238.8	210.0	10.42	15.86	0.233
9	24.91	223.8	206.8	10.38	15.51	0.242
11	35.35	157.7	168.1	9.08	13.81	0.296
12	36.88	151.2	157.9	8.61	13.61	0.302
14	47.28	117.9	129.2	7.48	12.39	0.343
15	48.94	113.9	135.5	7.92	12.23	0.349
17	59.28	94.0	147.1	9.16	11.58	0.389
18	69.72	80.0	93.8	6.19	11.00	0.423
19	71.41	78.1	80.5	5.35	10.88	0.427

Table 41. Experimental Results of Test Run No. 21

Temperature, ^{o}C	38.2	Test Material	Naphthalene	Date	11-04-65
Pipe Position	45^{o}	Density, $g/cm^3 \times 10^3$	1.107	Duration of Run, sec	12000
Reynolds Number	477	Viscosity, $g/cm\text{-}sec \times 10^4$	1.897	Average Diameter, in.	1.612
Schmidt Number	2.42	Diffusivity, cm^2/sec	0.071		

Section Number	z in Inches	ReScD/z	$N_{Aw} \times 10^{11}$	$(Nu_{AB})_{loc}$	$(Nu_{AB})_{lm}$	C_b^*
2	1.97	946.5	322.2	13.85	22.15	0.089
3	3.59	518.4	252.7	11.35	17.84	0.129
5	11.31	164.7	144.8	7.63	12.26	0.258
6	12.88	144.7	125.7	6.79	11.65	0.275
8	23.34	79.8	88.1	5.47	9.20	0.369
9	24.91	74.8	84.6	5.35	8.96	0.381
11	35.35	52.7	68.2	4.84	7.82	0.448
12	36.88	50.5	68.2	4.91	7.70	0.457
14	47.28	39.4	64.1	5.17	7.12	0.514
15	48.94	38.1	65.7	5.40	7.05	0.423
17	59.28	31.4	67.8	6.34	6.84	0.582
18	69.72	26.7	48.2	5.13	6.68	0.632
19	71.41	26.1	35.7	3.87	6.63	0.638

Table 42. Experimental Results of Test Run No. 22

Temperature, ^{o}C	38.2	Test Material	Naphthalene	Date	11-02-65
Pipe Position	45^{o}	Density, $g/cm^3 \times 10^3$	1.109	Duration of Run, sec	13000
Reynolds Number	953	Viscosity, $g/cm\text{-}sec \times 10^4$	1.897	Average Diameter, in.	1.610
Schmidt Number	2.42	Diffusivity, cm^2/sec	0.071		

Section Number	z in Inches	ReScD/z	$N_{Aw} \times 10^{11}$	$(Nu_{AB})_{loc}$	$(Nu_{AB})_{lm}$	C_b^*
2	1.97	1887.2	471.8	19.71	30.39	0.062
3	3.59	1033.7	377.1	16.26	24.79	0.091
5	11.31	328.3	243.7	11.82	17.55	0.193
6	12.88	288.5	216.2	10.69	16.79	0.208
8	23.34	159.1	159.3	8.79	13.66	0.291
9	24.91	149.1	151.8	8.50	13.34	0.301
11	35.35	105.1	119.1	7.30	11.74	0.361
12	36.88	100.7	112.1	6.95	11.55	0.368
14	47.28	78.6	91.1	6.08	10.45	0.413
15	48.94	75.9	92.3	6.22	10.30	0.419
17	59.28	62.7	90.0	6.51	9.61	0.459
18	69.72	53.3	70.6	5.47	9.07	0.494
19	71.41	52.0	64.9	5.08	8.99	0.499

Table 43. Experimental Results of Test Run No. 23

Temperature, ^{o}C	38.2	Test Material	Naphthalene	Date	11-03-65
Pipe Position	45^{o}	Density, $g/cm^3 \times 10^3$	1.109	Duration of Run, sec	11000
Reynolds Number	1432	Viscosity, $g/cm\text{-}sec \times 10^4$	1.897	Average Diameter, in.	1.615
Schmidt Number	2.42	Diffusivity, cm^2/sec	0.071		

Section Number	z in Inches	ReScD/z	$N_{Aw} \times 10^{11}$	$(Nu_{AB})_{loc}$	$(Nu_{AB})_{lm}$	C_b^*
2	1.97	2844.6	601.3	25.07	42.60	0.058
3	3.59	1558.1	464.5	19.88	33.51	0.082
5	11.31	494.9	313.9	14.79	22.57	0.167
6	12.88	434.8	282.9	13.54	21.55	0.180
8	23.34	239.8	201.8	10.58	17.33	0.251
9	24.91	224.8	194.0	10.29	16.90	0.260
11	35.35	158.4	154.1	8.78	14.73	0.311
12	36.88	151.8	148.6	8.55	14.48	0.317
14	47.28	118.4	132.9	8.13	13.13	0.358
15	48.94	114.4	136.2	8.42	12.97	0.365
17	59.28	94.4	128.9	8.48	12.18	0.403
18	69.72	80.3	98.6	6.87	11.51	0.436
19	71.41	78.4	81.9	5.75	11.38	0.441

Table 44. Experimental Results of Test Run No. 24

Temperature, °C	30.9	Test Material	Naphthalene	Date	10-15-65
Pipe Position	Horizontal	Density, $g/cm^3 \times 10^3$	1.124	Duration of Run, sec	14000
Reynolds Number	468	Viscosity, $g/cm\text{-}sec \times 10^4$	1.864	Average Diameter, in.	1.611
Schmidt Number	2.43	Diffusivity, cm^2/sec	0.068		

Section Number	z in Inches	ReScD/z	$N_{Aw} \times 10^{11}$	$(Nu_{AB})_{loc}$	$(Nu_{AB})_{lm}$	C_b^*
2	1.97	932.1	143.0	12.06	19.95	0.082
3	3.59	510.6	111.0	9.73	15.87	0.117
5	11.31	162.2	65.6	6.61	10.70	0.232
6	12.88	142.5	56.4	5.81	10.15	0.248
8	23.34	78.6	43.3	5.05	8.05	0.336
9	24.91	73.7	42.3	5.01	8.86	0.347
11	35.35	51.9	34.7	4.59	6.96	0.415
12	36.88	49.7	33.6	4.51	6.86	0.424
14	47.28	38.8	28.5	4.24	6.32	0.479
15	48.94	37.5	30.3	4.58	6.25	0.487
17	59.28	30.9	27.5	4.60	5.96	0.537
18	69.72	26.3	23.2	4.29	5.74	0.582
19	71.41	25.7	22.2	4.17	5.70	0.588

Table 45. Experimental Results of Test Run No. 25

Temperature, ^{o}C	30.9	Test Material	Naphthalene	Date	10-12-65
Pipe Position	Horizontal	Density, $g/cm^3 \times 10^3$	1.122	Duration of Run, sec	16000
Reynolds Number	990	Viscosity, $g/cm\text{-}sec \times 10^4$	1.864	Average Diameter, in.	1.601
Schmidt Number	2.43	Diffusivity, cm^2/sec	0.068		

Section Number	z in Inches	ReScD/z	$N_{Aw} \times 10^{11}$	$(Nu_{AB})_{loc}$	$(Nu_{AB})_{lm}$	C_b^*
2	1.97	1957.7	209.9	17.15	30.76	0.061
3	3.59	1072.3	159.2	13.35	23.76	0.085
5	11.31	340.6	98.0	8.99	15.24	0.164
6	12.88	299.2	86.1	8.01	14.42	0.175
8	23.34	165.1	65.6	6.61	11.25	0.239
9	24.91	154.7	66.8	6.81	10.96	0.247
11	35.35	109.0	57.2	6.26	9.66	0.298
12	36.88	104.5	54.4	6.01	9.51	0.305
14	47.28	81.5	50.3	5.92	8.73	0.349
15	48.94	78.7	51.5	6.13	8.64	0.355
17	59.28	65.0	53.1	6.77	8.26	0.398
18	69.72	55.3	40.8	5.57	7.95	0.437
19	71.41	54.0	38.2	.26	7.89	0.443

Table 46. Experimental Results of Test Run No. 26

Temperature, ^{o}C	30.9	Test Material	Naphthalene	Date	10-21-65
Pipe Position	Horizontal	Density, $g/cm^3 \times 10^3$	1.117	Duration of Run, sec	13000
Reynolds Number	1414	Viscosity, $g/cm\text{-}sec \times 10^4$	1.864	Average Diameter, in.	1.604
Schmidt Number	2.43	Diffusivity, cm^2/sec	0.069		

Section Number	z in Inches	ReScD/z	$N_{Aw} \times 10^{11}$	$(Nu_{AB})_{loc}$	$(Nu_{AB})_{lm}$	C_b^*
2	1.97	2801.8	256.7	20.68	35.53	0.049
3	3.59	1534.6	197.8	16.29	27.83	0.070
5	11.31	487.4	125.4	11.16	18.28	0.139
6	12.88	428.3	111.2	10.01	17.34	0.150
8	23.34	236.2	87.8	8.48	13.73	0.207
9	24.91	221.4	87.9	8.58	13.40	0.215
11	35.35	156.0	77.4	8.04	11.90	0.263
12	36.88	149.5	72.7	7.62	11.73	0.269
14	47.28	116.6	64.0	7.09	10.77	0.309
15	48.94	112.7	65.6	7.34	10.65	0.315
17	59.28	93.0	62.9	7.43	10.08	0.352
18	69.72	79.1	50.1	6.24	9.60	0.385
19	71.41	77.2	45.7	5.73	9.51	0.389

Table 47. Experimental Results of Test Run No. 27

Temperature, °C	30.9	Test Material	Naphthalene	Date	10-27-65
Pipe Position	Vertical	Density, $g/cm^3 \times 10^3$	1.125	Duration of Run, sec	13000
Reynolds Number	456	Viscosity, $g/cm\text{-}sec \times 10^4$	1.864	Average Diameter, in.	1.606
Schmidt Number	2.43	Diffusivity, cm^2/sec	0.068		

Section Number	z in Inches	ReScD/z	$N_{Aw} \times 10^{11}$	$(Nu_{AB})_{loc}$	$(Nu_{AB})_{lm}$	C_b^*
2	1.97	904.2	141.6	11.95	19.89	0.084
3	3.59	495.3	109.6	9.62	15.78	0.120
5	11.31	157.3	68.3	6.93	10.74	0.239
6	12.88	138.2	59.9	6.22	10.23	0.256
8	23.34	76.2	44.4	5.29	8.24	0.351
9	24.91	71.4	42.1	5.11	8.05	0.363
11	35.35	50.3	32.8	4.45	7.09	0.431
12	36.88	48.3	31.6	4.35	6.98	0.439
14	47.28	37.6	26.3	3.99	6.36	0.492
15	48.94	36.4	28.1	4.33	6.29	0.499
17	59.28	30.0	26.3	4.49	5.96	0.548
18	69.72	25.5	19.6	3.69	5.69	0.590
19	71.41	24.9	19.4	3.71	5.64	0.595

Table 48. Experimental Results of Test Run No. 28

Temperature, ^{o}C	30.9	Test Material	Naphthalene	Date	10-22-65
Pipe Position	Vertical	Density, $g/cm^3 \times 10^3$	1.113	Duration of Run, sec	13500
Reynolds Number	990	Viscosity, $g/cm\text{-}sec \times 10^4$	1.864	Average Diameter, in.	1.607
Schmidt Number	2.43	Diffusivity, cm^2/sec	0.069		

Section Number	z in Inches	ReScD/z	$N_{Aw} \times 10^{11}$	$(Nu_{AB})_{loc}$	$(Nu_{AB})_{lm}$	C_b^*
2	1.97	1965.1	214.1	17.35	28.63	0.057
3	3.59	1076.3	167.1	13.90	22.76	0.081
5	11.31	341.9	110.8	10.16	15.51	0.166
6	12.88	300.4	100.6	9.37	14.81	0.179
8	23.34	165.7	77.4	7.92	12.06	0.253
9	24.91	155.3	75.4	7.82	11.80	0.262
11	35.35	109.4	60.8	6.82	10.48	0.318
12	36.88	104.9	59.7	6.77	10.33	0.326
14	47.28	81.8	51.7	6.28	9.50	0.371
15	48.94	79.0	53.0	6.51	9.39	0.378
17	59.28	65.2	52.8	6.97	8.93	0.422
18	69.72	55.5	40.9	5.79	8.55	0.460
19	71.41	54.2	40.7	5.82	8.48	0.466

Table 49. Experimental Results of Test Run No. 29

Temperature, °C	30.9	Test Material	Naphthalene	Date	10-19-65
Pipe Position	Vertical	Density, $g/cm^3 \times 10^3$	1.124	Duration of Run, sec	14000
Reynolds Number	1453	Viscosity, $g/cm\text{-}sec \times 10^4$	1.864	Average Diameter, in.	1.606
Schmidt Number	2.43	Diffusivity, cm^2/sec	0.068		

Section Number	z in Inches	ReScD/z	$N_{Aw} \times 10^{11}$	$(Nu_{AB})_{loc}$	$(Nu_{AB})_{lm}$	C_b^*
2	1.97	2882.8	264.1	21.41	35.20	0.048
3	3.59	1579.0	206.8	17.13	28.00	0.068
5	11.31	501.5	139.8	12.57	19.10	0.141
6	12.88	440.7	123.4	11.23	18.22	0.152
8	23.34	243.0	102.6	10.11	14.85	0.217
9	24.91	227.8	100.0	9.96	14.55	0.225
11	35.35	160.5	82.6	8.82	13.03	0.277
12	36.88	153.9	78.3	8.44	12.85	0.284
14	47.28	120.0	67.9	7.76	11.81	0.325
15	48.94	115.9	69.6	8.03	11.67	0.332
17	59.28	95.7	66.8	8.18	11.05	0.370
18	69.72	81.4	50.6	6.54	10.50	0.403
19	71.41	79.5	49.8	6.50	10.41	0.408

Table 50. Experimental Results of Test Run No. 30

Temperature, ^{o}C	30.9	Test Material	Naphthalene	Date	11-12-65
Pipe Position	45^{o}	Density, $g/cm^3 \times 10^3$	1.124	Duration of Run, sec	15000
Reynolds Number	485	Viscosity, $g/cm\text{-}sec \times 10^4$	1.864	Average Diameter, in.	1.627
Schmidt Number	2.43	Diffusivity, cm^2/sec	0.968		

Section Number	z in Inches	ReScD/z	$N_{Aw} \times 10^{11}$	$(Nu_{AB})_{loc}$	$(Nu_{AB})_{lm}$	C_b^*
2	1.97	974.6	150.3	12.79	20.82	0.082
3	3.59	533.8	117.3	10.38	16.66	0.117
5	11.31	169.6	75.8	7.78	11.56	0.239
6	12.88	149.0	63.4	6.66	11.04	0.256
8	23.34	82.2	46.2	5.56	8.85	0.350
9	24.91	77.0	44.1	5.39	8.64	0.361
11	35.35	54.3	35.1	4.80	7.60	0.429
12	36.88	52.0	33.1	4.59	7.48	0.437
14	47.28	40.6	30.3	4.65	6.85	0.491
15	48.94	39.2	32.1	5.00	6.78	0.499
17	59.28	32.4	33.2	5.83	6.54	0.554
18	69.72	27.5	22.4	4.39	6.33	0.602
19	71.41	26.9	25.4	5.07	6.29	0.608

Table 51. Experimental Results of Test Run No. 31

Temperature, °C	30.9	Test Material	Naphthalene	Date	11-01-65
Pipe Position	45°	Density, g/cm^3 x 1	1.151	Duration of Run, sec	12500
Reynolds Number	982	Viscosity, g/cm-sec x 10^4	1.864	Average Diameter, in.	1.607
Schmidt Number	2.43	Diffusivity, cm^2/sec	0.068		

Section Number	z in Inches	ReScD/z	$N_{Aw} \times 10^{11}$	$(Nu_{AB})_{loc}$	$(Nu_{AB})_{lm}$	C_b^*
2	1.97	1949.5	208.1	17.05	26.00	0.052
3	3.59	1067.8	167.4	14.08	21.30	0.077
5	11.31	339.2	121.0	11.29	15.48	0.167
6	12.88	298.0	108.7	10.31	14.91	0.181
8	23.34	164.4	79.9	8.40	12.44	0.261
9	24.91	154.0	76.7	8.17	12.18	0.271
11	35.35	108.5	57.2	6.61	10.78	0.328
12	36.88	104.0	57.2	6.68	10.61	0.335
14	47.28	81.1	47.5	5.94	9.67	0.379
15	48.94	78.4	51.1	6.46	9.55	0.386
17	59.28	64.7	46.3	6.27	8.99	0.426
18	69.72	55.0	35.1	5.06	8.50	0.461
19	71.41	53.7	34.4	5.01	8.42	0.466

Table 52. Experimental Results of Test Run No. 32

Temperature, ^{o}C	30.9	Test Material	Naphthalene	Date	10-29-65
Pipe Position	45^{o}	Density, $g/cm^3 \times 10^3$	1.136	Duration of Run, sec	14000
Reynolds Number	1505	Viscosity, $g/cm\text{-}sec \times 10^4$	1.864	Average Diameter, in.	1.609
Schmidt Number	2.43	Diffusivity, cm^2/sec	0.068		

Section Number	z in Inches	ReScD/z	$N_{Aw} \times 10^{11}$	$(Nu_{AB})_{loc}$	$(Nu_{AB})_{lm}$	C_b^*
2	1.97	2991.3	253.9	20.72	33.07	0.043
3	3.59	1638.4	201.2	16.76	26.60	0.063
5	11.31	520.4	140.8	12.68	18.55	0.133
6	12.88	457.2	128.2	11.69	17.78	0.144
8	23.34	252.2	101.3	9.98	14.68	0.208
9	24.91	236.4	96.6	9.62	14.38	0.216
11	35.35	166.5	86.8	9.24	12.92	0.267
12	36.88	159.6	74.9	8.05	12.74	0.273
14	47.28	124.5	63.5	7.20	11.62	0.312
15	48.94	120.3	62.9	7.20	11.47	0.317
17	59.28	99.3	60.3	7.26	10.73	0.351
18	69.72	84.4	48.5	6.11	10.13	0.381
19	71.41	82.4	45.5	5.78	10.00	0.385

Table 53. Experimental Results of Test Run No. 33

Temperature, ^{o}C	30.9	Test Material	p-Dichlorobenzene	Date	12-08-65
Pipe Position	Horizontal	Density, $g/cm^3 \times 10^3$	1.131	Duration of Run, sec	7500
Reynolds Number	751	Viscosity, g/cm-sec $\times 10^4$	1.864	Average Diameter, in.	1.604
Schmidt Number	2.26	Diffusivity, cm^2/sec	0.073		

Section Number	z in Inches	ReScD/z	$N_{Aw} \times 10^{10}$	$(Nu_{AB})_{loc}$	$(Nu_{AB})_{lm}$	C_b^*
2	1.97	1383.8	195.2	13.26	22.15	0.062
3	3.59	758.0	151.5	10.59	17.53	0.088
5	11.31	240.7	104.0	8.08	11.99	0.181
6	12.88	211.5	95.7	7.58	11.49	0.195
8	23.34	116.7	81.6	7.24	9.67	0.282
9	24.91	109.3	76.5	6.90	9.50	0.294
11	35.35	77.0	68.5	6.87	8.73	0.365
12	36.88	73.9	73.7	7.51	8.67	0.375
14	47.28	57.6	66.7	7.63	8.43	0.443
15	48.94	55.7	67.3	7.84	8.40	0.453
17	59.28	45.9	62.0	8.16	8.33	0.516
18	69.72	39.1	48.4	7.17	8.24	0.570
19	71.41	38.1	48.4	7.30	8.22	0.578

Table 54. Experimental Results of Test Run No. 34

Temperature, °C	30.9	Test Material	p-Dichlorobenzene	Date	12-21-65
Pipe Position	Horizontal	Density, $g/cm^3 \times 10^3$	1.121	Duration of Run, sec	9000
Reynolds Number	729	Viscosity, $g/cm\text{-}sec \times 10^4$	1.864	Average Diameter, in.	1.620
Schmidt Number	2.26	Diffusivity, cm^2/sec			

Section Number	z in Inches	ReScD/z	$N_{Aw} \times 10^{10}$	$(Nu_{AB})_{loc}$	$(Nu_{AB})_{lm}$	C_b^*
2	1.97	1357.6	236.7	16.59	31.98	0.090
3	3.59	743.6	174.6	12.68	24.15	0.122
5	11.31	236.2	103.0	8.47	14.98	0.224
6	12.88	207.5	90.9	7.62	14.14	0.239
8	23.34	114.5	79.1	7.46	11.19	0.324
9	24.91	107.3	76.7	7.36	10.95	0.335
11	35.35	75.6	72.2	7.80	9.95	0.409
12	36.88	72.5	72.0	7.92	9.87	0.420
14	47.28	56.5	65.7	8.19	9.47	0.488
15	48.94	54.6	66.3	8.44	9.43	0.499
17	59.28	45.1	63.3	9.23	9.32	0.563
18	69.72	38.3	49.2	8.23	9.24	0.619
19	71.41	37.4	47.7	8.16	9.22	0.627

Table 55. Experimental Results of Test Run No. 35

Temperature, ^{o}C	30.9	Test Material	p-Dichlorobenzene	Date	12-09-65
Pipe Position	Horizontal	Density, $g/cm^3 \times 10^3$	1.133	Duration of Run, sec	7500
Reynolds Number	1386	Viscosity, $g/cm\text{-}sec \times 10^4$	1.864	Average Diameter, in.	1.598
Schmidt Number	2.26	Diffusivity, cm^2/sec	0.073		

Section Number	z in Inches	ReScD/z	$N_{Aw} \times 10^{10}$	$(Nu_{AB})_{loc}$	$(Nu_{AB})_{lm}$	C_b^*
2	1.97	2544.3	282.3	18.83	30.79	0.047
3	3.59	1393.6	221.5	15.10	24.55	0.068
5	11.31	442.6	153.2	11.34	16.88	0.141
6	12.88	388.9	137.7	10.34	16.14	0.153
8	23.34	214.5	122.3	10.00	13.47	0.222
9	24.91	201.0	114.1	9.44	13.23	0.232
11	35.35	141.6	101.3	9.05	12.06	0.289
12	36.88	135.8	101.9	9.20	11.94	0.296
14	47.28	105.9	88.1	8.57	11.27	0.347
15	48.94	102.3	86.7	8.54	11.18	0.354
17	59.28	84.5	88.6	9.39	10.79	0.400
18	69.72	71.8	71.8	8.18	10.49	0.443
19	71.41	70.1	71.3	8.22	10.44	0.449

Table 56. Experimental Results of Test Run No. 36

Temperature, °C	30.9	Test Material	p-Dichlorobenzene	Date	12-10-65
Pipe Position	Vertical	Density, $g/cm^3 \times 10^3$	1.131	Duration of Run, sec	8000
Reynolds Number	742	Viscosity, g/cm-sec $\times 10^4$	1.864	Average Diameter, in.	1.604
Schmidt Number	2.26	Diffusivity, cm^2/sec	0.073		

Section Number	z in Inches	ReScD/z	$N_{Aw} \times 10^{10}$	$(Nu_{AB})_{loc}$	$(Nu_{AB})_{lm}$	C_b^*
2	1.97	1366.8	203.2	13.90	24.45	0.069
3	3.59	748.7	154.8	10.92	19.02	0.097
5	11.31	237.8	99.2	7.80	12.49	0.190
6	12.88	208.9	88.0	7.04	11.88	0.203
8	23.34	115.2	70.8	6.28	9.55	0.282
9	24.91	108.0	67.9	6.11	9.34	0.292
11	35.35	76.1	55.1	5.43	8.29	0.353
12	36.88	72.9	55.9	5.58	8.17	0.361
14	47.28	56.9	47.6	5.16	7.56	0.412
15	48.94	55.0	49.3	5.41	7.48	0.420
17	59.28	45.4	46.6	5.57	7.14	0.467
18	69.72	38.6	33.2	4.28	6.81	0.506
19	71.41	37.7	31.7	4.14	6.75	0.512

Table 57. Experimental Results of Test Run No. 37

Temperature, ^{o}C	30.9	Test Material	p-Dichlorobenzene	Date	12-20-65
Pipe Position	Vertical	Density, $g/cm^3 \times 10^3$	1.114	Duration of Run, sec	7500
Reynolds Number	1425	Viscosity, $g/cm\text{-}sec \times 10^4$	1.864	Average Diameter, in.	1.610
Schmidt Number	2.23	Diffusivity, cm^2/sec	0.074		

Section Number	z in Inches	ReScD/z	$N_{Aw} \times 10^{10}$	$(Nu_{AB})_{loc}$	$(Nu_{AB})_{lm}$	C_b^*
2	1.97	2636.3	316.8	21.08	36.75	0.054
3	3.59	1444.0	242.7	16.54	28.65	0.076
5	11.31	458.6	174.7	13.01	19.24	0.154
6	12.88	403.0	156.6	11.84	18.42	0.167
8	23.34	222.3	129.2	10.70	15.23	0.239
9	24.91	208.3	122.5	10.27	14.93	0.249
11	35.35	146.8	99.5	9.02	13.38	0.305
12	36.88	140.7	94.6	8.66	13.19	0.313
14	47.28	109.7	79.7	7.80	12.10	0.357
15	48.94	106.0	80.5	7.95	11.96	0.363
17	59.28	87.5	74.0	7.79	11.25	0.402
18	69.72	74.4	57.6	6.42	10.63	0.435
19	71.41	72.7	52.7	5.92	10.52	0.440

Table 58. Experimental Results of Test Run No. 38

Temperature, ^{o}C	30.9	Test Material	p-Dichlorobenzene	Date	12-22-65
Pipe Position	45^{o}	Density, $g/cm^3 \times 10^3$	1.133	Duration of Run, sec	8000
Reynolds Number	724	Viscosity, g/cm-sec $\times 10^4$	1.864	Average Diameter, in.	1.628
Schmidt Number	2.26	Diffusivity, cm^2/sec	0.073		

Section Number	z in Inches	ReScD/z	$N_{Aw} \times 10^{10}$	$(Nu_{AB})_{loc}$	$(Nu_{AB})_{lm}$	C_b^*
2	1.97	1354.5	229.0	16.02	26.13	0.074
3	3.59	741.9	178.9	12.96	20.88	0.106
5	11.31	235.6	119.0	9.86	14.50	0.218
6	12.88	207.0	104.7	8.86	13.88	0.235
8	23.34	114.2	82.9	8.02	11.46	0.331
9	24.91	107.0	79.0	7.79	11.23	0.343
11	35.35	75.4	67.2	7.47	10.17	0.417
12	36.88	72.3	65.8	7.43	10.06	0.427
14	47.28	56.4	58.9	7.48	9.49	0.490
15	48.94	54.5	59.5	7.70	9.42	0.499
17	59.28	45.0	58.1	8.52	9.19	0.559
18	69.72	38.2	43.1	7.15	9.00	0.610
19	71.41	37.3	42.1	7.12	8.95	0.617

Table 59. Experimental Results of Test Run No. 39

Temperature, ^{o}C	30.9	Test Material	p-Dichlorobenzene	Date	12-29-65
Pipe Position	45^{o}	Density, $g/cm^3 \times 10^3$	1.135	Duration of Run, sec	7600
Reynolds Number	1360	Viscosity, g/cm-sec $\times 10^4$	1.864	Average Diameter, in.	1.634
Schmidt Number	2.26	Diffusivity, cm^2/sec	0.073		

Section Number	z in Inches	ReScD/z	$N_{Aw} \times 10^{10}$	$(Nu_{AB})_{loc}$	$(Nu_{AB})_{lm}$	C_b^*
2	1.97	2551.9	299.1	20.53	33.94	0.052
3	3.59	1397.7	233.6	16.42	26.96	0.074
5	11.31	444.0	154.2	11.83	18.28	0.152
6	12.88	390.1	137.0	10.66	17.42	0.164
8	23.34	215.1	112.8	9.55	14.15	0.231
9	24.91	201.6	109.5	9.38	13.86	0.240
11	35.35	142.1	94.6	8.74	12.45	0.296
12	36.88	136.2	92.5	8.64	12.29	0.303
14	47.28	106.2	79.2	7.92	11.41	0.349
15	48.94	102.6	79.3	8.01	11.30	0.356
17	59.28	84.7	76.0	8.21	10.74	0.398
18	69.72	72.0	62.7	7.23	10.29	0.435
19	71.41	70.3	61.4	7.15	10.22	0.441

Table 60. Results of Concentration Measurements

Run No. & Date	Temp., Position & Re No.	ReScD/z	R	Concentration Relative to Wall Concentration, C^*
13	38.2° C	27.8	0.86	0.75
10-05-65	Horiz.		0.78	0.66, 0.76, 0.71
	461		0.63	0.58, 0.67, 0.61
			0.31	0.48, 0.46
			0.00	0.40, 0.39, 0.35, 0.33
				0.43, 0.44, 0.27, 0.56
			0.31	0.38, 0.36
			0.63	0.60, 0.56
			0.78	0.70, 0.70
			0.86	0.77, 0.78
16	38.2° C	86.5	0.86	0.88, 0.87
10-01-65	Horiz.		0.78	0.77, 0.71, 0.86
	1426		0.63	0.35, 0.30, 0.30, 0.25
			0.31	0.28, 0.35
			0.00	0.29, 0.28
			0.31	0.38, 0.31, 0.30
			0.63	0.56, 0.44, 0.48, 0.51
			0.78	0.63, 0.72, 0.75
			0.86	0.78, 0.72
24	30.9° C	28.5	0.86	0.88, 0.91
10-15-65	Horiz.		0.78	0.83, 0.89, 1.04
	468		0.63	0.71, 0.83
			0.31	0.58
			0.00	0.46
			0.31	0.52
			0.63	0.68, 0.73
			0.78	0.71, 0.77
			0.86	0.83, 0.83
25	30.9° C	60.0	0.86	0.62, 0.67
10-12-65	Horiz.		0.78	0.52, 0.81, 0.65, 0.60
	990		0.63	0.41, 0.31, 0.36
			0.00	0.36, 0.34, 0.34
			0.63	0.57, 0.61
			0.78	0.64, 0.65
			0.86	0.72, 0.73

Table 60. (Continued)

Run No. & Date	Temp., Position & Re No.	ReScD/z	R	Concentration Relative to Wall Concentration, C^*
29 10-19-65	30.9° C Vert. 1453	88.3	0.86 0.78 0.63 0.31 0.00 0.31 0.63 0.78 0.86	0.68, 0.69 0.59, 0.53 0.46, 0.40 0.39, 0.39 0.38, 0.36 0.42, 0.40 0.54, 0.46, 0.46 0.68, 0.61, 0.65 0.73, 0.84, 0.71
30 11-12-65	30.9° C 45° 485	29.8	0.86 0.78 0.63 0.31 0.00 0.31 0.63 0.78 0.86	1.01, 1.10 0.94, 0.98 0.74, 0.78, 0.71 0.44, 0.40 0.45, 0.34, 0.33, 0.37 0.44, 0.40 0.60, 0.64 0.79, 0.81 0.95, 0.79, 0.70, 0.90

LITERATURE CITED

1. N. Macleod, M. D. Cox, and R. B. Todd, "A Profilometric Technique for Determining Local Mass-Transfer Rates," Chemical Engineering Science, 17, 923 (1962).

2. F. Kreith, J. H. Taylor, and J. P. Chong, "Heat and Mass Transfer from a Rotating Disk," Journal of Heat Transfer, Transactions ASME, Series C, 81, 95 (1959).

3. H. H. Sogin, "Sublimation from Disks to Air Streams Flowing Normal to their Surfaces," Transactions of the American Society of Mechanical Engineers, 80, 61 (1958).

4. H. H. Sogin and V. S. Subramanian, "Local Mass Transfer from Circular Cylinders in Cross Flow," Journal of Heat Transfer, Transactions ASME, Series C, 83, 483 (1961).

5. W. J. Christian and S. P. Kezios, "Sublimation from Sharp-Edged Cylinders in Axisymmetric Flow, Including Influence of Surface Curvature," Journal of the American Institute of Chemical Engineers, 5, 61 (1959).

6. R. L. Bosworth, "Mass Transfer in the Entrance Length of a Pipe-Laminar Flow," Georgia Institute of Technology, Ph.D. Thesis, 1962.

7. W. M. Kays, "Numerical Solutions for Laminar-Flow Heat Transfer in Circular Tubes," Transactions of the American Society of Mechanical Engineers, 77, 1265 (1955).

8. H. L. Langhaar, "Steady Flow in the Transition Length of a Straight Tube," Journal of Applied Mechanics, 9, Transactions ASME, 64, A-55 (1942).

9. B. Wilkins, Jr., "Nonisothermal Laminar Flow and Heat Transfer with Temperature Dependent Physical Properties," Georgia Institute of Technology, Ph.D. Thesis, 1965.

10. D. L. Ulrichson and R. A. Schmitz, "Laminar-Flow Heat Transfer in the Entrance Region of Circular Tube," International Journal of Heat and Mass Transfer, 8, 253 (1965).

11. R. B. Bird, W. E. Stewart, and E. N. Lightfoot, Transport Phenomena, John Wiley and Sons, Inc., New York, 1960.

12. W. J. Christian and S. P. Kezios, "Experimental Investigation of Mass Transfer by Sublimation from Sharp-Edged Cylinders in Axisym-

metric Flow with Laminar Boundary Layer," 1957 Heat Transfer and Fluid Mechanics Institute, Pasedena, California, p. 359.

13. M. A. Leveque, "Les Lois de la Transmission de Chalar par Convection," Annales de Mines, Series 12, 13, 201 (1928).

14. L. Graetz, "Ueber die Warmeleitungsfahigkeit von Flussigkeiten," Annalen der Physik und Chemie, 25, 337 (1885).

15. E. Pohlhausen, "Der Warmeaustaush zwischen festen Korpern und Flussigkeiten mit kleiner Reibung und kleiner Warmeleitung," Zeitschrift für angewandte Mathematik und Mechanik, 1, 115 (1921).

16. T. W. Jackson, J. M. Spurlock, and K. R. Purdy, "Combined Free and Forced Convection in a Constant Temperature Horizontal Tube," Journal of the American Institute of Chemical Engineers, 7, 38 (1961).

17. W. H. McAdams, Heat Transmission, Third Edition, McGraw-Hill Book Company, Inc., New York, 1954.

18. D. R. Oliver, "The Effect of Natural Convection on Viscous-Flow Heat Transfer in Horizontal Tubes," Chemical Engineering Science, 17, 335 (1962).

19. R. C. Martinelli and L. M. K. Boelter, "The Analytical Prediction of Superposed Free and Forced Viscous Convection in a Vertical Pipe," University of California Publications in Engineering, 5, 23 (1942).

20. R. L. Pigford, "Nonisothermal Flow and Heat Transfer Inside Vertical Tubes," Chemical Engineering Progress Symposium Series, 51, 79 (1955).

21. E. R. Gilliland and T. K. Sherwood, "Diffusion of Vapors Into Air Streams," Industrial and Engineering Chemistry, 26, 516 (1934).

22. L. M. K. Boelter, "Note of the Diffusion of Vapors Into an Air Stream Flowing Viscously and Vertically," Transactions of the American Institute of Chemical Engineers, 39, 557 (1943).

23. T. M. Hallman, "Combined Forced and Free-Laminar Heat Transfer in Vertical Tubes with Uniform Internal Heat Generation," Transactions of the American Society of Mechanical Engineers, 78, 1831 (1956).

24. T. J. Hanratty, E. M. Rosen, and R. L. Kabel, "Effects of Heat Transfer on Flow Field at Low Reynolds Numbers in Vertical Tubes," Industrial and Engineering Chemistry, 50, 815 (1958).

25. G. F. Scheele, E. M. Rosen, and T. J. Hanratty, "Effect of Natural Convection on Transition to Turbulence in Vertical Pipes," Canadian

Journal of Chemical Engineering, 38, 67 (1960).

26. C. K. Brown and W. H. Gauvin, "Combined Free-and-Forced Convection, II. Heat Transfer in Opposing Flow," Canadian Journal of Chemical Engineering, 43, 313 (1965).

27. R. W. Hornbeck, W. T. Rouleau, and F. Osterle, "Laminar Entry Problem in Porous Tubes," The Physics of Fluids, 6, 1649 (1963).

28. L. Lapidus, Digital Computation for Chemical Engineers, McGraw-Hill Book Company, Inc., New York, 1962.

29. M. Jakob, Heat Transfer, Sixth Printing, John Wiley and Sons, New York, 1949.

30. W. J. Lee, "A Theoretical Study of Nonisothermal Flow and Heat Transfer in Vertical Tubes for Fluids with Variable Physical Properties," Georgia Institute of Technology, Ph.D. Thesis, 1962.

31. T. W. Jackson, W. B. Harrison, and W. C. Boteler, "Combined Free and Forced Convection in a Constant-Temperature Vertical Tube," Transactions of the American Society of Mechanical Engineers, 80, 739 (1958).

32. Tables of Thermal Properties of Gases, United States Bureau of Standards Circular 564, 33, 69 (1955).

33. T. K. Sherwood and H. S. Bryant, Jr., "Mass Transfer Through Compressible Turbulent Boundary Layers," The Canadian Journal of Chemical Engineering, 35, 51 (1957).

34. J. S. G. Thomas, "The Evaporation of Naphthalene in Dry Air and in Moist Coal Gas," Journal of the Society of Chemical Industry, 35, 506 (1916).

35. C. H. Bedingfield, Jr., and T. B. Drew, "Analogy Between Heat Transfer and Mass Transfer," Industrial and Engineering Chemistry, 42, 1164 (1950).

36. P. N. Walsh and N. O. Smith, "Sublimation Pressure of α-p-Dichloro-, β-p-Dichloro-, p-Dibromo-, and p-Bromochlorobenzene," Journal of Chemical and Engineering Data, 6, 33 (1961).

37. International Critical Tables, Vol. III, McGraw-Hill Book Company, Inc., New York, 1929.

38. T. K. Sherwood and O. Trass, "Sublimation Mass Transfer Through Compressible Boundary Layers on a Flat Plate," Journal of Heat Transfer, Transactions ASME, Series C, 82, 313 (1960).

39. R. C. Reid and T. K. Sherwood, The Properties of Gases and Liquids,

McGraw-Hill Book Company, Inc., New York, 1958, Ch. 8.

40. I. E. Mack, Jr., "Average Cross-Sectional Area of Molecules by Gaseous Diffusion Methods," Journal of the American Chemical Society, 47, 2468 (1925).

41. J. M. Jakob, S. P. Kezios, A Sinila, H. H. Sogin, and M. Spielman, "Aircraft Windshield Heat and Mass Transfer," AF Technical Report No. 6120, Part 5, p. 417 (1952).

VITA

William Dinsmore Holland was born in Atlanta, Georgia on November 9, 1933. He attended public schools in Atlanta and was graduated from Henry W. Grady High School.

He entered the Georgia Institute of Technology, Atlanta, Georgia in June, 1951, and majored in Chemical Engineering. In June, 1955, he received the Bachelor of Chemical Engineering degree. After two years service in the U. S. Navy, he entered the Massachusetts Institute of Technology where he received the Master of Science in Chemical Engineering degree in September, 1958.

From September, 1958 to September, 1960, he was employed full-time by the Lockheed-Georgia Company, Marietta, Georgia, in the capacity of Research Engineer in the Engineering Development Test Laboratory. Upon entering the Graduate Division of the Georgia Institute of Technology in September, 1960, he continued his employment with Lockheed-Georgia Company on a part-time basis until June, 1965.

In June, 1961, he married the former Caroline deRosset Cooke of Richmond, Virginia. They have two daughters.